WEAR MECHANISM EVALUATION AND MEASUREMENT IN FUEL-LUBRICATED COMPONENTS

INTERIM REPORT
BFLRF No. 286

By

P.I. Lacey
Belvoir Fuels and Lubricants Research Facility (SwRI)
Southwest Research Institute
San Antonio, Texas

Under contract to

U.S. Army TARDEC
Mobility Technology Center–Belvoir
Fort Belvoir, Virginia

Contract No. DAAK70-92-C-0059

Approved for public release; distribution unlimited

September 1994

Disclaimers

The findings in this report are not to be construed as an official Department of the Army position unless so designated by other authorized documents.

Trade names cited in this report do not constitute an official endorsement or approval of the use of such commercial hardware or software.

DTIC Availability Notice

Qualified requestors may obtain copies of this report from the Defense Technical Information Center, Cameron Station, Alexandria, Virginia 22314.

Disposition Instructions

Destroy this report when no longer needed. Do not return it to the originator.

REPORT DOCUMENTATION PAGE

Form Approved
OMB No. 0704-0188

1. AGENCY USE ONLY (Leave blank)	2. REPORT DATE	3. REPORT TYPE AND DATES COVERED
	Submitted 1994 Jan Issued 1994 Sep	Interim Jan 92 to Sep 93

4. TITLE AND SUBTITLE

Wear Mechanism Evaluation and Measurement in Fuel-Lubricated Components (U)

5. FUNDING NUMBERS

DAAK70-87-C-0043; WD 18
DAAK70-92-C-0059; WD 10

6. AUTHOR(S)

Lacey, Paul I.

7. PERFORMING ORGANIZATION NAME(S) AND ADDRESS(ES)

Belvoir Fuels and Lubricants Research Facility (SwRI)
Southwest Research Institute
P.O. Drawer 28510
San Antonio, Texas 78228-0510

8. PERFORMING ORGANIZATION REPORT NUMBER

BFLRF No. 286

9. SPONSORING/MONITORING AGENCY NAME(S) AND ADDRESS(ES)

Department of the Army
Mobility Technology Center-Belvoir
10115 Gridley Road, Suite 128
Ft. Belvoir, Virginia 22060-5843

10. SPONSORING/MONITORING AGENCY REPORT NUMBER

11. SUPPLEMENTARY NOTES

12a. DISTRIBUTION/AVAILABILITY STATEMENT

Approved for public release; distribution unlimited

12b. DISTRIBUTION CODE

13. ABSTRACT (Maximum 200 words)

Previous studies have demonstrated that the durability of some fuel injection systems on compression-ignition engines will be adversely affected by fuels of sufficiently low lubricity. However, no widely accepted lubricity measure is available; indeed, the wear mechanisms present have not been conclusively defined. The results of the present study indicate that oxidative corrosion is the predominant mechanism with very highly processed fuels, resulting in catastrophic wear and rapid failure. A laboratory test procedure directed toward the oxidative wear mechanism was evaluated and a number of modifications suggested.

Two closely related laboratory wear test procedures that rely on the transition from mild boundary lubricated wear to adhesive scuffing were also developed. The resulting procedures allow the fuels to be either ranked using a continuous scale or separated using a simple pass/fail criteria. All the procedures are sensitive to the addition of trace quantities
of lubricity additives and show directional correlation with refinery severity, as measured by sulfur and aromatic content. As a result, the tests produced excellent correlation with full-scale equipment tests performed at a number of locations, as well as the criteria necessary for oxidative corrosion. However, the scuffing load tests show greatly increased separation between good and unacceptable fluids compared to the oxidative corrosion tests. Evaluation of commercially available fuels indicates that fuel lubricity is decreasing and that very poor lubricity fuels are occasionally observed.

14. SUBJECT TERMS

Humidity	Boundary Lubrication	Corrosive Wear
Bench Test	Diesel	Viscosity
Corrosion Inhibitor	Oxidative Wear	Adhesive Wear

15. NUMBER OF PAGES

157

16. PRICE CODE

17. SECURITY CLASSIFICATION OF REPORT	18. SECURITY CLASSIFICATION OF THIS PAGE	19. SECURITY CLASSIFICATION OF ABSTRACT	20. LIMITATION OF ABSTRACT
Unclassified	Unclassified	Unclassified	

EXECUTIVE SUMMARY

Problems and Objectives: To reduce its logistics burden, the U.S. Army is using aviation turbine fuel in compression ignition-powered vehicles. Similar fuels are commonly used in arctic conditions, with no apparent durability problems. However, previous full-scale pump stand tests, as well as field experience gained during Operation Desert Shield/Storm, indicate that severe wear is produced with neat Jet A-1 fuel. Wear rate was reduced by addition of a corrosion inhibitor. However, it was believed that wear mechanisms other than oxidative corrosion, such as mild scuffing, were also involved. The objective of the work contained in this report is to define the mechanisms present and develop accurate laboratory-scale wear tests to evaluate their severity.

Importance of Project: Fuel injection system durability is highly dependent on fuel lubricity, which is decreasing. However, the wear mechanisms and lubricity requirements of fuel-lubricated components are only partially defined. As a result, no minimum fuel lubricity standard exists, and the limitations of lubricity additives under adverse conditions are unknown.

Technical Approach: Full-scale pump stand tests were performed under conditions of controlled humidity to define the relative importance of oxidative corrosion and adhesive wear. The measured wear was then correlated with nonstandard BOCLE tests, as a function of humidity and applied load. The laboratory wear test data were also compared to independent test data provided by equipment manufacturers.

Accomplishments: The availability of moisture is a predominant variable controlling the onset of severe wear with low-lubricity fuels that are susceptible to an oxidative corrosive material removal mechanism. This wear process may be effectively controlled by use of corrosion inhibitors and evaluated using the ASTM standard BOCLE test. However, long-term pump durability in the absence of oxidative wear may be affected by other fuel attributes, such as adhesive wear resistance. As a result, several laboratory wear tests that model scuffing load conditions were also developed and evaluated using a wide range of fuel compositions. The scuffing load tests provide improved discrimination between good and unacceptable lubricity fuels and excellent correlation with full-scale equipment for fuels above a critical minimum viscosity.

Military Impact: The results of this study confirm that use of highly refined Jet A-1 in a temperate climate will produce very rapid wear of rotary fuel injection pumps. Use of Jet A-1 in very cold conditions is less likely to produce severe wear, possibly due to reduced moisture content in the fuel. Use of JP-8 will reduce wear, although long-term durability and maximum power output are likely to be lower than with DF-2. Aviation turbine fuels that have acceptable boundary lubricating characteristics may promote increased wear due to their low viscosity. The lubricity of low-sulfur, low-aromatics fuels is also marginally lower than that of conventional high-sulfur fuel. However, the effect of this decrease on equipment durability has not been defined. Lubricity additives significantly reduce scuffing wear, particularly when used at high concentrations (>200 ppm).

FOREWORD/ACKNOWLEDGMENTS

This work was performed by the Belvoir Fuels and Lubricants Research Facility (BFLRF) at Southwest Research Institute (SwRI), San Antonio, TX, under Contract No. DAAK70-87-C-0043 for the period January 1992 through September 1992 and Contract No. DAAK70-92-C-0059 for the period October 1992 through September 1993. Work was funded by the U.S. Army TARDEC, Mobility Technology Center-Belvoir (MTCB), Fort Belvoir, VA, with Mr. T.C. Bowen (AMSTA-RBFF) serving as contracting officer's representative. Project technical monitor was Mr. M.E. LePera (AMSTA-RBF) of MTCB.

The author would like to acknowledge the efforts of BFLRF personnel, including Messrs. D.M. Yost and S.R. Westbrook, who provided much advice and technical assistance; R.E. Grinstead, who provided fuel injection pump expertise and conducted the pump stand experiments; and J.J. Dozier, who performed the bench wear tests. The author also acknowledges the editorial assistance provided by Mr. J.W. Pryor, Ms. M.M. Clark, and Ms. L.A. Pierce in the preparation of this report. Stanadyne Automotive Inc. and Robert Bosch, GMBH and ARCO Alaska, Inc. provided much of the data presented in Figs. 3, 7, 15, and 16. Finally, the author would like to thank the Southwest Research Institute Advisory Committee for Internal Research for financial assistance that allowed development of the test surfaces detailed in Appendix J.

TABLE OF CONTENTS

TABLE OF CONTENTS (Cont'd)

LIST OF ILLUSTRATIONS

LIST OF TABLES

I. INTRODUCTION

Many fuels provide a limited range of contact conditions in which successful lubrication is possible and injection components on compression ignition equipment rely on the fuel to provide the required lubrication. At present, both military and commercial fuel specifications are being revised.(1)* This process may result in the production of more severely refined fuels, devoid of the reactive components necessary for effective lubrication and wear prevention. Relatively little research has concentrated on fuel-lubricated wear in ground vehicles. Lubricity additives are available; however, no specification for minimum acceptable protection due to variation in additive quality or concentration exists. The present report reflects a portion of the U.S. Army-sponsored study to define the effects of highly refined fuels on injection system wear in ground vehicles. The ultimate objective is to develop laboratory wear tests that may be used to screen fuels and additives and assure acceptable products are procured for military use.

Effective laboratory wear test simulation of a real environment typically requires accurate reproduction of the principal contact conditions, such as metallurgy, surface finish, lubricant condition, geometry, and interfacial temperature.(2) Other variables such as sliding speed and contact load/pressure should also reflect the final application. However, in the present instance, the objective is not to characterize a single contact, but rather to characterize the effects of a given fuel on the range of injection systems within the military fleet. Moreover, the most critically fuel-sensitive components are undefined, and it is likely that the relative importance of the wear mechanisms in each contact will be influenced by both fuel viscosity and composition.(3,4) As a result, the approach taken was to broadly define the wear mechanisms present using wear maps and then develop laboratory tests that define the minimum acceptable resistance to each mechanism.

A multitude of commercial wear test apparatus are available, in a range of configurations (5), and the four-ball machine, Dennison Tribotester, Lucas Dwell Tester, and the Thornton Aviation Fuel Lubricity Evaluator (TAFLE) have all been utilized with fuels.(6) In the present study, test procedures for the Ball-on-Cylinder Lubricity Evaluator (BOCLE) were developed, based on

* Underscored numbers in parentheses refer to the list of references at the end of this report.

wear mechanism data obtained using the Cameron-Plint test apparatus.(7,8) The resulting tests provided excellent correlation with the wear observed in full-scale equipment for fuels above a critical minimum viscosity. The BOCLE apparatus has the additional benefit of previous application with aviation turbine fuels and widespread availability in the fuels industry.

II. OBJECTIVE

The overall objectives of this project are (a) to better define the effects of low-lubricity fuels on diesel injection system wear with particular reference to Jet A-1/JP-8, and (b) to develop bench wear tests that reflect the wear mechanisms observed in full-scale equipment.

III. BACKGROUND

This report discusses a portion of the U.S. Army study to define the effects of highly refined fuels on injection system wear. The study to date includes both full-scale pump stand tests, as well as bench-scale wear test evaluation, resulting in a number of reports and publications.(7–14) As far as possible, this report follows the format of those earlier in the series, while providing the minimum duplication of information necessary to remain complete.

The U.S. Department of Defense is moving toward the use of a single fuel on the battlefield (1); Jet A-1 (15) or JP-8 (16) will be used in ground equipment, and widespread use of fuels not meeting these specifications will be curtailed. This directive is currently being implemented, and aviation kerosene accounted for approximately 21 percent of U.S. Army fuel procured during financial year 1991*.(17) At present, the U.S. Army fulfills much of its remaining CONUS requirements with commercial-type fuels meeting VV-F-800D.(18) However, the specification defining commercial fuel is also being revised to reduce vehicle exhaust emissions. The Environmental Protection Agency (EPA) has specified a maximum sulfur content of

* Total fuel procured includes DF-A, DF-1, DF-2, JP-8, and Jet A-1. Note some kerosene fuel is used in aviation equipment rather than compression-ignition engines, which are the primary concern of the present study.

0.05 mass% for all on-highway fuel nationwide to be effective 01 October 1993. This fuel must have a minimum cetane index of 40 or a maximum of 35 vol% aromatics. The California Air Resources Board (CARB) mandates a more stringent requirement of 10 vol% aromatics, also effective 01 October 1993. In Europe, sulfur content is limited to 0.3 mass% max and is expected to fall to 0.05 mass% by 1996.

In each instance, the necessary reduction in sulfur content may typically be achieved using more severe refinery processes, such as hydrogen treating. However, these processes may result in a fuel devoid of reactive components necessary for effective lubrication and wear prevention. Indeed, increased failure rates were reported for certain types of rotary fuel injection pumps operating on Jet A-1 during Operation Desert Shield/Storm, due in part to fuel lubricity.(10, 11) Similarly, very high fuel injection system failure rates have been reported in Scandinavia, due to the commercial sale of highly refined low-sulfur fuels. As a result, a number of organizations, including the U.S. Army and the International Organization for Standardization (ISO/TC22/SC7/WG6), are attempting to define the minimum lubricity requirements of the diesel fuel injection system.

Controlled full-scale equipment tests performed by individual participants under laboratory conditions confirmed that the durability of the rotary injection pump system is highly dependent on fuel lubricity. Most importantly, from a military perspective, severe wear was observed with neat Jet A-1.(3) However, overall wear rate was successfully reduced by suitable lubricity additives or improved metallurgy on critical components. DF-A, which is very similar to Jet A-1, has been successfully used by the U.S. forces in Alaska for many years. Arctic diesel fuel (DF-A) comprised approximately 5 percent of the total U.S. Army fuel consumption (DF-1, DF-2, DF-A, JP-8, and Jet A-1) for FY91, 99 percent of which was used in Alaska. DF-1 fuel accounted for approximately 9 percent of total fuel usage.(17) The successful use of this fuel in arctic conditions may be attributed to a number of conditions including cool ambient weather, very low atmospheric moisture content, and occasional operation on good lubricity fuel.

Previous publications in the present study (7,8) have described the development and application of a wear-mapping technique using the Cameron-Plint test apparatus. This apparatus provides

a reciprocating motion and a range of contact conditions appropriate to the injection system. Wear mechanism maps were developed in conjunction with wear rate maps to allow comparison of the bench-scale wear tests with the material removal processes observed in full-scale applications. This technique delineated the principal wear mechanisms likely to exist at the conditions present in various segments of the fuel injection system. At lower loads, material removal with fuels devoid of natural or artificial corrosion inhibitors was primarily described by an oxidative wear mechanism. Regulation of either moisture or oxygen availability greatly affected wear rate in laboratory tests under these conditions. However, the weak boundary and surface oxide films present were easily removed, resulting in intermetallic adhesion and severe scuffing at slightly higher loads. In this study, scuffing describes conditions of severe friction and wear produced by welding of the subsurface material due to failure of the boundary film or surface oxide layers.

Typical boundary lubricants at low loads consist of oxygenates, among which are those materials based on dilinoleic acid specifically approved as boundary lubricating and corrosion-inhibitor additives. In contrast, antiwear and extreme pressure (EP) fuel compounds must provide a boundary lubricating film stronger than the surface oxide layer they replace. As a result, imperfect correlation exists between the wear rate under lightly loaded conditions and adhesive wear resistance. Similarly, decreased moisture content may reduce wear under low loads, but also decrease the scuffing load capacity of the fuel by eliminating the protective surface oxide layer.

The surface oxidation mechanism has been widely observed in aviation equipment operating on kerosene fuels and effectively controlled using corrosion-inhibitor additives. As a result, a standard test procedure exists for the Ball-on-Cylinder Lubricity Evaluator (BOCLE), (ASTM D 5001) (19) referred to as *Procedure A* in the present work. (The principal test parameters for the various wear-test procedures discussed in the present study are detailed in Appendix A.) This technique is commonly used by the U.S. Air Force to measure aviation turbine fuel lubricity and is believed to correlate with lightly loaded aircraft fuel system components such as spool valves. The lightly loaded *Procedure A* test corresponds closely to the mild wear portion of the wear maps and primarily reflects the fuel's resistance to oxidative corrosion. Previously, oxidation of

metallic contact surfaces was demonstrated to be a contributing wear mechanism in pumps from compression-ignition equipment operating on very low lubricity fuel.(3,14) However, both adhesive and fretting corrosion wear were also indicated, and the relative importance of each mechanism was unclear (scuffing failure has also been reported on the highly stressed areas on the teeth of aviation gear pumps). Finally, the wear maps indicate that the ASTM standard BOCLE test alone (*Procedure A*) may not adequately consider the range of metallurgy, humidity, and contact severity present in practical applications.(8)

IV. TECHNICAL APPROACH

The primary objective of this study is to develop a laboratory wear test that reflects the fuel lubricity requirements of full-scale equipment. Two principal wear mechanisms have been suggested. As a result, the work is separated into two distinct phases: a) evaluation and development of a wear test for oxidative corrosion; and b) development of a wear test based on the transition to adhesive scuffing.

However, the technical performance of the work is most easily separated as follows: a) full-scale pump stand tests to define the predominant wear mechanisms; and b) development of bench-scale wear tests that model these mechanisms. Brief summaries of the technical approach in both areas follow. The bulk of the supporting full-scale equipment tests is provided in the appendices, with the results discussed in the body of the text as required.

A. Full-Scale Pump Stand Tests

Pump tests were performed to define the effects of variables such as fuel moisture content, temperature, and running-in on injection system wear. Detailed descriptions of these tests are included in Appendix B. Unless otherwise stated, a standard and an arctic pump were tested simultaneously using recirculated fuel. Five standard and three arctic pumps were procured. For ease of reference, a code number was assigned to each pump, as described in TABLE 1. The pumps were similar in configuration, but the arctic unit contained an improved metallurgy in

TABLE 1. Fuel Injection Pump Code Sheet

Code No.	Pump Type	Serial No.	Model No.	Condition
1	Standard	5608689	DB2829-4524	Rebuilt
2	Standard	5608690	DB2829-4523	Rebuilt
3	Standard	6627499	DB2829-4524	New
4	Arctic	6624980	DB2829-4523	New
5	Standard	7136688	DB2829-4979	New
6	Arctic	6913740	DB2829-4980	New
7	Standard	7136689	DB2829-4979	New
8	Arctic	6913741	DB2829-4980	New

certain critical components. Pump Nos. 1 through 4 are identical to those used in Reference 3. Pump Nos. 5 through 8 are very similar in configuration to the remaining units, but have slightly different calibration, as described in Appendix C. Pump Nos. 1 and 2 were previously operated, but were completely rebuilt to the manufacturer specifications using standard components. These rebuilt pumps were used in particularly destructive tests, in which the use of new pumps could not be justified.

Each of the tests was performed during regular 8-hour shifts, with a warm-up period of 30 minutes to attain the normal operating temperature of 79°C (175°F). Pump performance was continuously monitored so that the test could be terminated prior to catastrophic failure. Samples of the test fuels were drawn every 20 hours, and a BOCLE wear test performed to ensure that lubricity was not affected by oxidation [fuel-oxidation reactions from oxygenated species (i.e., carboxylic acids, aldehydes, alcohols, etc.) that, because of their polar nature, act as good lubricity agents]. Overall degradation in pump performance was defined by operating each unit on an engine and a calibration stand, both before and after each test. Pretest and post-test measurements were also taken with an unused pump to ensure that the test equipment was

self-consistent. Finally, each pump was completely disassembled, and qualitative and quantitative wear measurements performed, with the results provided in Appendix D.

The pretest engine power for each of the pumps is plotted in Appendix E. Pump Nos. 1 through 4 produced approximately 10 percent higher maximum engine power than the remaining pumps due to the difference in calibration. The engine power produced with Jet A-1 (conforming to ASTM D 1655) (15) in each of the new pumps is approximately 14 percent lower than with diesel fuel (VV-F-800D) (18) over the complete speed range. This result is in good agreement with previous measurements with this type of pump.(3)

B. Laboratory Wear Tests

Laboratory wear tests were performed using the Ball-on-Cylinder Lubricity Evaluator (BOCLE) and the Cameron-Plint test apparatus. A more detailed description of both apparatus may be obtained in Reference 3. The Cameron-Plint test apparatus provides a reciprocating contact geometry with a wide load range and so may be more suited to this application than the BOCLE test. However, the majority of tests were based on the BOCLE, due to its widespread availability and its more accurately controlled test environment.

Initial testing concentrated on minor variations to the ASTM standard procedure (*Procedure A*): fuel moisture content and temperature were adjusted to produce significantly improved correlation with full-scale equipment. It is not suggested that each of the modified procedures should be incorporated in the standard test. However, the improved correlation achieved by minor changes in test parameters to better reflect full-scale operation indicates the similarity of the wear mechanisms in each instance and the utility of the ASTM standard BOCLE test. Nonetheless, the results of this and preceding reports indicate that the oxidative corrosion tests defined in *Procedures A* and *B* may only partially reflect the more highly loaded contacts present in some fuel injection equipment. In addition, they provide poor discrimination between good and unacceptable lubricity fluids. As a result, considerable emphasis has been placed on developing alternate wear tests that reflect the scuffing load capacity of the fuel (*Procedures C, D, E,* and *F*).

Both the full-scale and laboratory wear test procedures used the fuels detailed in TABLE 2. The fuels were selected to provide widely varying lubricity characteristics and composition, while reflecting fuel types likely to be procured around the world by the U.S. Army. The resulting data base facilitated a broad comparison between the fuels as a function of composition and will also be of interest to commercial users.

Fuels A, B, C, and F are identical to those used in References 7 through 14 and are also used in the full-scale pump tests described in Appendix B. Fuels B and C consist of Jet A-1 (Fuel A) with 15 mg/L DCI-4A and 71/227 mg/L BIOBOR-JF/FOA-15 added, respectively. Fuels G, H, I, J, N, Q, T, U, V and W were provided by ISO/TC22/SC7/WG6 and have also been evaluated by that group. Fuels N and Q are ostensibly similar unadditized Class 1 fuels from Scandinavia. However, Fuel N provides a low BOCLE result and has uncharacteristically good wear properties. As a result, it is likely that this fuel was inadvertently additized or contaminated. Fuels D, E, O, P, R, and S are experimental, noncommercially available fluids produced by batch distillation and were provided courtesy of ARCO Alaska, Inc. Fuel L is a standard calibration fluid for use with diesel injection systems and contains an antiwear additive. Fuel W corresponds to Fuel J clay treated according to ASTM D 3948. Fuel Y is a synthetic fuel from Canada.

V. EVALUATION OF OXIDATIVE CORROSION

A. Previous Work

Figs. 1a and 1b are wear maps for AISI E-52100 steel lubricated with neat clay-treated Jet A-1 in a controlled test environment of air and nitrogen, respectively.(7) In each instance, the Y axis is the ambient humidity in the test chamber, while the vertical axis reflects Archard's wear coefficient, as defined in Reference 20. The lightly loaded region of the wear map is highly dependent on the moisture content in the fuel, indicating an oxidative/corrosive material removal process. This portion of the map was found to have good directional correlation with the BOCLE.

TABLE 2. Principal Characteristics of Fluids Used in Wear Tests

Fluid	Fuel Type	Sulfur, mass%	Aromatics, mass%	Olefins, mass%	Viscosity at 40°C, cSt
A	Jet A-1	0.002	8	0	1.07
B	JP-8	0.002	8	0	1.07
C	Jet A-1 + Add	0.002	8	0	1.07
D	DF-A	0.05	19	1.5	1.02
E	DF-A	0.041	13.9	0.5	1.0
F	DF-2	0.39	38	3.7	3
G	DF-1	0.081	27	3.4	1.51
H	DF-2	0.296	44	4.0	2.02
I	DF-2	0.0053	22	4.4	2.2
J	DF-2	0.0041	10.4	3.9	1.9
K	DF-2	0.31	--	--	2.65
L	Cal. Fl.	0.13	10.0	--	2.48
M	ISOPAR M	0	0	0	3.11
N	Class 1	0.001	5	--	1.84
O	DF-A	0.07	22	1	1.29
P	DF-A	0.204	20.1	--	1.37
Q	Class 1	0.001	4.4	1.9	1.83
R	Experim.	0.01	20.1	1.6	--
S	Experim.	0.004	13.2	1.4	--
T	Bosch	0.001	1.1	--	2.35
U	Bosch	0.15	--	--	2.79
V	Class II	0.001	--	--	2.3
W	CT J	<0.0041	--	--	1.9
X	Experim.	0.001	2.7	1.9	1.8 at 20°
Y	Synthetic	--	--	--	1.37
Z	Q + Add	0.001	4.4	1.9	1.83

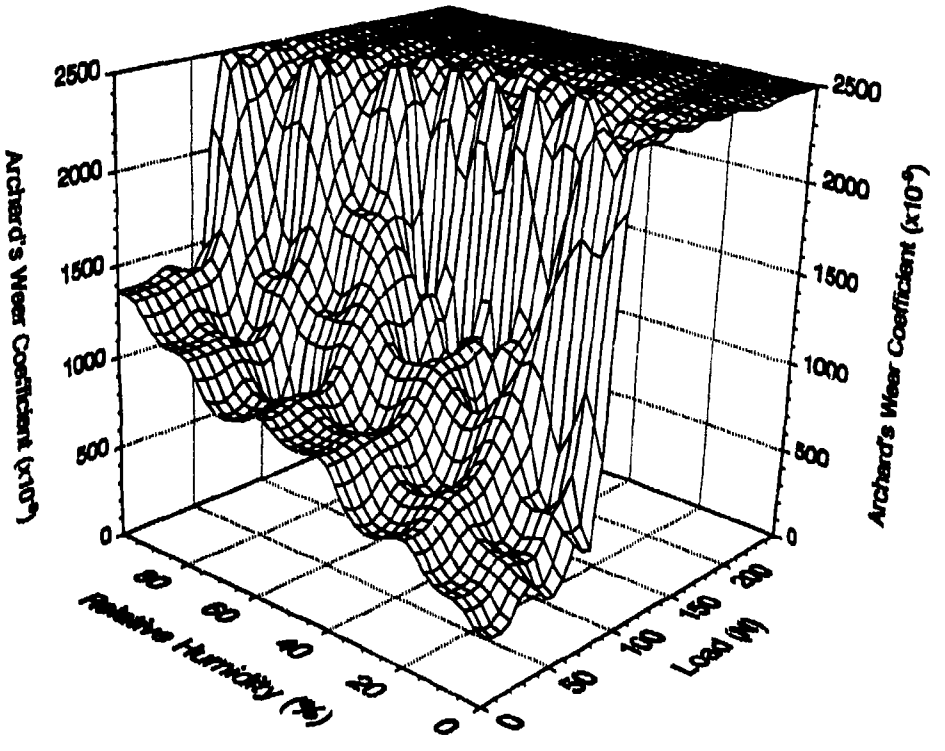

a. Tests Performed in Air

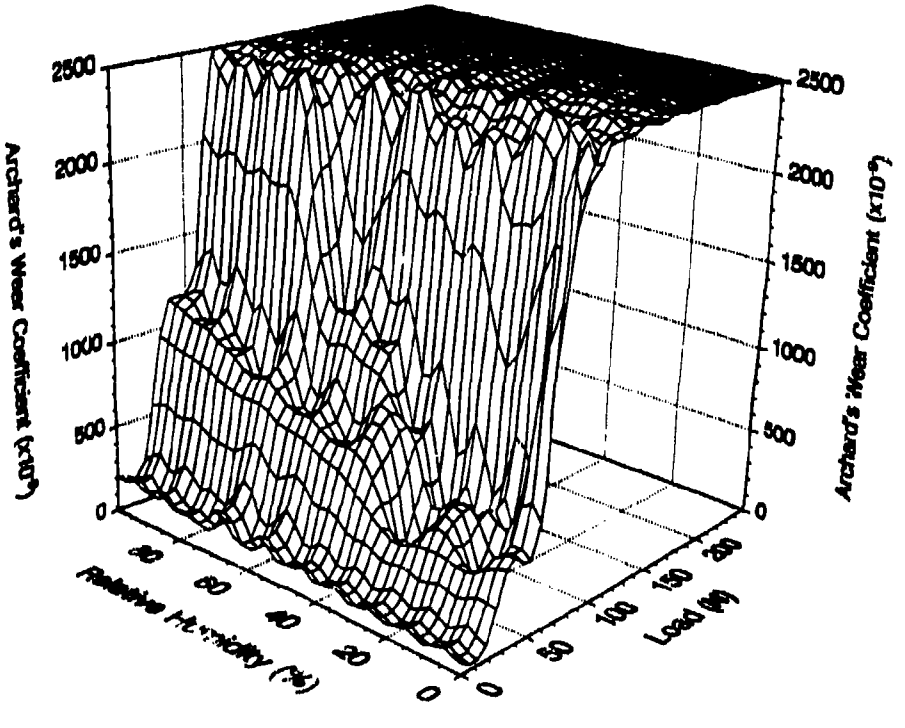

b. Tests Performed in Nitrogen

Figure 1. Wear maps plotted as a function of humidity and applied load for Jet A-1

In contrast, at higher loads, the presence of up to 50 percent relative humidity actually increases the scuffing load capacity of the fuel. These results indicate that the effects of moisture content on the full-scale pump will depend on the applied load and the pertinent wear mechanisms. Previously, a primary wear mechanism in pumps operating on neat clay-treated Jet A-1 was oxidation of the metallic surfaces, and a brown oxide coating was present on the inside of the pump at the conclusion of the test.(3) However, some adhesive wear was also indicated. Therefore, the effects of moisture content on the wear rate in the full-scale pump are unknown, as its effects on the wear map results were shown to depend on contact load. Decreasing moisture content may reduce oxidative wear at the expense of increased adhesive scuffing for Jet A-1. Similarly, moisture may reduce the scuffing load capacity of JP-8 under certain conditions.

B. Evaluation of Oxidative Corrosion in the Full-Scale Pump

Controlled variations in atmospheric moisture content within the fuel reservoir were made during full-scale pump tests to define the predominant material removal process, as described in Appendix B. At relative humidity values less than 100 percent, the amount of water dissolved in the fuel will be correspondingly less than the saturation values, in accordance with Henry's Law. Fuels A, B and F (described in TABLE 2) were used and correspond to neat low-lubricity fuel, additized low-lubricity fuel, and a fuel with good natural lubricity, respectively.

Normalized wear coefficients for lightly loaded areas of the pumps are plotted in Fig. 2a, while results for more highly loaded components are plotted in Fig. 2b. The results of nonstandard BOCLE wear tests performed as a function of atmospheric humidity are also shown for comparison (the remaining test parameters follow *Procedure A*). Each of the wear measurements was normalized using Archard's coefficient (20) to eliminate the effects of sliding distance and applied load. Nonetheless, the normalized wear rate varied significantly, depending on fuel and test conditions. In general, the nonstandard BOCLE results were almost an order of magnitude greater than the corresponding pump test data. This difference is probably due to the relatively high surface roughness of the standard BOCLE ring (0.56 to 0.71 μm), combined with its different metallurgy when compared to the full-scale pump.

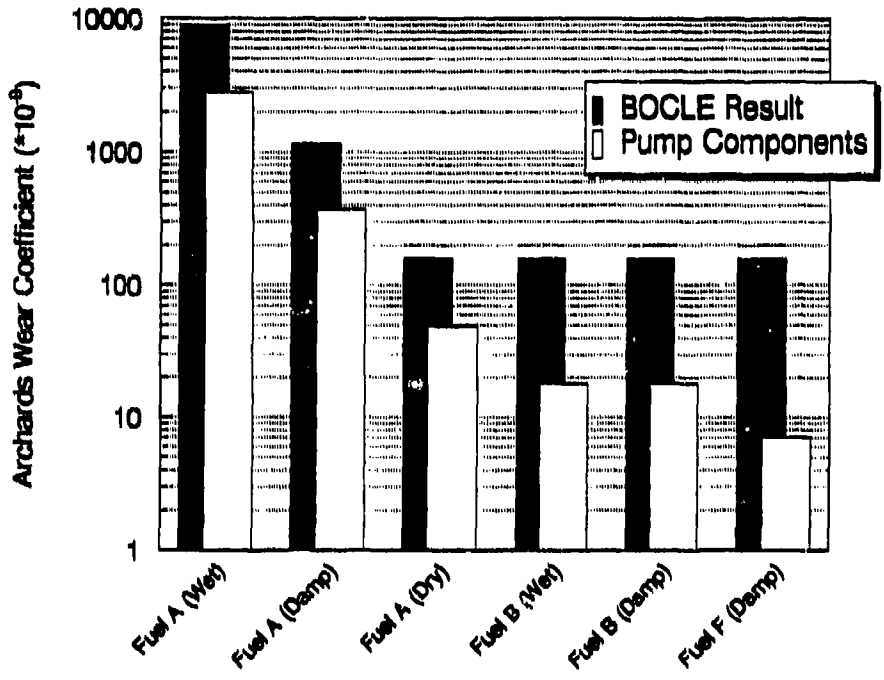

a. Lightly Loaded Pump Components

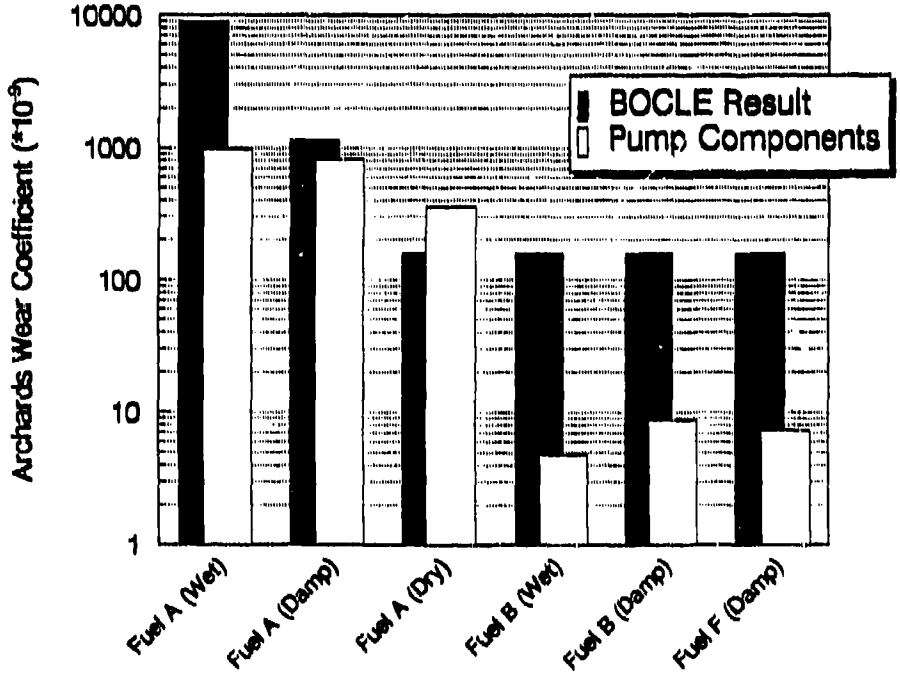

b. Highly Loaded Pump Components

Figure 2. Comparison between normalized BOCLE results and average wear measurements taken from components in the full-scale pump

At low loads, wear rate is a strong function of test humidity in both the BOCLE and the full-scale pumps. Moreover, the effects of humidity are dependent on fuel type and are especially great for the neat low-lubricity fuel, producing a fifty-fold increase in wear volume. The dilinoleic acid-based corrosion inhibitor successfully reduced wear in each instance and made the fuel independent of humidity. These results indicate the almost complete dependence of these lightly loaded areas of the pump on an oxidative corrosive wear mechanism. Clearly, the ASTM standard BOCLE test described as *Procedure A* cannot be expected to provide direct quantitative correlation with pump stand tests performed at an atmospheric humidity other than 10 percent. As in previous studies, Fuel F was marginally more successful than predicted by the BOCLE, probably due to the combined effects of increased viscosity and superior adhesive wear resistance compared to Fuels A and B.

Directional correlation is also apparent between the BOCLE results and the wear measurements on the more highly loaded pump components, as plotted in Fig. 2b. Variation in moisture content has less effect on the wear observed with the low-lubricity fuel under these conditions, probably due to the onset of alternate mechanisms independent of oxidative corrosion. Nonetheless, wear rate was reduced by the corrosion-inhibitor additive, even though extensive laboratory tests indicate that it has little effect on adhesive wear at this concentration, as shown in Fig. 14 of Section VI.C. In general, the very highly loaded areas within the injection system are only subjected to low amplitude lateral motion conducive to fretting corrosion, which has a more complex interrelationship with surface oxidation. The BOCLE test produces oxidative wear with no fretting motion and little adhesion. As a result, the overall correlation is less than that for the lightly loaded contacts. The results indicate a more complex combination of wear mechanisms in the highly loaded contacts, probably including adhesive welding, oxidative corrosion, three-body abrasion by oxide wear particles, and fretting. In general, however, oxidative corrosion plays a major role in these contacts, and wear rate is greatly reduced by the use of corrosion-inhibitor additives.

C. Evaluation of Oxidative Corrosion in the BOCLE

All fuels consist of many distinct compounds. Reactive species such as dilinoleic acid are effective in reducing oxidative/corrosive wear at a concentration of only a few parts per million, and previous workers have indicated that many naturally occurring compounds may contribute to lubricity.(21,22) Typical diesel fuels do contain trace amounts of oleic-acid compounds, which may act as lubricity additives. To evaluate the importance of these components, Cat 1-H diesel was rinsed with sodium bicarbonate in deionized water and dried using sodium sulfonate. This procedure removes compounds more acidic than phenols, but has little effect on the oxidative/corrosive wear resistance of the fuel as measured using the BOCLE. As a result, it is likely that other unknown compounds also serve as corrosion inhibitors. At present, fuel composition may not be used to predict lubricity from a theoretical basis, and an empirically derived wear test procedure is needed.

Increasingly severe refinery processes to reduce sulfur content will inadvertently remove aromatic, olefin, and a range of other undefined compounds, as shown in TABLE 2 and Appendix F. As a result, sulfur content is only a broad measure of refinery severity, rather than the primary component responsible for lubricity. Indeed, the presence of sulfur was previously shown to increase wear under certain conditions, probably due to a corrosive mechanism.(3) Although some exceptions exist, both aromatic and olefin contents of the fuels detailed in TABLE 2 are broadly related to sulfur content, as shown in Appendix F, Fig. F-1a. Clearly, each of the fuel parameters is partially interrelated and is dependent on the severity of the refinery process; in general, more severe refinery processes increase the fraction of nonreactive saturated hydrocarbons.

The preceding pump test data were primarily confined to a single fuel, the lubricity of which was defined using additives and ambient humidity. The complexity of performing full-scale equipment tests prohibits more detailed testing with a wide range of fuels at this laboratory. However, good correlation exists between the wear mechanisms of the BOCLE and wear observed in full-scale pumps performed at this and other laboratories, as shown in Fig. 2 and,

later in this report, Fig. 7. As a result, the BOCLE apparatus was selected to rapidly evaluate the oxidative corrosion process and its relationship to fuel composition.

The ASTM standard BOCLE wear characteristics (*Procedure A*) of the fuels detailed in TABLE 2 are plotted in Fig. 3 as a function of sulfur content. The results obtained from fuels known to contain lubricity additives are not plotted (i.e., Fuels B, C, and L), to avoid artificial bias of the results. [An unpublished study of 50 fuels that contain corrosion-inhibitor additives qualified under MIL-I-25017 (23) showed no relationship between BOCLE data and any measured physical or chemical characteristic other than additive concentration.] Clearly, only very general trends may be expected from correlation with these bulk physical properties, as minute amounts of contaminant may greatly affect wear characteristics, so no universal correlation was observed. However, a statistically significant increase in the BOCLE result is evident for the most severely refined fuels (olefins below 0.5 percent, aromatics below 10 percent, and sulfur below 0.05 percent), corresponding to an eight-fold increase in Archard's wear coefficient. The wear mechanisms responsible for this increase require further definition, although it is likely to be due to increased susceptibility to oxidative corrosion as observed in the full-scale pump tests.

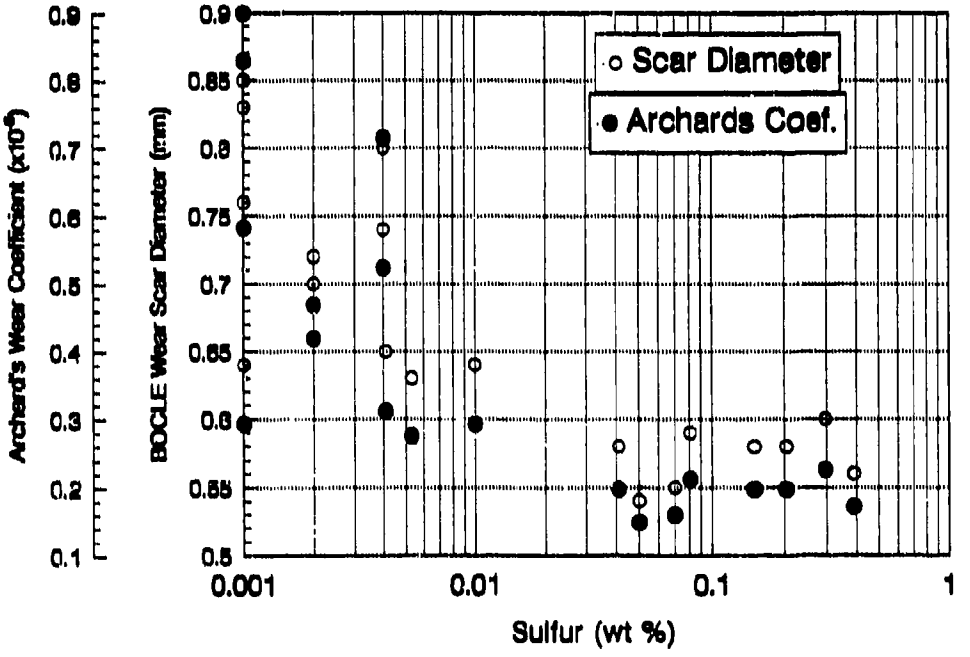

Figure 3. Correlation between BOCLE wear result performed according to *Procedure A* and refinery severity as measured using fuel-sulfur content

More detailed BOCLE tests to define the effects of decreasing sulfur content on the wear mechanisms present were performed using Fuels O and P in TABLE 2. These fuels have sulfur contents of 0.079 and 0.204 mass%, respectively, and the distillation properties provided in Appendix F. The end point of both fuels was sequentially reduced using a batch distillation process to produce a range of fuels with naturally decreasing sulfur content and a slight corresponding change in aromatic and olefin content. The majority of sulfur-containing compounds is contained in the higher molecular weight fuel components, as shown in Appendix F, Fig. F-2. Clearly, this batch distillation process will not accurately reflect the fuel composition achieved using refinery techniques such as hydrogen or furfural treatment. However, the procedure is being considered by isolated refineries, and the results may be used to indicate the properties of low-sulfur products derived from a single base stock.

The results of BOCLE wear tests plotted as a function of increasing sulfur content (end point) are shown in Fig. 4, at 0-, 10-, and 100-percent relative humidity (Rh). A slight, but repeatable,

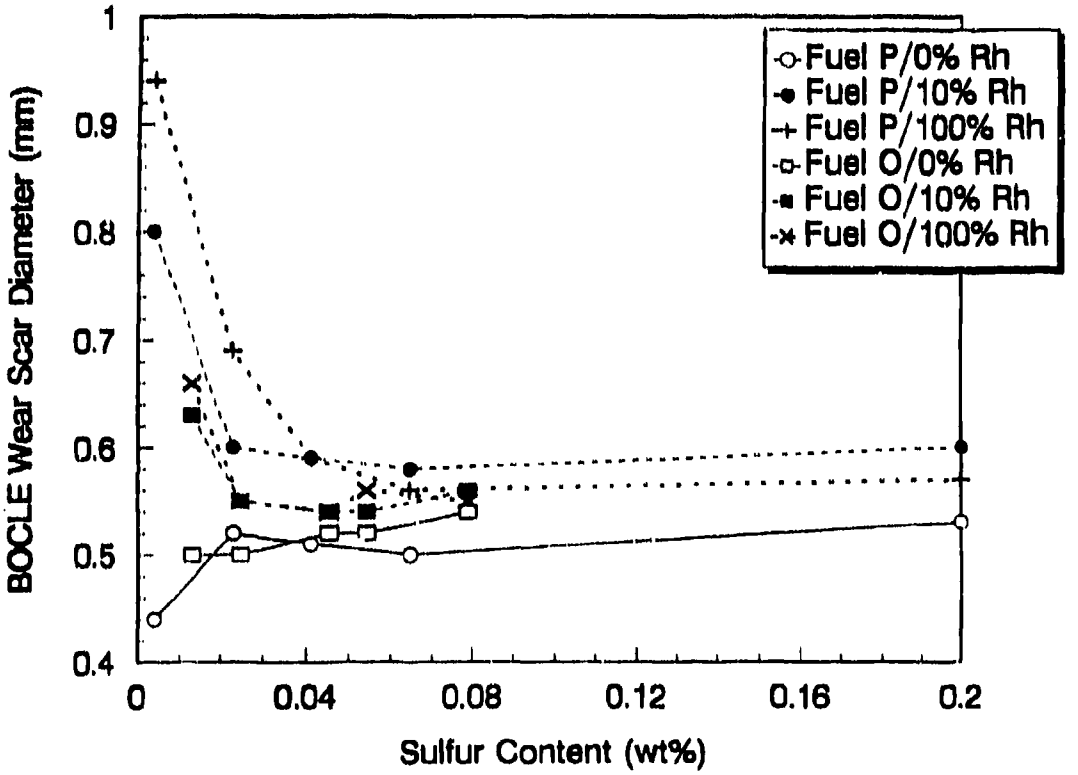

Figure 4. BOCLE wear scar diameter (*Procedure A* at 0, 10, and 100 percent Rh) as a function of sulfur content in Fuels O and P varied using batch distillation

decrease in the average wear scar diameter occurs during the initial reduction in sulfur content. Directionally similar results have been observed with artificial sulfur additives (di-*tert*-butyl disulfide) probably due to the elimination of a mild corrosive wear mechanism.(3) In the presence of moisture, a further reduction in end point/sulfur content produced a dramatic increase in wear rate for both fuels. However, with no moisture present, the wear rate remains low over the complete end point range studied. The natural corrosion inhibitors in each fuel (not necessarily sulfur) appear to be eliminated if the end point of the fuel is sufficiently low, facilitating the severe oxidative/corrosive wear mechanism observed in the full-scale pump tests. The wear mechanisms observed during the systematic treatment of Fuels O and P duplicate the effects previously observed for the full range of fuels. No relationship is apparent between wear rate and composition or humidity for fuels that contain a significant volume of reactive species; however, if the refinery process is sufficiently severe, a sudden increase in wear rate occurs due to an oxidative corrosion mechanism.

Nonstandard BOCLE wear tests were performed on fuels detailed in TABLE 2 to demonstrate that the preceding relationship between refinery severity and oxidative corrosion holds for fuels of varying composition. Once again, the tests were performed at relative humidities of 0 and 100 percent in addition to the ASTM standard conditions of 10 percent, with the results shown in Fig. 5. The sulfur and aromatic contents of each fuel are also plotted to allow comparison with the wear test data. Less refined fuels with a sulfur content above approximately 0.025 mass% have a relatively small BOCLE wear scar diameter of less than 0.62 mm in the ASTM standard BOCLE test described in *Procedure A*. The BOCLE results for these fuels are almost independent of both moisture and sulfur content. In contrast, more severely refined fuels produce greatly increased wear and are highly sensitive to moisture. The relationship between moisture content and wear rate is erratic for the most severely refined fuels, probably due to trace amounts of contaminant not reflected by the very low sulfur level. Clearly, however, fuel lubricity and resistance to oxidative corrosion are adversely affected by severe refinery treatment to reduce sulfur and aromatic content.

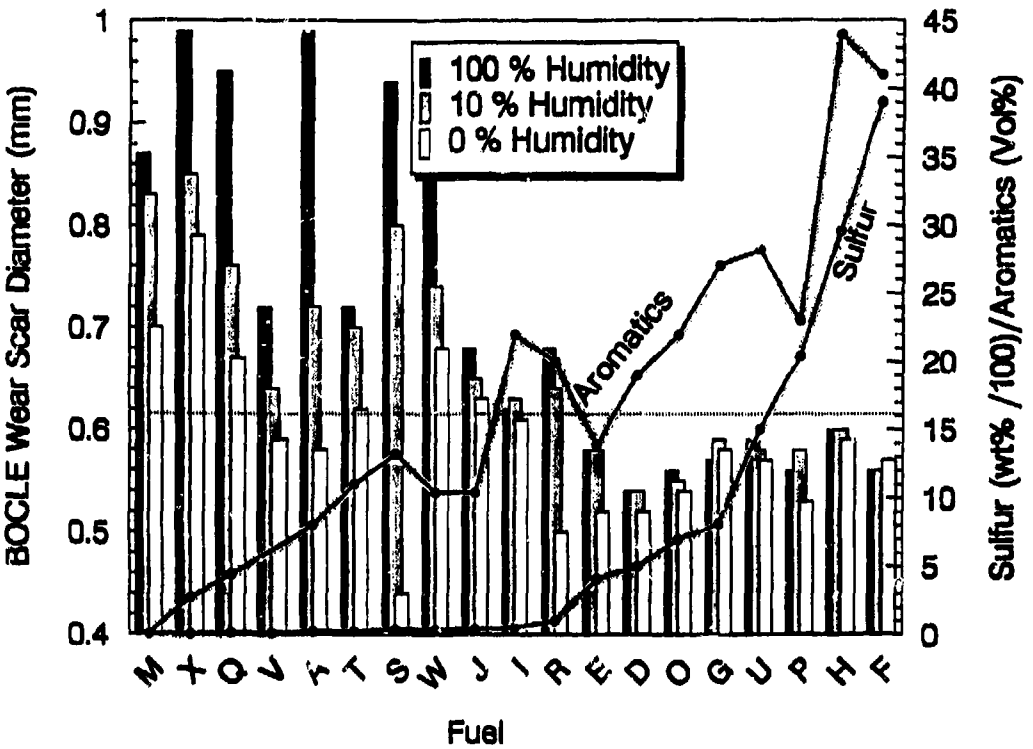

Figure 5. BOCLE wear scar diameter (*Procedure A* at 0, 10, and 100 percent Rh) as a function of sulfur/aromatic content in fuels detailed in TABLE 2

As usual, tests with additized fuels were not included in Fig. 5. The addition of corrosion inhibition and commercially available lubricity additives to severely refined fuels typically results in a BOCLE wear scar between 0.55 and 0.6 mm. This value is in general agreement with the preceding results obtained with natural inhibitors. A single boundary additive containing more reactive boron compounds has been shown to provide wear protection in addition to eliminating corrosion, and it produces a wear scar diameter of less than 0.4 mm (14), which is similar to that obtained for formulated engine oils.

D. Evaluation of a Revised BOCLE Wear Test at High Humidity

Preceding sections indicate that the BOCLE diameter of 0.65 mm specified by the U.S. Air Force (23) approximates the elimination of natural and artificial corrosion inhibitors from the fuel. The principal difficulty with the ASTM standard BOCLE test is the small separation between acceptable and poor lubricity fuels. However, the results of the preceding section also indicate that greater separation may potentially be obtained by increasing the level of humidity in the test

cell. A more detailed evaluation of this approach follows. The effects of varying other test parameters were also briefly evaluated with mixed results. For some fluids, oxidative wear was emphasized by decreasing the applied load and speed, although the improvement was not universal. Clearly, a more detailed evaluation of the remaining test parameters is also required, but is beyond the scope of the present work.

The repeatability of the ASTM standard BOCLE test (*Procedure A*) was originally verified using a round-robin evaluation. That work indicated that tests performed at 10 percent humidity had better precision than those at 50 percent humidity.(22) However, it is unclear if the decreased accuracy outweighs the benefits achieved due to increased separation of the test results. Initial repeatability tests in the present study were performed at a test humidity of 60 percent to prevent formation of condensation in the test reservoir. However, reproducibility was decreased, possibly due to inaccuracy of the humidity meter on the BOCLE apparatus. Subsequent tests were performed under saturated atmospheric moisture conditions (*Procedure B*; 100 percent relative humidity), thereby eliminating the requirement for humidity measurement. The results are shown

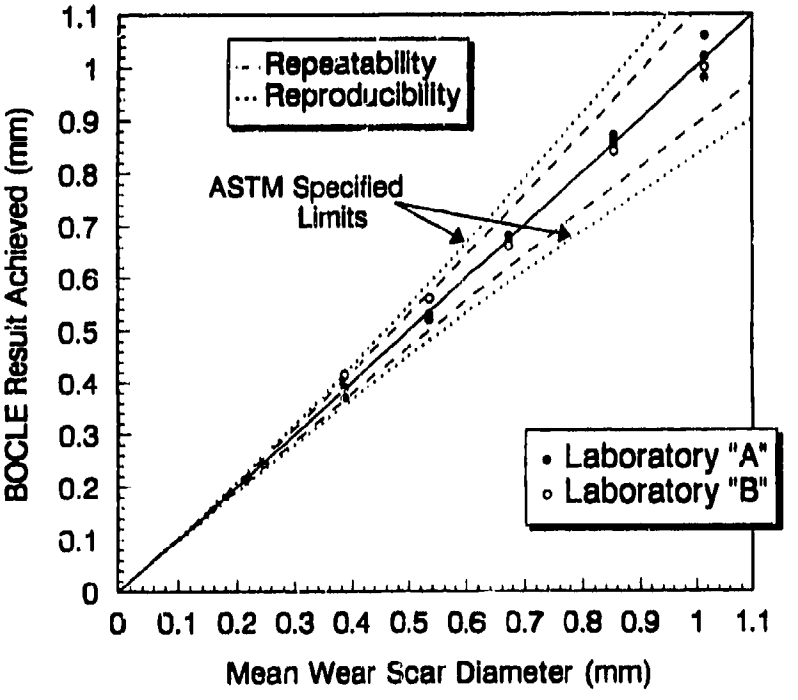

Figure 6. Comparison of modified BOCLE results at 100 percent humidity (*Procedure B*) with maximum acceptable test repeatability and reproducibility as defined in ASTM D 5001 (*Procedure A*)

in Fig. 6. The solid and hollow symbols each denote 1 of 20 single tests performed within BFLRF and an independent laboratory, respectively, using identical fuel. (Note: Three tests were performed with each of the fluids in Laboratory A, although some points are not visible due to overlapping results.) The broken lines define the maximum acceptable repeatability within a given lab and reproducibility between independent test apparatus, as defined in Equations 1 and 2. The difference between any two test results should not exceed these values in more than 1 case in 20.(19) The repeatability and reproducibility in each of the nonstandard tests at 100 percent humidity are comparable to those expected from the ASTM standard procedure at 10 percent humidity.

$$\text{Repeatability } (2*\text{Std Deviation}) = 0.109*D^{1.8} \qquad \text{(Eq. 1)}$$

$$\text{Reproducibility } (2*\text{Std Deviation}) = 0.167*D^{1.8} \qquad \text{(Eq. 2)}$$

where D is the wear scar diameter produced in tests performed according to ASTM D 5001.(19)

Results from the revised BOCLE test procedure at 10 and 100 percent relative humidity (*Procedures A* and *B*) are compared with the wear observed in full-scale pump tests in Fig. 7, using hollow and solid symbols, respectively. As in preceding tests, the distinction between good and unacceptable lubricity fluids is increased by the revised BOCLE procedure at 100 percent and good directional correlation was observed with full-scale equipment, if Fuel G is excluded.

Clearly, however, the likely range of test repeatability (95 percent confidence from Fig. 6) forms a significant portion of the discrimination between good and unacceptable fuels, while the effects of interlaboratory reproducibility will be greater yet. The correlation is likely to be partially degraded by the accuracy of the pump tests, the repeatability of which has not been defined. These pump tests were performed at three locations with differing equipment, operating conditions, and rating procedures, with no attempt being made to control fuel moisture content.

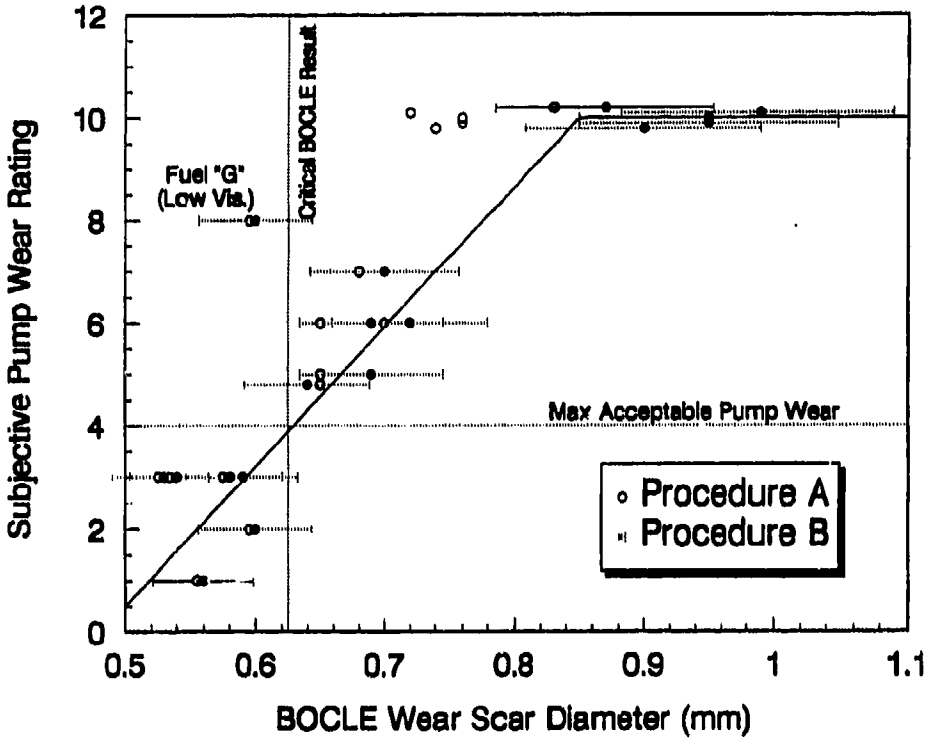

(Error bars show 95 percent confidence interval for *Procedure A* or *B* BOCLE tests as discussed in Fig. 6.)

Figure 7. Relationship between subjective measure of full-scale pump wear and results obtained using *Procedures A* and *B* with the same fuels

The unexpectedly severe pump wear with Fuel G may be partially due to its relatively low viscosity when compared with the remaining better lubricity fuels, as defined in TABLE 2 (the BOCLE result is largely independent of viscosity). Many of the pump tests were performed by the manufacturers*, who indicate that a rating in excess of 4 represents unacceptable wear. Only low-lubricity fuels are sensitive to moisture, with the result that the transition from mild to severe pump wear still occurs at approximately 0.62 mm for both the revised and standard BOCLE procedure, corresponding to the requirements of MIL-I-25017 (23) and the onset of oxidative corrosion.

* Some pump wear-test data provided through ISO/TC22/SC7/WG6 courtesy of Stanadyne Automotive, Inc., and Robert Bosch GMBH. It should be noted that many of the fluids are experimental in nature and in no way reflect the durability expected with this equipment under field conditions.

Previously, it was noted that low-lubricity fuels that produce a BOCLE result above 0.65 mm have been successfully used in arctic conditions, with no apparent effect on durability. Full-scale pump tests over a range of temperatures higher than those found in the arctic [32° to 90°C (90° to 194°F)] failed to show any correlation with temperature, as detailed in Appendix B. However, the nonstandard low-temperature BOCLE test described in Appendix G showed a decrease in wear (-7° to 50°C), probably due to reduced solubility of water in the fuel, combined with increased viscosity.

VI. DEVELOPMENT OF A SCUFFING LOAD WEAR TEST

A. Need for a Scuffing Load Test

The preceding section indicated that severe wear is produced by an oxidative mechanism with highly refined fuels devoid of naturally occurring corrosion inhibitors. However, the ASTM standard test (*Procedure A*) provides relatively narrow separation between fuels of good and unacceptable lubricity, and a revised procedure, also based around oxidative corrosion (*Procedure B*), produced only marginally improved discrimination. In addition, certain aspects of fuel lubricity were not reflected by the lightly loaded contact conditions of either *Procedure A* or *B*. Preceding studies using wear maps indicate that adhesive wear and scuffing under severe contact conditions are not directly related to oxidative corrosion at low loads, as shown in Fig. 8. Composition changes commonly produced proportionately greater variation in the applied load required for the onset of scuffing than wear under conditions of continuous boundary lubrication.

As a result, direct correlation between a reproducible wear mechanism transition and full-scale equipment may greatly reduce the measurement errors and uncertainty associated with the ASTM standard BOCLE (*Procedure A*). Preceding studies have indicated that the Cameron-Plint test apparatus provides a very distinct transition from mild oxidative corrosion to adhesive scuffing.(8) However, the BOCLE apparatus is more suitable due to its widespread availability and previous application in aviation.(4, 22-25) Moreover, the preceding section indicates that the BOCLE at least partially reflects oxidative corrosion in fuel injection systems from ground

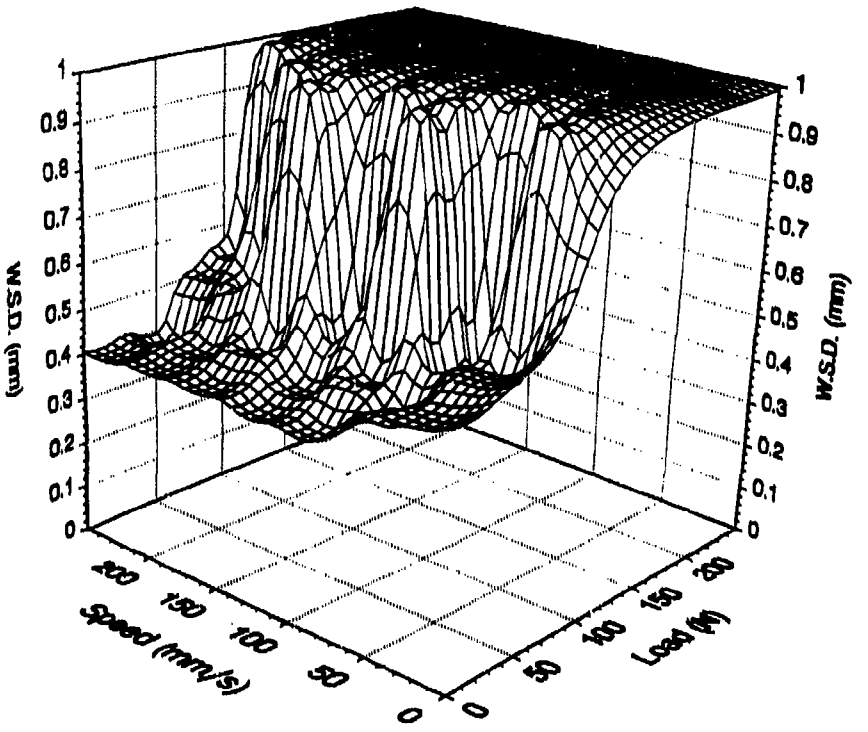

a. Poor Lubricity Fuel (Fuel A)

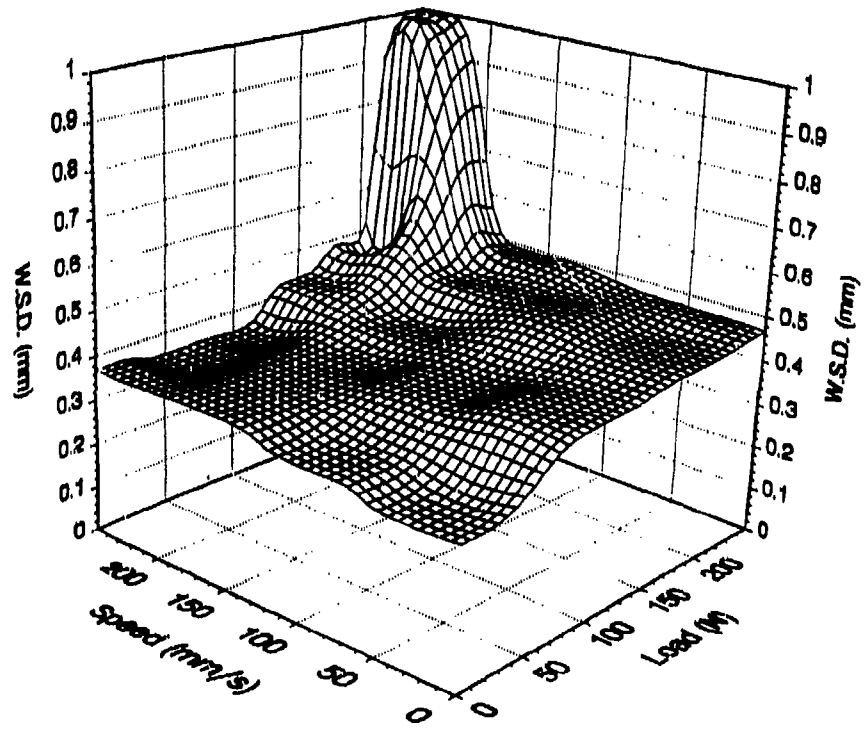

b. Good Lubricity Fuel (Fuel F)

Figure 8. Wear maps plotted as a function of sliding speed and applied load

vehicles. A scuffing load procedure developed around this apparatus would simplify the equipment requirements for complete description of fuel lubricity.

Many scuffing failure criteria are derived from Blok's hypothesis wherein a system will scuff if the total contact temperature exceeds a certain critical level.(26) As a result, the scuffing onset conditions for a given contact junction will depend on surface finish, applied load, sliding speed, and the lubricity of the fluid. Moreover, composition changes commonly produce proportionately greater variation in the applied load required for the onset of scuffing compared to corresponding changes in wear scar diameter under conditions of boundary lubrication, as shown in Fig. 8 at the test conditions defined in *Procedure E*. (Note: The true wear volume is proportional to the more commonly reported wear scar diameter to the fourth power and is more closely related to scuffing load capacity.)

B. Development of a Scuffing Test Using the BOCLE

Hadley and Blackhurst (4) developed a modified procedure to ensure that the BOCLE operated in the scuffing mode, summarized in Appendix A as *Procedure C*. In this procedure, a series of 1-minute tests is performed, each with a finite load increment and new test specimens. At a critical load, failure of the weak boundary layers formed by the fuel will occur as indicated by an increase in wear scar diameter at that point. The procedure requires that the tests be run (and preconditioned) with nitrogen to reduce the strength of the oxide film and promote adhesive welding between the substrate materials. Hadley and Blackhurst (4) used Auger Electron Spectroscopy to define the predominant wear mechanisms. In the present study, the results obtained using a specially prepared friction force measurement arm were found to be in general agreement with the results obtained using Auger at considerably reduced cost.

Test results obtained using *Procedure C* are provided in Appendix H, for selected fuels from TABLE 2. In most instances, the friction coefficient provided a more precise measure of scuffing onset than wear scar diameter. The average friction force during boundary lubrication prior to scuffing was typically between 0.12 and 0.24, while the friction coefficient during scuffing increased to between 0.25 and 0.35. As a result, the critical load required for the onset

of scuffing with the BOCLE may be best derived from consideration of both friction and wear. Qualitative comparison between different fuels is possible using *Procedure C*, particularly if multiple tests are performed at each load. However, in most instances, only a gradual transition to scuffing is evident from consideration of the wear scar. Moreover, the test repeatability was comparable to the variation between good and bad fuels and provided little benefit compared to *Procedures A* and *B*.

The instantaneous friction force measured during *Procedure C* BOCLE scuffing tests at various loads with Fuel F are plotted in Fig. 9. The variation in friction coefficient observed between boundary lubrication and scuffing is relatively small. Moreover, a distinct transition from effective boundary lubrication to adhesive scuffing does not occur at any single load, even within a short 60-second test. Rather, intermediate loads produce initial scuffing, followed by recovery and the onset of effective boundary lubricated wear with reduced friction. This change in wear mechanism is probably due to decreasing contact pressure as the counterformal contact area increases.

The contact conditions during tests performed according to *Procedure C* at an applied load of 450 g with Fuels A, B, and F are plotted in Fig. 10, as a function of test duration. (Note: The applied load is half the specimen contact load due to the geometry of the BOCLE test apparatus.) The wear scar diameter produced after only 10 seconds of testing is approximately 0.29 mm for each fuel, with a mean contact pressure of 150 N/mm^2. By comparison, the Hertzian diameter for the unworn counterformal contact is only 0.15 mm, with a mean contact pressure of 578 N/mm^2, as described in Appendix I. Adhesive scuffing is unlikely to be the primary wear mechanism, as continuous low friction was observed under these conditions for Fuel F, as shown in Fig. 9. In addition, each fuel produced similar wear, although the scuffing resistance of Fuel F is significantly greater than Fuels A and B.

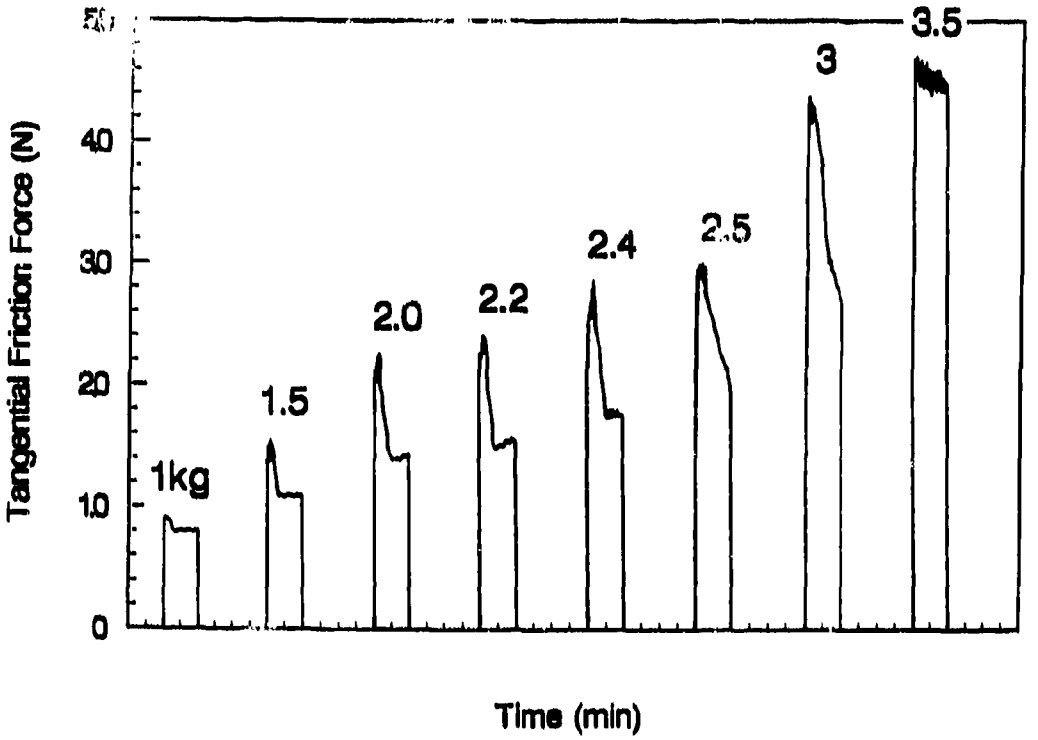

Figure 9. Friction traces obtained during scuffing load tests

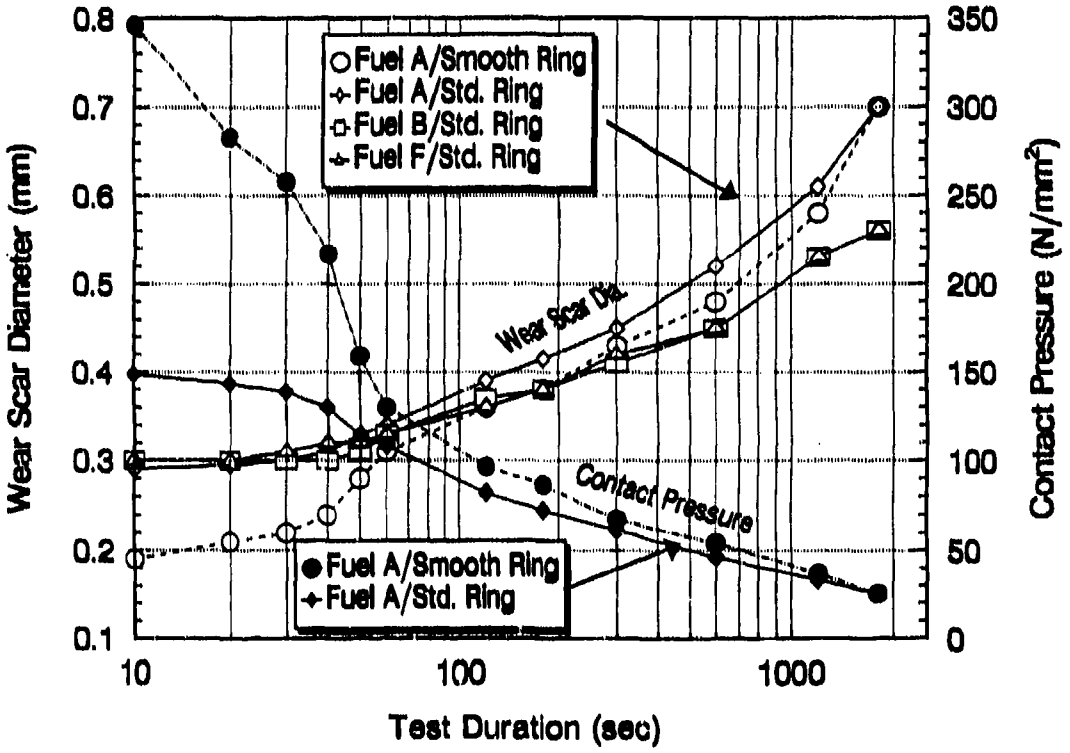

Figure 10. Variation in BOCLE wear scar diameter as a function of time during tests performed according to *Procedure A* with test rings of different surface finish

The unexpectedly high friction and wear in the absence of severe scuffing is due to the circumferential surface texture on the ASTM standard test ring (19), which promotes a number of unwanted effects, including: abrasion, rapid removal of the surface oxide layers, and distortion of the Hertzian contact. The resulting combined wear mechanism is likely to decrease the severity of the transition observed. Initial wear rate was greatly reduced by polishing the ring specimen to a mirror finish, depicted by circular characters in Fig. 10. Indeed, the diameter of the wear scar produced by the polished ring after 10 seconds of testing is only marginally greater than predicted from elastic deformation of the surfaces. Wear rate increases after approximately 40 seconds, and little variation exists between the results of the polished and standard rings after an extended test period. This minimal variation is probably due to the formation of an irregular surface texture on the polished ring opposed by removal of the texture from the standard specimen.

ASTM standard specimens were sequentially polished, resulting in "two process" surfaces that consist of the original profile, with the higher peaks removed. As a result, the surface deformation necessary to achieve a given bearing area is reduced, as shown in Fig. 11. The results are plotted using a probabilistic X axis, such that a Gaussian (normal) cumulative distribution function maps to a straight line. The original ground surface approximates a true random distribution, while the surfaces of intermediate roughness (0.59 and 0.25 μm) retain their original characteristics only at high bearing areas (high loads). The final specimen (0.015 μm) has a mirror finish and retains none of the original surface characteristics. A more detailed description of the surfaces and their manufacture may be obtained in Appendix J.

The results of scuffing load tests (in air) with ISOPAR M (Fuel M), ISOPAR M + 60 mg/L DCI-4A corrosion-inhibitor additive, and Fuel F are plotted in Fig. 12 as a function of the Root Mean Square (Rq) surface roughness of the test ring. A dramatic increase in the apparent scuffing load capacity of the better fuels was observed for surface finishes better than approximately 0.18 μm. Comparatively little change was observed for the poor lubricity fuels, resulting in greatly improved discrimination. In addition, the transition from boundary lubrication to adhesive scuffing with each fuel was more distinct for the smoother surfaces.

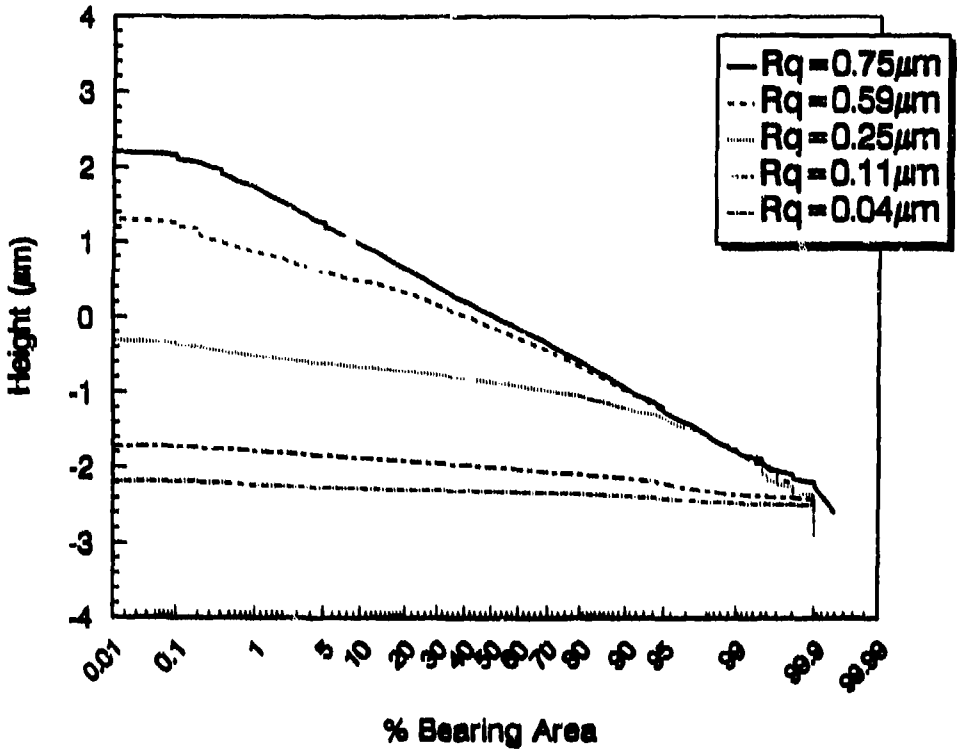

Figure 11. Bearing area curves for ring specimens used in scuffing load tests, plotted using a probabilistic X axis

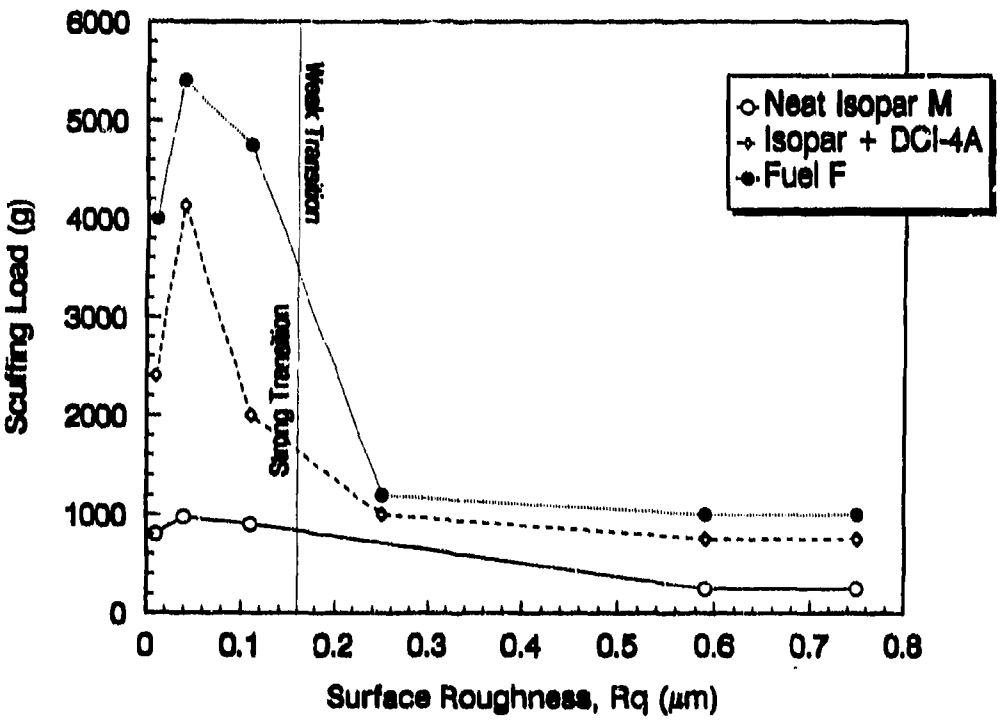

Figure 12. Effect of surface roughness on the applied load required for the onset of scuffing

Clearly, specimens with a surface roughness of 0.04 μm provide the optimum test format as load-carrying capacity with the more lubricious fuels decreases for very highly polished specimens. A polishing technique was developed to produce specimens with this surface finish using various grades of diamond paste. However, test **specimen** manufacture and repeatability are optimized for the most highly polished specimen, which has no additional roughness requirements. The ring specimens used in the remainder of this study have a surface finish of 0.04 μm unless stated otherwise. However, similar but more accurate results were obtained using the highly polished specimens (0.18 μm) with a 30-second break-in period at an applied load of 500 g at a test humidity of 50 percent. This initial break-in period produced the correct surface finish on the test cylinder without appreciable material removal from the ball specimen. Future studies will use the break-in period. The increased humidity minimizes the effect of accidental atmospheric contamination and also provides distinctly increased additive response.

Preliminary tests indicated that scuffing could not be induced on the more highly polished ring specimens (<0.04 μm) with better lubricity fuels in the load range available (<6 kg applied load or <12 kg contact load), at the ASTM standard test speed of 240 rpm. However, severe scuffing was produced at 525 rpm with each fuel in TABLE 2. The resulting methodology is summarized as *Procedure D* in Appendix A, while a detailed description of the test methodology may be obtained in Appendix K. The preliminary tests also confirm the importance of meticulous cleaning of the specimens prior to testing.

C. Test Results

The friction and wear results from scuffing load tests with a ring specimen roughness of 0.04 μm, performed according to *Procedure D* (without a break-in period) may be obtained in Appendix H. In each instance, the transition from mild to severe friction and wear is more apparent than previously observed in *Procedure C*, while the variation in applied load required to produce scuffing for the best and worst fuels was also significantly increased. Nonetheless, directional correlation was achieved between *Procedures C* and *D*, as shown in a subsequent section. Microscopic examination of the ball specimen prior to transition confirms that plastic deformation due to adhesion and abrasion is reduced by the polished ring. As a result, the

pretransition friction coefficient produced by the smooth specimen topography never exceeds 0.12. In contrast, the tangential force and surface damage produced during adhesive scuffing is similar to that observed with the textured specimen. Indeed, in many instances, the level of scuffing forced premature test termination, artificially reducing the wear scar produced.

At applied loads close to the transition point, only a brief period of high friction was observed during a number of tests, particularly with low-lubricity fluids. Typically, an initial period of low friction was observed, followed by a sharp friction spike. Previous studies of scuffing failure have noticed a similar effect.(27) The delayed transition is probably due to the gradual formation of an irregular wear scar on the polished ring specimen (Fig. 10) (28), increasing specimen temperature (29), or possibly near-surface transformation of the contact metallurgy.(30) In each instance, the tabulated friction coefficient was the absolute maximum achieved during the test. Scuffing was considered to have occurred if the maximum friction coefficient exceeded 0.175. Continuous scuffing was observed at marginally higher loads, although even transient scuffing produced a significant increase in scar size.

In general, the scuffing load capacity of the fuel is a function of composition, as shown in Fig. 13. The results obtained for each fuel using *Procedure B* are also plotted to allow comparison. No perfect correlation exists between the test procedures for oxidative corrosion (*Procedures A* or *B*) and adhesive scuffing (*Procedures C* or *D*), as previously noted in Reference 8. Nonetheless, the results of both techniques are directionally similar and seldom contradictory. Both oxidative corrosion and scuffing load tests are sensitive to the effects of artificial lubricity additives in ISOPAR M, as shown in Fig. 14. The scuffing load test (*Procedure D*) demonstrates a proportionately greater change than the ASTM standard BOCLE result, with a very distinct increase in scuffing load capacity for additive concentrations above 25 mg/L. The scuffing load test remains sensitive to additive concentration until approximately 50 mg/kg. The ASTM standard BOCLE test highlights the effects of oxidative corrosion and is sensitive to lower concentrations of the dilinoleic acid-based corrosion-inhibitor additive. It may be assumed that low additive concentrations prevent formation of a surface oxide layer without providing a more durable boundary film.

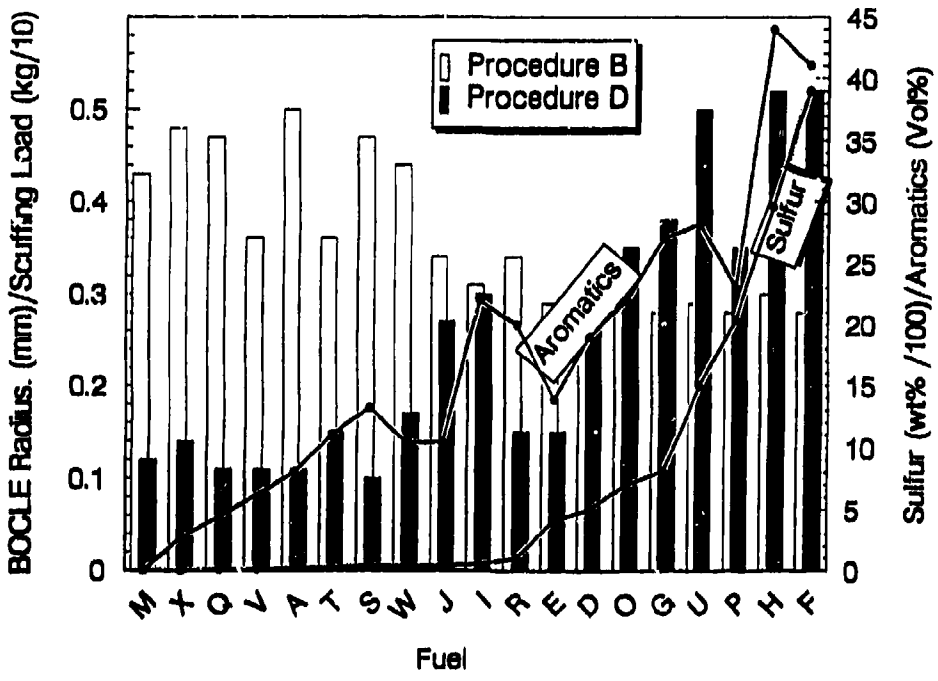

(Test results obtained using *Procedure B* are also plotted for comparison.)

Figure 13. Effect of refinery severity on scuffing load capacity measured using *Procedure D* with fuels from TABLE 2

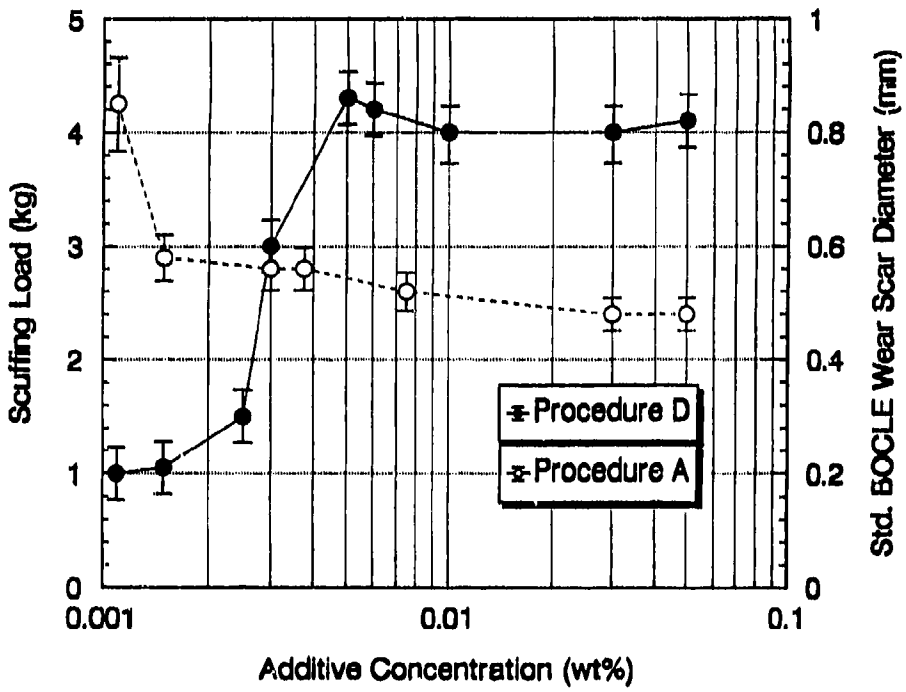

(Error bars define 95 percent confidence interval for *Procedures A* and *D* as described in ASTM D 5001 and TABLE 3, respectively.)

Figure 14. Sensitivity of *Procedures A* and *D* to additive concentration in ISOPAR M

TABLE 3. Test Repeatability of *Procedure D* With Additized ISOPAR M

Add Conc., mg/L	Scuffing Load, g					Mean	Std Dev	Coefficient of Var
Iteration	1	2	3	4	5			
LABORATORY A								
Batch A								
0	1000	1000	900	1000	--*	975	50	5.1
30	2700	3000	3100	--	--	2933	208	7.1
60	4300	4000	4100	--	--	4133	152	3.7
Batch B								
0	900	900	800	800	700	820	84	10.2
30	2000	2100	1900	2100	2100	2040	89	4.4
60	3900	4100	4200	4000	4000	4040	114	2.8
LABORATORY B								
Batch B								
0	900	800	1100	--	--	933	152	16.2
60	3700	3800	3800	--	--	3766	57.7	1.5
LABORATORY C								
Batch B								
0	800	800	1000	--	--	866	115	13.2
60	3800	4000	3700	--	--	3833	152	3.9

*-- Indicates test not repeated here.

Note: Batch B was clay treated immediately prior to inclusion of additive. Direct comparison may not be made between Batch A and Batch B. The test-ring specimens had a surface finish of 0.04 µm. Test humidity = 10 percent.

Both neat and additized ISOPAR M containing 30 mg/kg of corrosion-inhibitor additive are specified as reference fluids in ASTM D 5001. The results of repeat tests performed according to *Procedure D* at additive concentrations 0, 30, and 60 mg/kg are provided in TABLE 3. Two batches of ISOPAR M were used (the data in Fig. 14 applies to Batch A), and a distinct variation between the fluids is apparent, particularly at an additive concentration of 30 mg/L (statistical probability >95 percent). Both samples produced a wear scar in excess of 0.8 mm in tests performed according to ASTM D 5001. However, Batch B was clay treated immediately prior to use, as its lubricity was superior to that of Batch A in the as-received condition, while Batch B

had been clay treated approximately 20 months prior to use, possibly removing oxidation inhibitor additives. The variation in the ASTM standard BOCLE result obtained with Batch A over the intervening 20-month period is shown in Appendix F (Fig. F-3). Both *Procedures A* and *D* appear affected by the age of the reference fluid.

The standard deviation of the test results obtained using *Procedure D* is 115 g and provides the basis for the error bars in Fig. 14 (95 percent confidence). Bartlett's test shows no statistically significant variation in the standard deviation of the test results across the load range examined, and the coefficient of variation ranges from 2 to 10 percent. By comparison, the ASTM standard BOCLE results (*Procedure A*) produced by most real fuels (unlike ISOPAR M) are within the range of 0.55 to 0.72 mm, with a corresponding standard deviation range of 0.019 to 0.032 mm, as defined in Equation 1. The coefficient of variation ranges from approximately 4 to 5 percent, which is comparable to that observed in *Procedure D*. Clearly, however, the effects of test variability will be less significant in *Procedure D* than *Procedure A*, as the ratio between the standard deviation and typical span of the results observed is reduced from approximately 15 to 3 percent.

D. Correlation of *Procedure D* With Full-Scale Pump Results

The results of scuffing load wear tests performed according to *Procedure D* are compared with wear produced by the same fuels in full-scale pump tests in Fig. 15. Fig. 15a shows the results obtained in tests performed with a 30-second break-in period at 50 percent humidity. Fig. 15b was obtained using specimens that have a slight surface texture and a surface finish of 0.04 μm but without a break-in period at 10 percent humidity. Similar results were obtained in both procedures, and good directional correlation was observed in each instance. [Note: Good correlation was obtained with Fuel G at high humidity.] Moreover, the correlation is likely to be partially degraded by the accuracy of the pump tests, which were performed at three locations with differing equipment, operating conditions, and rating procedures with no control of fuel moisture content. Clearly, the slightly textured specimen provides increased discrimination, although it is believed that test variability is correspondingly increased. Very low lubricity fuels

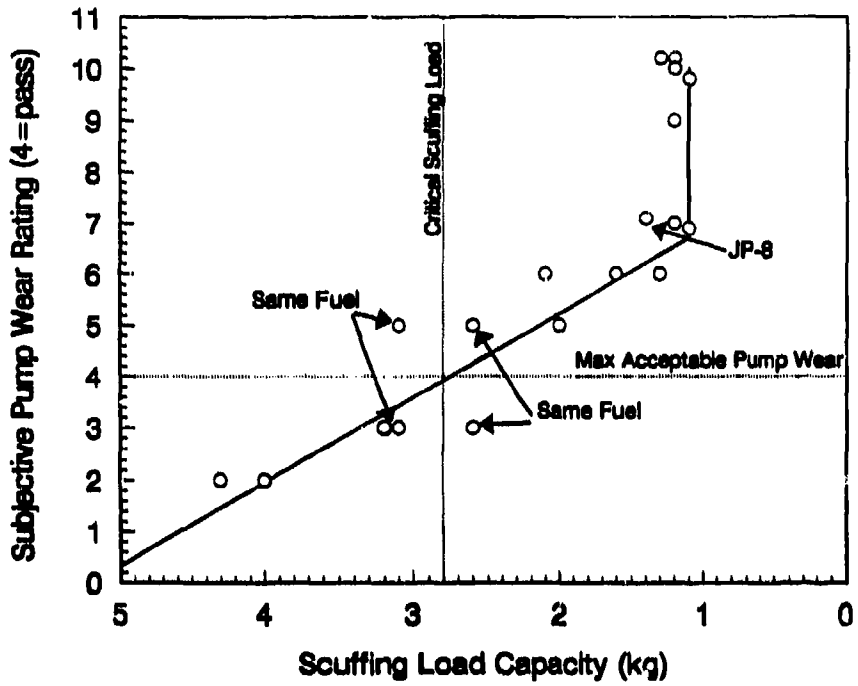

a. Surface Roughness of Test Ring = 0.015 μm (30-second break-in period at 500-gram load, 50 percent humidity)

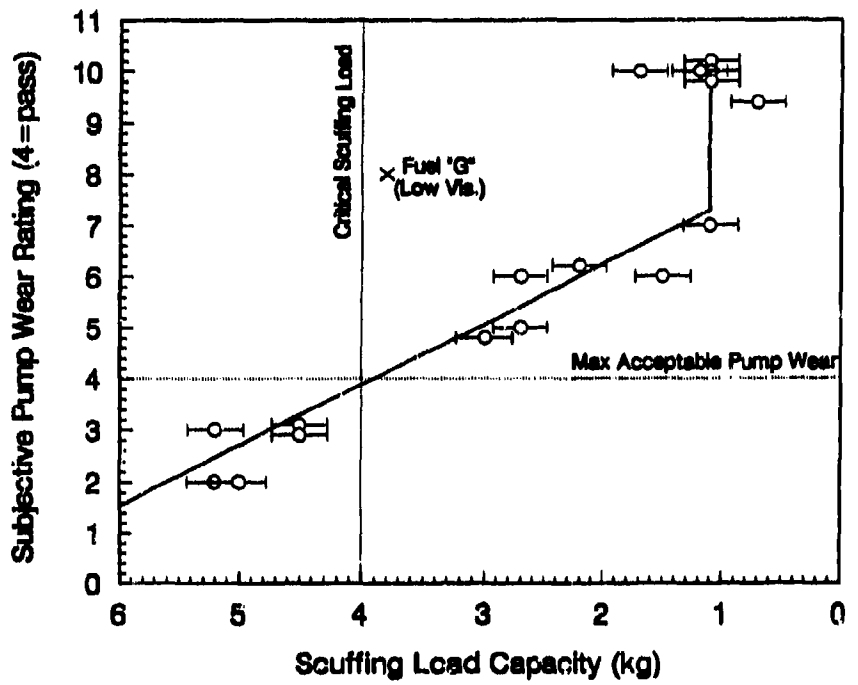

b. Surface Roughness of Test Ring = 0.04 μm (no break-in period, 10 percent humidity)

(Error bars in Fig. 8 define 95 percent confidence interval as defined in TABLE 3.)

Figure 15. Relationship between subjective measure of full-scale pump wear and results obtained using *Procedure D* with the same fuels

typically caused severe pump wear and catastrophic pump failure, denoted by a subjective pump rating of 10. These sudden failures produce a discontinuity at a scuffing load capacity of approximately 1.2 kg. Both the laboratory and full-scale equipment tests predict relatively severe wear with JP-8. The equipment manufacturers indicate that this level of wear protection would not be acceptable in commercial equipment.

Many of the equipment tests were performed by the original manufacturers. Those tests indicate that a subjective rating in excess of 4 corresponds to unacceptable field wear. Clearly, a scuffing load capacity in excess of 4 kg for the slightly textured specimens (or 2.8 kg with the 30-second break-in) indicates that a given fuel is likely to produce acceptable wear in full-scale equipment (subjective rating <4). The results of laboratory wear tests performed at an applied load of 2.8 kg with highly polished specimens of 0.015 μm roughness (*Procedure E*) are shown in Fig. 16 for tests performed with a 30-second break-in. Clearly, a significant difference is present between the pass and fail fuels. The single 2-minute test unambiguously discriminates between good- and bad-lubricity fuels, based on the needs of full-scale equipment. Many tests with low-lubricity fuels had to be terminated prematurely due to excessive friction and severe scuffing, resulting in artificially low friction and wear measurements. The BOCLE apparatus is presently being modified to allow completion of these tests.

E. Comparison and Correlation Between Scuffing Load Tests

Three distinct techniques to define the scuffing wear resistance of fuels have been evaluated, two of which use the BOCLE (*Procedures C* and *D*) and one uses the Cameron-Plint test apparatus (*Procedure F*). *Procedure C* was previously shown to produce good correlation with the well-established Thornton Aviation Fuel Lubricity Evaluator (4) and so was used as the baseline in the present comparison. *Procedure E* is derived from *Procedure D* and was not considered in the present analysis. The test methodology used for the Cameron-Plint tests corresponds to that of the wear maps, with the raw data shown in Appendix H.

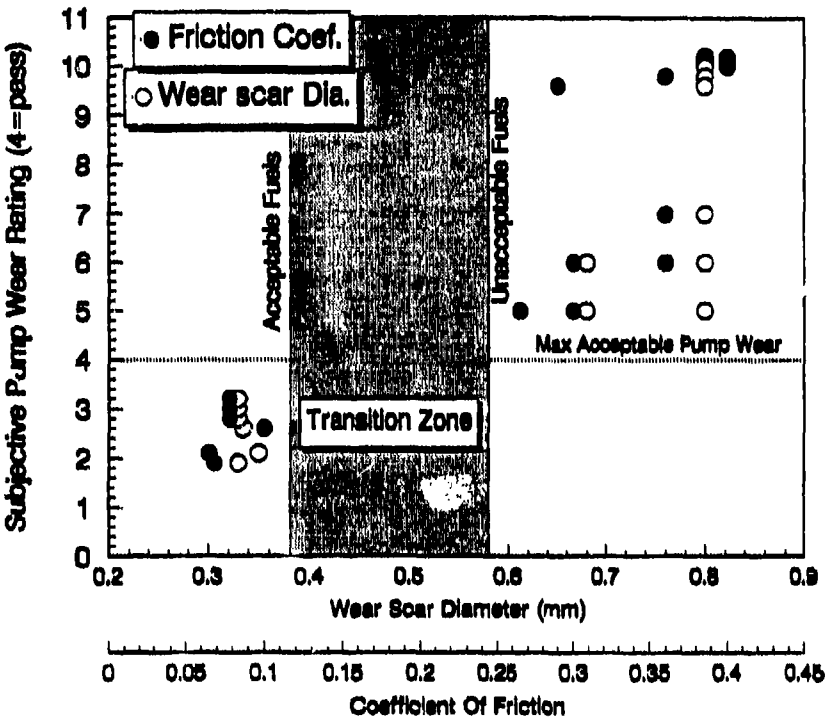

(Specimen Ring Roughness = 0.015 μm, 30-second break-in at applied load of 500 g, 50 percent humidity)

Figure 16. Relationship between subjective measure of full-scale pump wear and results obtained using *Procedure E* with the same fuels

Good directional correlation was achieved between *Procedures C* and *D*, as shown in Fig. 17a. The applied load required to produce scuffing in *Procedures D* and *E* is several times that required in *Procedure C*, despite the fact that the sliding speed is increased from 240 to 525 rpm. Clearly, the differentiation among fuels provided by the polished ring is an order of magnitude better than the standard specimen, resulting in greatly improved utility. Similarly, the transition to severe wear and scuffing using the Cameron-Plint test apparatus is more severe than that previously observed with either BOCLE test, as shown in Fig. 17b. The applied load required to produce scuffing in the Cameron-Plint test apparatus is approximately 10 times greater than for *Procedure C*. This dramatic difference in required loading is due to the polished surface topography of the Cameron-Plint specimens, combined with its relatively low average sliding speed. (*Procedure A* = 0.616 m/s; *Procedure D* = 1.53 m/s; *Procedure F* = 0.238 m/s).

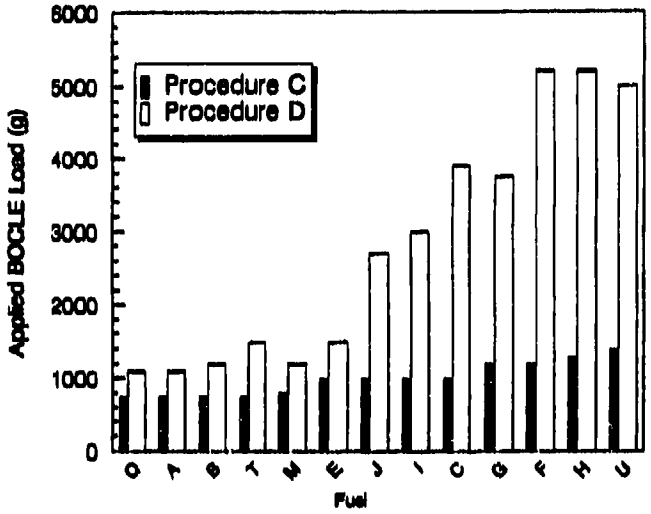

a. Procedure C Versus Procedure D

b. Procedure C Versus Procedure F

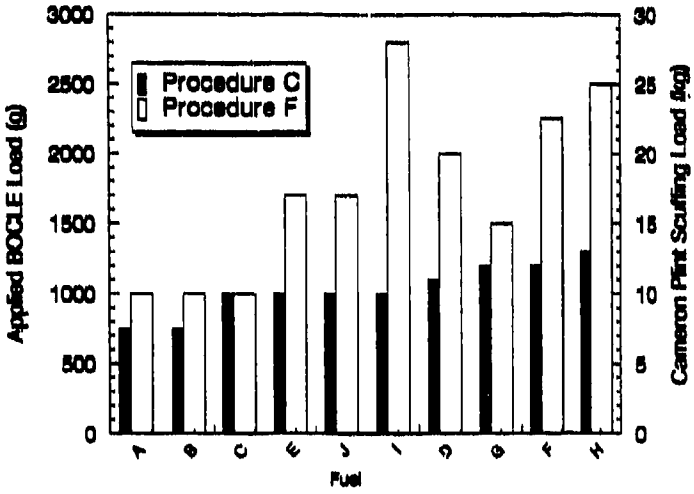

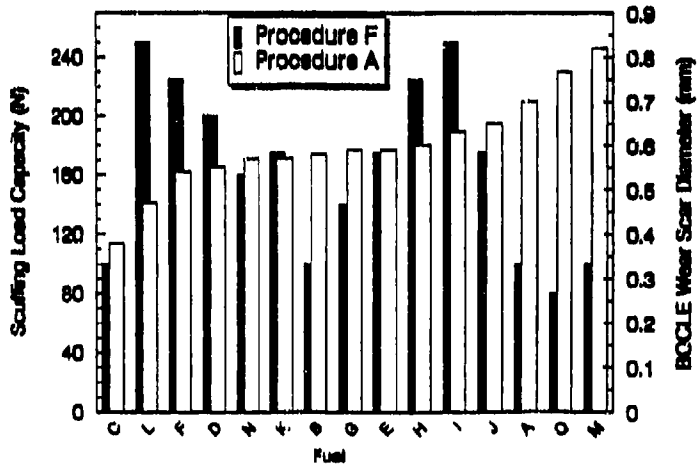

c. Procedure F Versus Procedure A

Figure 17. Comparison of scuffing load test results with fuels detailed in TABLE 2

Procedure A gives a directionally similar ranking to scuffing load capacity, as measured by both *Procedures D* and *F* shown in Figs. 11 and 17c, respectively. However, the correlation is not perfect, and Fuels I and J provide unexpectedly good scuffing load characteristics when compared to their performance during boundary lubrication, particularly in the Cameron-Plint tests. In addition, the scuffing load capacity for the Jet A-1 fuel is less sensitive to low additive concentrations (i.e., Fuel B), than the standard BOCLE test. Poor correlation between the oxidative corrosion and adhesive wear mechanisms has been suggested by previous workers.(4) Sensitivity to additive concentration was increased during BOCLE tests performed at high (50 percent) humidity, probably due to the increased importance of the oxidative corrosion mechanism.

No quantitative comparison was made between the Cameron-Plint and the BFLRF-modified BOCLE scuffing load procedure, as Fig. 17a indicates that the results of both BOCLE techniques are closely related.

VII. DISCUSSION

Fuel lubricity and wear resistance are two of the few properties that may be degraded by certain refinery processes.(22) The present study addresses the evaluation of fuel lubricity in two ways: a) full-scale equipment tests were performed to understand better the wear mechanisms present, and b) laboratory tests were developed and compared with the results obtained in the full-scale equipment tests. The premise for the wear mechanism evaluation was that oxidative corrosion may be controlled by varying moisture availability or use of corrosion-inhibitor additives. Indeed, oxidative wear appears broadly proportional to humidity, indicating that availability of moisture is the rate-limiting parameter in the surface oxidation reaction. It is recognized that the related mechanism of fretting corrosion and, to a lesser extent, adhesion and scuffing will also be slightly affected by fuel moisture content. However, it is assumed that these effects are negligible in the present context.

Oxidative corrosion was found to be the primary wear mechanism under lightly loaded conditions with the most severely refined fuels. Indeed, the wear rate produced by this mechanism was

sufficient to cause complete pump failure in less than 8 hours. Even pumps containing an improved (Arctic) metallurgy failed rapidly in damp conditions, due to severe wear of remaining nonimproved components. Wear of highly loaded components was partially reduced but not eliminated by removal of moisture, and the remaining wear may be attributable to adhesion. As a result, the severe material removal in highly loaded contacts with these fuels is not solely due to adhesive scuffing, and a combined wear mechanism is likely. The direct relationship between moisture availability and wear rationalizes the successful use of highly refined fuels such as Jet A-1 in military vehicles under arctic conditions. Laboratory wear tests in Appendix G confirmed that wear rate is reduced at low ambient temperatures.

The present work demonstrated better correlation between full-scale pumps and the BOCLE apparatus than previous studies, which did not fully consider the effects of moisture.(3,13-14) Therefore, the standard BOCLE wear test as defined in ASTM D 5001 (*Procedure A*) does reflect both wear rate and mechanism in the fuel injection system with very low lubricity fuel devoid of corrosion inhibitors. The BOCLE result of approximately 0.62 mm simultaneously reflects the onset of catastrophic surface oxidation and unacceptable pump wear and closely reflects the requirements of the U.S. Air Force in aviation equipment.(23) Marginally improved separation between good and unacceptable fluids was achieved by increasing the level of humidity in the test cell (*Procedure B*), with no apparent decrease in repeatability. However, the principal difficulty with both oxidative corrosion wear tests is poor differentiation between good and unacceptable fluids.

Improved results were obtained by measuring the applied load required for transition from boundary lubricated wear to adhesive scuffing and a detailed test procedure was developed based around ASTM D 5001. A polished test ring replaces the standard textured specimen to minimize the asperity tip stresses, resulting in mild wear at all loads prior to scuffing and severe material removal and surface deformation during scuffing. The scuffing load tests may be used to provide either a continuous quantitative comparison (*Procedure D*) or a simple pass/fail criteria (*Procedure E*) and provide greatly increased separation between good and poor lubricity fuels with no apparent increase in test error.

Production of an accurate surface finish on the ring specimen is critical to the accuracy of the scuffing-load wear test procedures. In general, the surface may not be completely defined using a profilometer, due to the very smooth finish and the significant effect of small variations in roughness. The load-carrying capacity of the contact is found to decrease significantly if the surfaces are excessively smooth. This anomalous effect is probably due to a rapid increase in the real area of contact within the apparent or geometric contact area, as elastic deformation accommodates the small surface irregularities. Lubricant flow into the contact may then be decreased due to the lack of a convenient flow path. Hirst and Hollandar (31) also indicate that in these conditions the surface damage more easily builds up to serious proportions because there are no longer any interruptions to prevent the growth of small welded junctions. The results of the present study indicate that a slight surface texture (visible as a haze) provides optimum discrimination; however, the perfectly polished surface may be more accurately reproduced, and correspondingly superior test repeatability is obtained when a 30-second break-in period is used.

The scuffing load test produced better correlation with the oxidative corrosion mechanism of the ASTM standard BOCLE procedure (*Procedure A*) than would have been predicted by the wear maps. Both tests are sensitive to the effects of boundary-lubricant additives and produced qualitative correlation with refinery severity, as defined by sulfur and aromatic content. The scuffing load test magnifies the effect of the additives, but requires higher additive concentration and strength when compared to the ASTM standard BOCLE procedure. However, the ASTM standard BOCLE test is designed to highlight the effects of oxidative corrosion and is therefore sensitive to lower concentrations of the dilinoleic acid-based corrosion inhibitor additive. It may be assumed that low additive concentrations prevent formation of a surface oxide layer without providing a more durable boundary film. Preceding studies performed with the TAFLE (32) also indicate that the onset of adhesive scuffing and seizure is relatively insensitive to low concentrations of corrosion inhibitor additives. Increased additive sensitivity is provided by the scuffing load wear test at high humidity, probably due to increased importance of surface oxidation.

Similarly, full-scale pump tests with JP-8 fuel show unacceptably severe wear (this fuel corresponds to Jet A-1 aviation turbine fuel with a low concentration of corrosion inhibitor

additive). By definition, JP-8 produces a small (<0.65 mm) wear scar in the ASTM standard BOCLE test (*Procedure A*). This result indicates that scuffing-load capacity and adhesive wear resistance is more closely related to the wear process in full-scale equipment than tests for oxidative corrosion. Each of the BOCLE tests examined was highly sensitive to fuel contamination. The importance of the remaining contact parameters such as humidity and temperature on *Procedures D* and *E* is yet to be defined. Preceding results using the ASTM standard test ring would indicate that these contact parameters may also have a significant effect.(12) A number of tests have been performed using an AISI E-52100 steel ring in place of the ASTM standard specimen (SAE 8720) to reduce compatibility (increase mutual solubility) with the opposing test ball. However, this variation had little apparent effect on the severity of the transition obtained, possibly due to the relatively high indentation hardness of the specimens.(2) Full-scale equipment appeared less sensitive than the laboratory tests and were largely unaffected by initial running-in with a good lubricity fuel prior to operation on Jet A-1.

In general, good correlation was achieved between the laboratory wear tests and full-scale equipment. However, the BOCLE tests are largely independent of viscosity, while many pump manufacturers specify a minimum viscosity of approximately 1.8 cSt at pump operating temperature. As a result, low-viscosity fuels that provide acceptable boundary protection in the laboratory tests may still produce severe pump wear. The effects of viscosity are less apparent for fuels that have low inherent lubricity and produce severe wear irrespective of physical characteristics. The results of the present study indicate that a scuffing load capacity below 3 kg (as defined using *Procedure D* or *E*) will produce unacceptable equipment wear. However, this value is unlikely to be absolute and will vary as a function of fuel viscosity, equipment operating temperature, and individual equipment requirements.

A model defining the effects of hydrodynamic/elastohydrodynamic lubrication on minimum acceptable chemical lubricity is needed. Sulfur and aromatic content are partially related to kinematic viscosity, as shown in Appendix F, particularly for straight-run distillate fuels (processes such as solvent extraction, clay treatment, or catalytic hydrogenation are capable of producing clean fuels with high viscosity). In addition, both fuel composition and kinematic viscosity (υ) are related to density (32), although kinematic viscosity may be converted to the

more fundamental dynamic viscosity (η) using Equation 3. Clearly, thick-film and boundary lubrication are separate mechanisms that are partially interrelated in some instances.

$$\upsilon = \frac{\eta}{\rho} \qquad \text{(Eq. 3)}$$

The volumes of aromatics, olefins, and sulfur were found to be loosely interrelated and together appear to form a broad measure of the severity of the refining process. Oxidative corrosion increased dramatically for severely refined fuels with a sulfur content below approximately 0.025 mass%. However, no universal relationship was found between *Procedures A* or *B* (which measure oxidative corrosion) and fuel composition; indeed, these tests are independent of composition for less highly refined fuels. Trace amounts of a reactive compound greatly affect the oxidative corrosion mechanism, and small changes in refinery parameters such as endpoint produced a significant change in lubricity. In contrast, *Procedures C* and *D* remain sensitive to aromatic, sulfur, and artificial additive content for the range of fuels evaluated. Boundary film strength and resistance to adhesive scuffing in the absence of a surface oxide layer appears sensitive to the concentration of reactive species present in fuels. Aviation research in the late 1960s also indicated that fuel lubricity is dependent on the presence of polar compounds, most probably high molecular weight aromatics.(32) The composition of these better lubricity fuels is highly complex and is not easily represented by any simple collection of parameters. In contrast, it may eventually be possible to predict the expected boundary lubricating performance of severely refined fuels, as the majority of reactive compounds have been removed.(34) The results support Hadley's conclusion (4) that the relative performances of the fuel in both the mild and scuffing regime are dependant on different aspects of fuel composition.

The effects of low-lubricity fuels have been observed by isolated commercial users in the United States and also in Sweden. Light-duty vehicles operating on Jet A-1 that meets ASTM D 975 have experienced poor startability in warm ambient conditions in Phoenix, AZ.(35) This effect is in good agreement with the results of the present study. although it is unclear if this poor performance is due to low viscosity and internal pump leakage or increased pump wear.(36) In conclusion, the results of the present study indicate that JP-8 provides only marginal boundary film protection in rotary fuel injection systems, while Jet A-1 is acceptable only under cold

ambient conditions. In addition, replacing DF-2 with JP-8 or Jet A-1 will reduce maximum engine power/startability and will produce an additional undefined decrease in rotary fuel injection system durability, due to reduced viscosity and poor adhesive wear resistance. The decrease in durability will depend on a number of factors, including fuel viscosity, composition, and temperature.

Neat Class 1 low-sulfur fuel, currently on sale in Scandinavia (Fuel Q in TABLE 2) has similar lubricity to Jet A-1, as measured using the laboratory tests described in the present study. Durability problems associated with the Scandinavian fuel appear to have been eliminated through the use of additives, partially validating the results of the present work. By comparison, most tests performed with U.S. low-sulfur/low-aromatics fuel indicate intermediate lubricity, with occasional instances of poor lubricity. Many commercial additives are available that significantly improve lubricity; however, their effectiveness appears to be fuel composition-sensitive.

The test procedures for oxidative corrosion and scuffing described in this paper reflect the principal wear mechanisms for lower lubricity fuels, defined by the wear mechanism maps. It is likely that other individual mechanisms and combinations also exist in full-scale equipment. These mechanisms may include corrosive fretting, abrasion by hard metallic oxides, fatigue, and sulfur corrosion.(33) The present approach attempted to isolate the predominant mechanisms and model each individually. Overall, the BOCLE apparatus is an effective tool; however, a number of effects combine to decrease the repeatability obtained. In particular, the calibration of the humidity (below saturation) and speed controls requires regular adjustment, while temperature control, although critical to accuracy, is not automated. More subtle effects such as accidental fuel contamination, or even the gradual formation of oxygenated species during storage, greatly affect lubricity and apparent test repeatability, particularly with highly refined fuels. Previous workers have also emphasized the importance of these effects.(22) However, such variation is indicative of an accurate test configuration that is highly sensitive to small changes in fuel composition. Clearly, no single test will fully represent each of the permutations possible. However, it is hoped that the wear test procedures suggested in the present work may be used to represent the most critical contacts in full-scale equipment.

VIII. CONCLUSIONS

As a result of this study, the following conclusions are made:

1. Wear test procedures based around the transition from mild oxidative wear to adhesive scuffing were developed for the BOCLE and provide greatly improved differentiation between good and unacceptable lubricity fuels.

2. The scuffing transition test provided good repeatability. Unacceptable pump wear occurs for fuels that provide a scuffing load result below 3 kg.

3. The adhesive scuffing test showed directional correlation with preceding tests, such as those developed by Hadley and the Thornton Aviation Fuel Lubricity Evaluator (TAFLE).

4. Fuel lubricity is adversely affected by refinery severity.

5. Injection system durability will be reduced by use of JP-8.

6. Relatively small changes in refinery treatment may have a significant effect on lubricity after a critical fuel composition is achieved.

7. Wear-related failures of rotary fuel injection pumps may be produced in a matter of hours with very low lubricity fuels such as neat Jet A-1 in a severe operating environment.

8. Laboratory wear tests indicate that the wear rate with Jet A-1 is reduced at low temperatures approaching the freezing point of water.

9. The ASTM standard BOCLE procedure is accurate and repeatable, but provides little separation between good and unacceptable lubricity fuels.

10. Addition of dilinoleic acid-based corrosion inhibitors to Jet A-1 (such as those used in JP-8, 15 to 22 ppm) greatly reduced oxidative wear.

11. Good directional correlation was achieved between the ASTM standard BOCLE test and the onset of very severe oxidative corrosion in the full-scale pump.

12. Corrosion inhibitors have little effect on scuffing load capacity at the very low concentration recommended in MIL-I-25017. However, a significant improvement in scuffing load capacity is observed at significantly higher concentrations (i.e., 250 ppm).

13. The ASTM standard BOCLE is largely insensitive to the lubricity of less highly refined fuels not susceptible to oxidative wear (in the absence of very strong artificial boundary lubricant additives).

14. The scuffing load test remains sensitive to the lubricity of less highly refined fuels that do not produce oxidative wear.

15. Wear with good lubricity fuels (BOCLE <0.62 mm) appears to be independent of moisture content. The wear rate associated with poor lubricity fuels that produce a BOCLE wear scar diameter greater than approximately 0.62 is highly sensitive to the availability of moisture and the associated effects of temperature on water solubility.

16. Engine power is reduced by approximately 14 percent when operated on Jet A-1 in place of a conventional DF-2. (Note: The Jet A-1 used in the present study has especially low viscosity and represents a worst-case example.)

17. The lubrication qualities of standard test fluids such as ISOPAR M is not constant and improves slightly with time.

18. Scuffing wear resistance of fuel-lubricated contacts is highly sensitive to surface roughness.

19. Load-carrying ability is significantly reduced for excessively smooth surfaces produced during initial manufacture or subsequent mild wear.

20. In general, a dramatic increase in oxidative corrosion wear occurs after a critical level of refinery severity is achieved, as defined by sulfur, aromatic, and olefin content. Other mechanisms include adhesive scuffing, three-body abrasion by oxide particles, and fretting.

21. The improved metallurgy or "arctic" kits available for some rotary fuel injection pumps fails to prevent wear in the remainder of the pump when operated with very low-lubricity fuels.

22. Initial break-in of the pumps with good lubricity fuels has little effect on the subsequent wear rate observed with low-lubricity fuels.

23. Limited experience with commercially available low-sulfur/low-aromatics fuels would indicate intermediate and occasionally poor lubricity.

24. Additive effectiveness appears to be fuel composition-sensitive.

IX. RECOMMENDATIONS

Additional work on this subject is recommended in order to answer the following questions:

1. Is acceptable long-term durability guaranteed in the absence of oxidative corrosion, particularly in highly loaded unit injection systems?

2. What is the importance of viscosity, particularly on long-term durability?

3. What is the influence of viscosity on the correlation between the laboratory wear tests and full-scale equipment?

4. Is there a relationship between minimum acceptable lubricity and viscosity/temperature?

5. What was the typical lubricity of high-sulfur diesel fuels available prior to October 1993?

6. What is the typical lubricity of the currently available low-sulfur/low-aromatics fuels?

7. Will reformulated diesel fuels available to the U.S. Army suffer from the oxidative corrosion wear mechanism seen in Scandinavia?

8. The ASTM standard BOCLE test is independent of composition for fuels containing a significant amount of nonsaturated hydrocarbons. Is pump wear also independent of composition for fuels of this type?

9. What components in the fuel are responsible for lubricity?

10. Are the same fuel components responsible for wear under conditions of both oxidative corrosion and adhesive scuffing?

11. What are the effects of fuel lubricity on more highly loaded unit injection systems?

X. LIST OF REFERENCES

1. Department of Defense Directive 4140.43, subject: "Fuel Standardization," March 1988.

2. *Wear Control Handbook*, Peterson, M.B., Winwer, W.O., ed., American Society of Mechanical Engineers, United Engineering Center, 345 East 47th Street, New York, NY 10017, 1980.

3. Lacey, P.I., "The Relationship Between Fuel Lubricity and Diesel Injection System Wear," Interim Report BFLRF No. 275 (AD A247927), prepared by Belvoir Fuels and Lubricants Research Facility, Southwest Research Institute, San Antonio, TX, January 1992.

4. Hadley, J.W. and Blackhurst, P., "An Appraisal of the Ball-on-Cylinder Technique for Measuring Aviation Turbine Fuel Lubricity," Society of Tribologists and Lubrication Engineers, Vol. 47, No. 5, pp. 404–411, 1991.

5. Catalog of Friction and Wear Devices, Second Ed., American Society of Lubrication Engineers, Park Ridge, IL, 1977.

6. Datchefski, G., "History Development and Status of the Ball-on-Cylinder Lubricity Evaluator for Aero Gas Turbine Fuels," Procurement Executive Ministry of Defence, Directorate of Engines Eng 2a, St. Giles Court, London WC2H 8LD, UK, Reference D/DEngl(PE)33/25/1, 1991.

7. Lacey, P.I., "Wear With Low-Lubricity Fuels, Part I - Development of a Wear Mapping Technique," *Wear*, 160, pp. 325–332, 1993.

8. Lacey, P.I., "Wear With Low-Lubricity Fuels, Part II - Correlation Between Wear Maps and Pump Components," *Wear*, 160, pp. 333–343, 1993.

9. Lacey, P.I., "Evaluation of Oxidative Corrosion in Diesel Fuel Lubricated Contacts," ASME Tribology Transactions, Preprint No. 93-TC-2E-1, presented at the ASME/STLE Tribology Conference in New Orleans, LA, October 24–27, 1993.

10. Lacey, P.I. and Lestz, S.J., "Failure Analysis of Fuel Injection Pumps From Generator Sets Fueled With Jet A-1," Interim Report BFLRF No. 268 (AD A234930), prepared by Belvoir Fuels and Lubricants Research Facility (SwRI), Southwest Research Institute, San Antonio, TX, January 1991.

11. Lacey, P.I. and Lestz, S.J., "Wear Analysis of Diesel Engine Fuel Injection Pumps From Military Ground Equipment Fueled With Jet A-1," Interim Report BFLRF No. 272 (AD A239022), prepared by Belvoir Fuels and Lubricants Research Facility (SwRI), Southwest Research Institute, San Antonio, TX, May 1991.

12. Lacey, P.I. and Lestz, S.J., "Fuel Lubricity Requirements for Diesel Injection Systems," Interim Report BFLRF No. 270 (AD A235972), prepared by Belvoir Fuels and Lubricants Research Facility (SwRI), Southwest Research Institute, San Antonio, TX, February 1991.

13. Lacey, P.I., "Effect of Low-Lubricity Fuels on Diesel Injection Pumps-Part I: Field Performance," SAE Technical Paper No. 920823, Society of Automotive Engineers, 400 Commonwealth Drive, Warrendale, PA 15096, February 1992.

14. Lacey, P.I., "Effect of Low-Lubricity Fuels on Diesel Injection Pumps-Part II: Laboratory Evaluation," SAE Technical Paper No. 920823, Society of Automotive Engineers, 400 Commonwealth Drive, Warrendale, PA 15096, February 1992.

15. "Aviation Turbine Fuel, Grades Jet A-1/Jet A," American Society for Testing and Materials Standard D 1655, ASTM, 1916 Race Street, Philadelphia, PA, 1989.

16. Military Specification MIL-T-83133C, "Turbine Fuels, Aviation Turbine Kerosene Types," NATO F-34 (JP-8) and NATO F-35, 22 March 1990.

17. Compilation of Fuel, Lubricant, and Engine Statistics, Department of the Army, U.S. Army Belvoir Research, Development and Engineering Center, Fort Belvoir, VA, 28 May 1992.

18. Federal Specification VV-F-800D, "Fuel Oil, Diesel," Grade DF-2, 27 October 1987.

19. American Society for Testing and Materials Method D 5001-89, "Test Method for Measurement of Lubricity of Aviation Turbine Fuels by the Ball-on-Cylinder Lubricity Evaluator (BOCLE)," ASTM, 1916 Race Street, Philadelphia, PA, 1989.

20. Archard, J.F., "Contact and Rubbing of Flat Surfaces." *J. Appl. Phys.* **24**, pp. 981–988, 1953.

21. Wei, D. and Spikes H.A., "The Lubricity of Diesel Fuels," *Wear*, **111**, 2, 1986.

22. "Aviation Fuel Lubricity Evaluation," CRC Report No. 560, Coordinating Research Council, 219 Perimeter Center Parkway, Atlanta, GA, July 1988.

23. Military Specification MIL-I-25017E, "Inhibitor, Corrosion/Lubricity Improver, Fuel Soluble (Metric)," 15 June 1989.

24. "Handbook of Aviation Fuel Properties," CRC Report No. 530, Coordinating Research Council, 219 Perimeter Center Parkway, Atlanta, GA, 1983.

25. Biddle, T.B. and Edwards, W.H., "Evaluation of Corrosion Inhibitors as Lubricity Improvers," AF Wright Aeronautical Laboratories (AD A198743), July 1988.

26. Blok, H., "Les Temperatures de Surface Dans des Conditions de Graissage Sous Pression Extreme," Proceedings of the 2nd World Petroleum Congress, Paris, June 1937.

27. Durkee, D.B. and Cheng, H.S., "An Examination of a Possible Mode of Scuffing Failure in Simple Sliding," *Wear*, **59**, pp. 223–230, 1980.

28. Odi-Owei, S., Roylance, B.J., and Xie, L.Z., "An Experimental Study of Initial Scuffing and Recovery in Sliding Wear Using a Four-Ball Machine," *Wear*, **117**, pp. 267–287, 1987.

29. Yamamoto, Y. and Hirano, F., "Relation Between Scuffing Resistance and the Increase in Surface Hardness During Tests Under Conditions of Rolling/Sliding," *Wear*, **63**, pp. 165–173, 1980.

30. Torrance, A.A. and Cameron, A., "Surface Transformations in Scuffing," *Wear*, **28**, pp. 299–311, 1974.

31. Hirst, W. and Hollander, A.E., "Surface Finish and Damage in Sliding," Proc. Roy. Sol. Lond., Ser. A. 337, pp. 379–394, 1974.

32. Goodger, E. and Vere, R., *Aviation Fuels Technology*, Macmillan, New York, NY, 1985.

33. Hadley, J.W., "A Method for the Evaluation of the Boundary Lubricating Properties of Aviation Turbine Fuels," *Wear*, 101, pp. 219–253, 1985.

34. Hadley, J.W., "The Effect of Composition on the Boundary Lubricating Properties of Aviation Turbine Fuels," text of presentation given at MOD/IOP Seminar "Tribology of Aviation Turbine Fuel Systems" at the Institute of Physics, London, England, December 13, 1989.

35. Excerpts from letter dated August 25, 1992 Mike Lopker, Public Works Dept., City of Phoenix to Mike Millar, Ford Motor Company. Letter was edited by Mr. P.T. Henderson and circulated as item N1008 in the ISO/TC22/SC7/WG6 record.

36. Lacey, P.I., "Development of a Fuel Lubricity Test Based on the Transition From Oxidative Corrosion to Adhesive Wear Mechanisms," Paper No. 93111, in press with Journal of Lubrication Engineering.

APPENDIX A

Laboratory Test Conditions

TABLE A-1. Summary of Conditions Used in Laboratory Wear Tests Discussed or Developed in the Present Study

	Oxidative Corr. (Some Adhesion)			Adhesive Scuffing (Some Oxidative Corr.)		
Procedure Type:	A	B	C	D	E	F
App. Load, kg	0.5	0.5	0.5 to 2.0	0.5 to 8.0	3	1 to 25.0
Speed, rpm	240	240	240	525	525	0 to 50 (Hz)
Break-in, sec/kg	None	None	None	30/0.5	30/0.5	30/0.5
Duration, min.	30	30	1	2	2	142.8 (meters)
Ring Texture	Standard	Standard	Standard	Polished	Polished	--
Atmosphere	Air	Air	Nitrogen	Air	Air	Air
Humidity, %Rh	10	100	10	50	50	50
Pass/Fail	0.65 mm	0.65 mm	1 kg (Aprx)	3 kg	No Scuffing	--
Reference	19	--	4	--	--	7

Notes:

1. Test specimen metallurgy and cleaning procedure as defined in ASTM Method D 5001-89.
2. The load refers to the applied load (BOCLE only) and corresponds to half that on the test specimens.
3. In each instance, the test is preceded by a 15-minute preconditioning period at the appropriate conditions of atmosphere and humidity.
4. The root mean square surface (RMS) roughness of the ASTM standard ring must be between 0.56 and 0.71 μm. The surface roughness of the polished specimen must be less than 0.05 μm RMS as defined in Appendix J of this report.
5. Severe scuffing may necessitate premature termination of tests performed according to *Procedures D* and *E*.
6. The fuel sample was changed after every fifth test in *Procedure D* in the absence of scuffing and after every test that produced very severe scuffing.
7. A detailed description of the test methodology for *Procedure D* may be obtained in Appendix K of this report.
8. All of the results reported in the present study (except Figs. 15a and 16) used *Procedure D* without a break-in period and 10 percent humidity. Future work will use the break-in period and 50 percent humidity, resulting in marginally different results.

APPENDIX B

Summary of Full-Scale Pump Tests

SUMMARY OF FULL-SCALE PUMP TESTS

A. Pump Stand Test Methodology

An arctic and a standard fuel pump were tested simultaneously on a Unitest stand with a common fuel supply. To ensure a realistic test environment, the mounting arrangement and drive gear duplicate that of the GM 6.2L engine. For this study, 1,000 liters of test fuel were maintained in an enclosed reservoir and continuously recirculated throughout the duration of each test. A centrifugal supply pump provided a positive head of 3 psi at the inlet to the test pumps. A primary (sock) filter (AC Part No. T935) and a cartridge filter corresponding to that used on the 6.2L engine in the High-Mobility Multipurpose Wheeled Vehicle (HMMWV) (GM Part No. 14075347) were used to remove wear debris and particulate contamination. Finally, a 5-kW Chromalox explosion-resistant circulation heater produced the required fuel inlet temperature. The heater has a relatively low watt density of 15 W/in.^{2} to minimize fuel degradation due to flash heating, and a 40-liter (11-gal.) reservoir was placed in line after the heater to ensure that the fuel supply temperature remained stable as the thermostat cycled. Each pump was fully insulated using rockwool to ensure that the temperature of the complete unit is similar to that of the incoming fuel.

The high-pressure outlets from the pumps were connected to eight NA52X fuel injectors from a GM 6.2L engine and assembled in a collection canister. Fuel from both canisters was then returned to the bulk storage tank via a common return line. A separate line to the bulk storage tank was used to carry excess fuel from the governor housing. Fuel-to-water heat exchangers on both the return lines from the injector canisters and the governor housing were used to control the temperature of the fuel. The fuel reservoir was maintained below the minimum flash point of Jet A-1 to minimize evaporation of the lighter fractions in the fuel. A pressure gauge was placed at the inlet to each pump, and a separate tool was manufactured to allow continuous measurement of the internal transfer pump pressure during normal operation.

B. Effect of Dissolved Moisture on Pump Wear

Two full-scale pump stand tests were performed to confirm the effects of dissolved moisture on fuel system wear. Standard (nonarctic) reconditioned pumps were used, as the arctic components appear to be largely independent of oxidative wear.(1,2)* During these tests, 200 liters of fuel were contained in a sealed reservoir, with a single vent to the atmosphere. During the initial test, dry compressed air was bubbled through Jet A-1 at a rate of 0.33 ft^3/min, to define the baseline wear rate in the absence of moisture. A prepurge period of 24 hours was performed to remove existing moisture from the fuel. The neat Jet A-1 fuel was continuously clay treated during the test, further reducing the residual moisture content within the closed system.

In the second test, 4 liters of water were placed at the bottom of the fuel tank to ensure that the fuel was saturated with dissolved moisture. The flow and return pipes to the pump were positioned so that no bulk water was transported to the pump. A Stanadyne Model 80 filter (No. 27288) with integral water separator was placed in line before the pump to remove any free water from the fuel supply. However, no free water was found in the filter at the conclusion of the test. The fraction of dissolved water was determined to be approximately 57 ppm, which is close to the saturation level for Jet A-1 at the reservoir temperature of 33°C (93°F).(3) Free water is commonly formed in vehicular fuel tanks due to the effects of condensation (i.e., a drop of 10°C in fuel temperature when that fuel is water saturated will create 15 to 25 ppm of undissolved or free water).(3)

The fraction of dissolved moisture present in the fuel greatly affected pump durability. The transfer pump pressure and fuel delivery remained almost unchanged during 80 hours of testing with dry fuel, as shown in Fig. B-1. In contrast, the measured transfer pump pressure and total fuel delivery changed dramatically after only 8 hours of testing with wet fuel. In addition, the interior of the pump that had been operated on wet fuel had an oxide coating, confirming the presence of a corrosive wear mechanism.

* Underscored numbers in parentheses refer to the list of references at the end of this appendix.

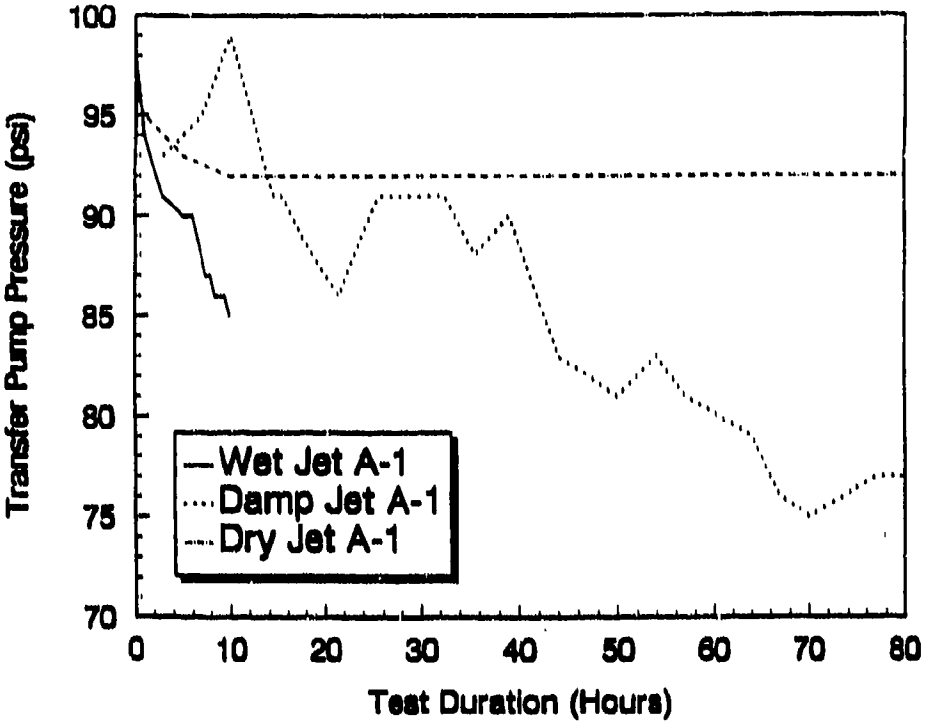

a. Transfer Pump Pressure

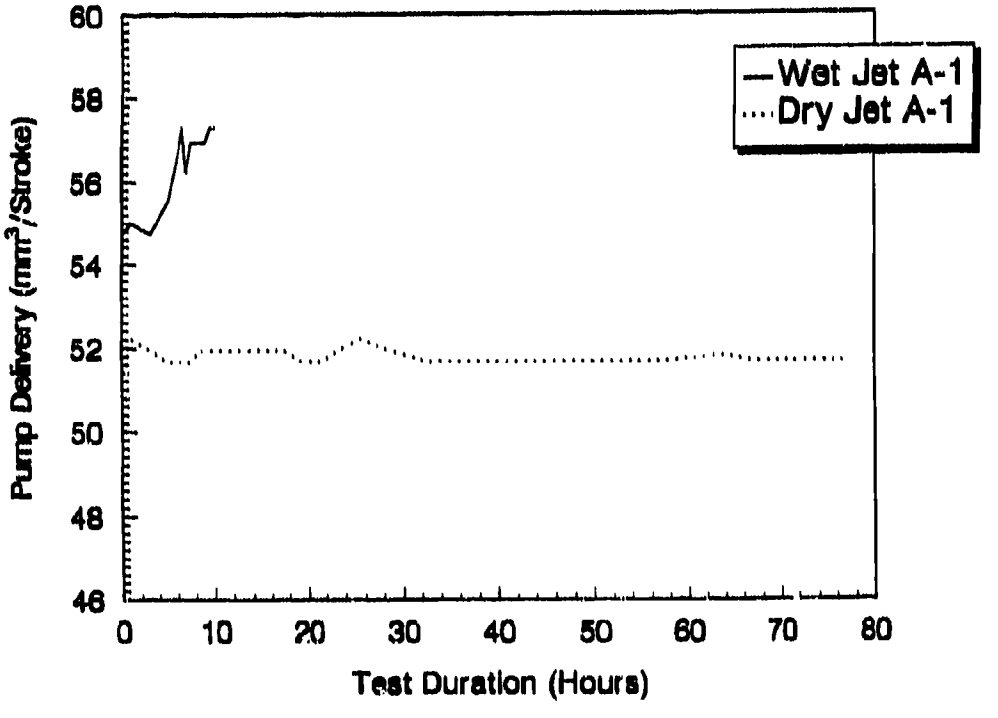

b. Pump Delivery

Figure B-1. Pump operating characteristics measured during tests with Fuel A (Jet A-1) with and without the presence of moisture

The transfer pump pressure measured during a previous full-scale pump stand test with Jet A-1 in an open reservoir (1) is also plotted in Fig. B-1. The decrease in transfer pump pressure in this test is less severe than with saturated fuel, probably due to the intermediate moisture content in the absence of bulk water. At relative humidity values less than 100 percent, the amount of water dissolved in the fuel will be correspondingly less than the saturation values, in accordance with Henry's Law. The average relative humidity during this test was 63 percent.(1) This proportional relationship between relative humidity and measured wear is in qualitative agreement with the lightly loaded region of the wear map in Fig. 1 of the main report. The post-test operating characteristics of the pumps were not evaluated using a test stand, due to the very severe wear present on Pump No. 2 and the fact that both pumps were reconditioned.

C. Effect of Lubricity Additive on Corrosive Wear Under Saturated Moisture Conditions

Previous reports noted that the addition of additives qualified under MIL-I-25017 to form JP-8 greatly reduced corrosive wear under conditions of slight, but unknown humidity.(1) However, the effects of these additives on full-scale pump wear under more severe, saturated moisture conditions are unknown. As a result, 200-hour tests were performed using Pump Nos. 5 and 6 (TABLE 1 of the main report) with moisture-saturated Jet A-1 containing 20 mg/L DCI-4A corrosion-inhibitor additive. This additive is qualified under MIL-I-25017 and is formulated from dilineolic acid, effectively corresponding to JP-8 aviation turbine fuel.

The addition of corrosion-inhibitor additive greatly improved the pump's durability under the present operating conditions. The pump operating characteristics measured during the 200-hour test are plotted in Fig. B-2. The measured transfer pump pressure decreased over the first 100 hours for both pumps. The decrease observed is marginally greater than that seen with dry Jet A-1, but is appreciably better than neat Jet A-1 under similar damp conditions. The fuel delivery rate decreased by approximately 10 percent for the arctic pump but remained constant for the standard unit. This decrease was also evident in the post-test engine power curves shown in Appendix E of this report, and the post-test pump calibration stand measurements in Appendix C. However, in each instance, the pump operating characteristics measured on the

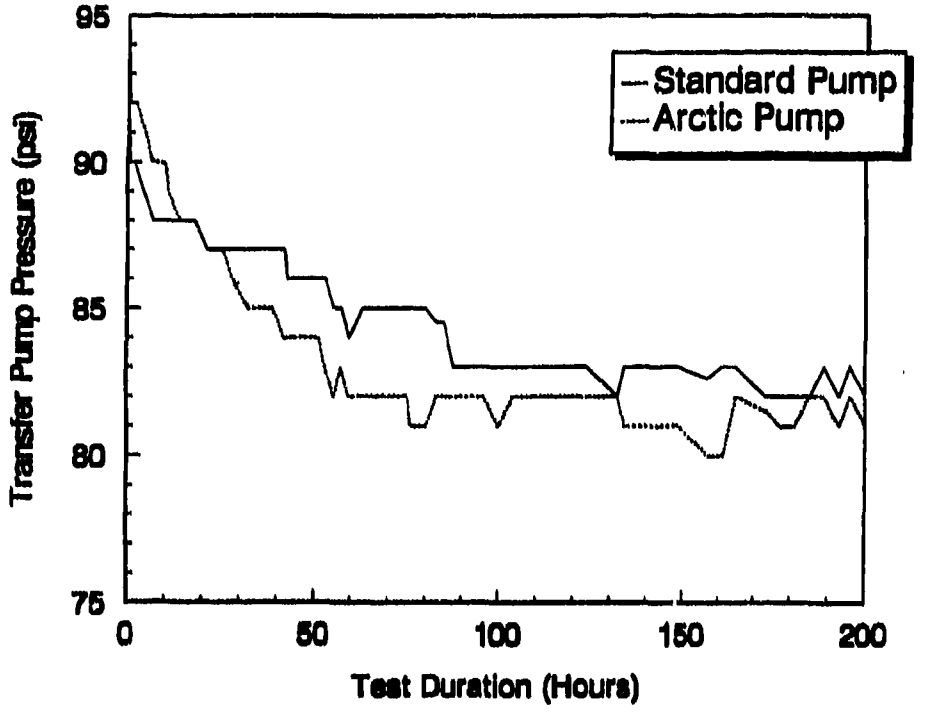

a. Transfer Pump Pressure

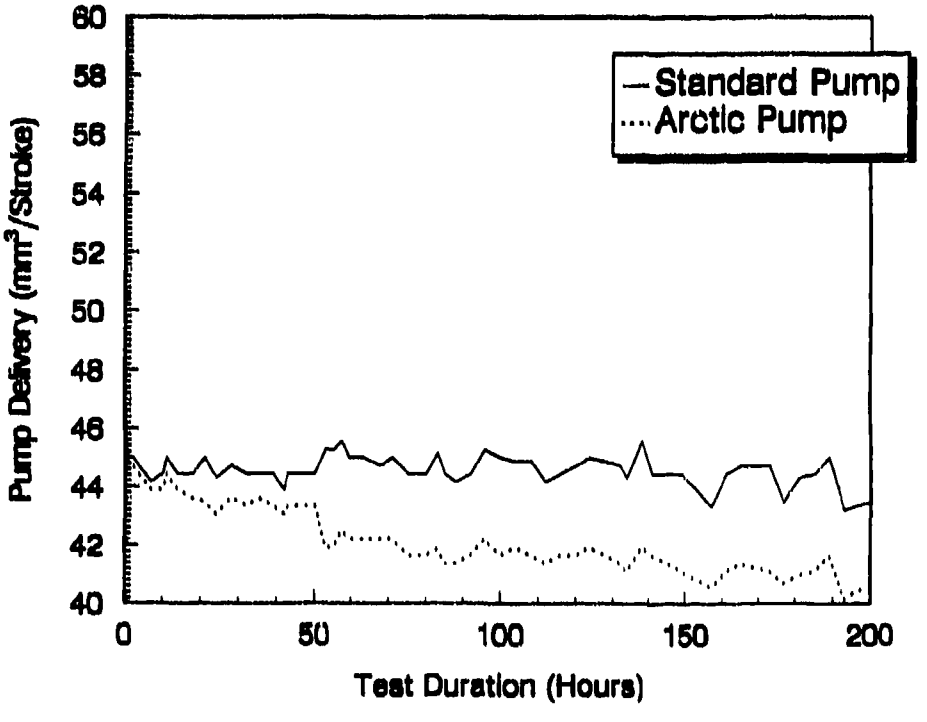

b. Total Pump Delivery

Figure B-2. Pump operating characteristics with Fuel B (JP-8) with moisture present

calibration stand remain within the manufacturer's specifications after 200 hours of operation on wet JP-8, as detailed in Appendix D. Clearly, the corrosion inhibitors remain effective at high fuel moisture content.

D. Effect of Temperature on Pump Wear Under Saturated Moisture Conditions

As previously stated, U.S. Army ground forces have used Jet A-1 and Arctic diesel fuel (DF-A) on compression-ignition equipment in Alaska for many years, with no apparent durability problems. The decreased wear under arctic conditions may be due to the low ambient temperatures combined with reduced atmospheric moisture. Temperature is likely to have a significant effect on pump wear, as hydrodynamic and elastohydrodynamic lift provide partial or complete separation among many components. Furthermore, the oxidation rate of the metallic surfaces during corrosive wear is likely to be defined by an Arrhenius equation and the availability of moisture (4), both of which are highly temperature dependent. In an attempt to evaluate the importance of this effect, full-scale pump stand wear tests were performed using Pump Nos. 7 and 8 with unheated fuel, producing an inlet temperature of approximately 32°C (90°F) throughout the test. As in the preceding pump tests, 4 liters of water were placed at the bottom of the 1,000-liter Jet A-1 reservoir to simulate condensation and to facilitate oxidative/corrosive wear.

Very severe degradation in performance was observed with the standard injection pump at this temperature. Pump delivery increased gradually during the first 25 hours of operation, due to wear between the roller shoes and blade spring, as shown in Fig. B-3. Transfer pump pressure decreased gradually over the same time period. However, a dramatic decrease in transfer pump pressure occurred after approximately 26 hours with a corresponding decrease in fuel delivery, due to very severe wear of the transfer pump blades. In addition, it is likely that the pump blades stuck in the rotor, as occasional resistance was felt if the pump shaft was manually rotated. Little or no wear was present on the arctic blades, and the engine test characteristics of the arctic pump remained unchanged, as shown in Appendix E. No post-test engine evaluation was performed on the standard pump due to the very severe wear present. A more detailed

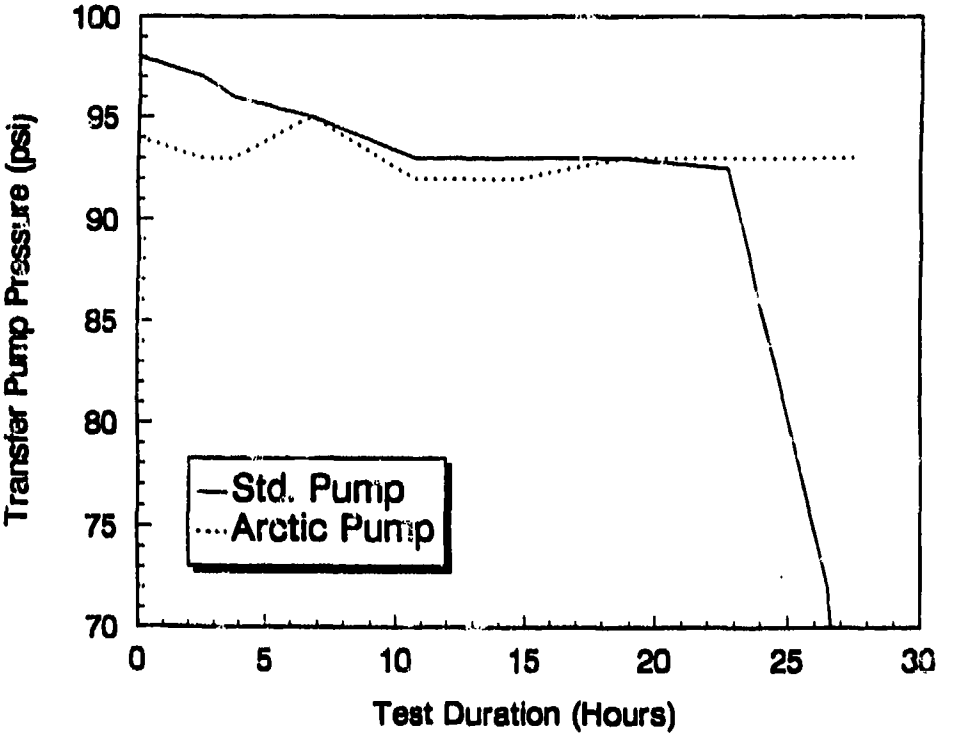

a. Transfer Pump Pressure

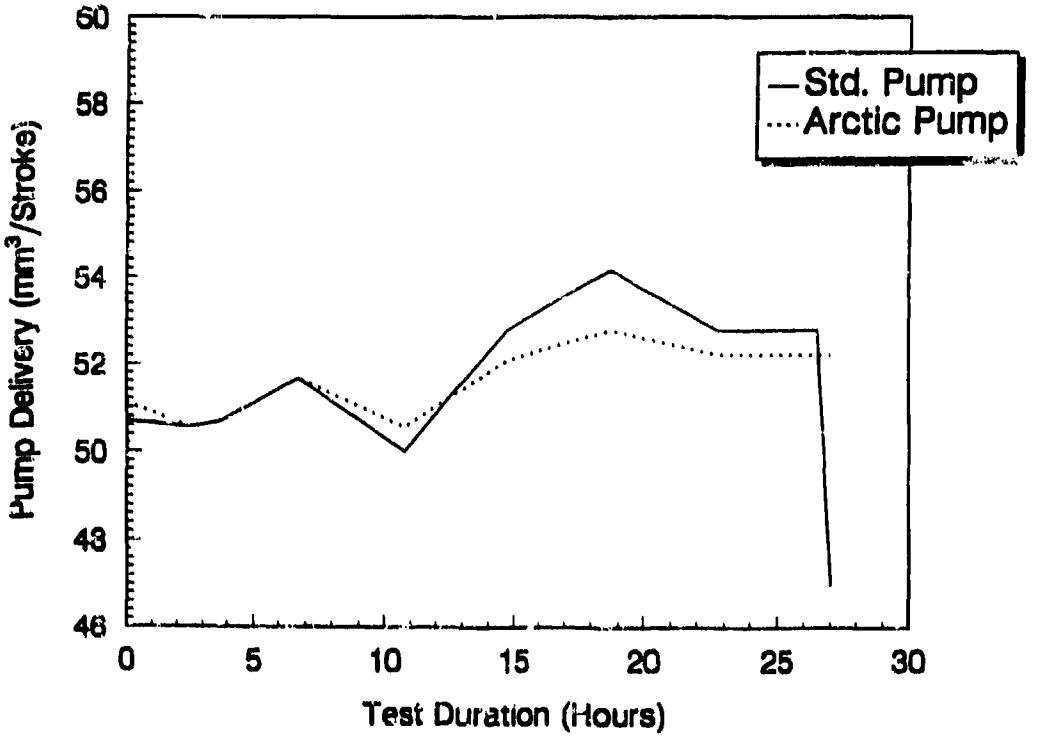

b. Pump Delivery

Figure B-3. Pump operating characteristics at ambient temperature with Fuel A (Jet A-1) with moisture present

description of the wear rate as well as comparison with the remaining pumps is given in Appendix D.

The wear rate observed in the present test with no in-line fuel heater was at least as severe as that observed in the preceding tests at 79°C (175°F) with Jet A-1. However, the quantity of dissolved moisture in the fuel is likely to be defined by the temperature of the reservoir, as no additional moisture is available after the fuel enters the pump stand system. The temperature of the fuel reservoir was approximately 32°C (90°F) in tests performed at both ambient and high temperatures. This temperature is likely to be well above the fuel storage temperatures present under arctic conditions, even in an operating vehicle. Thus, the availability of moisture within the pump is greatly increased. The effects of moisture content on wear are evaluated in more detail using laboratory wear tests for a range of fuels in Appendix G.

E. Effect of Break-in With Good Lubricity Fuel

The initial period of operation, or break-in, is the most critical period in the life of many contacts. Mild wear during this period may produce a smooth conforming interface between the opposing surfaces, reducing the asperity tip contact pressure. In many instances, surface chemical films may also have a finite initiation time or temperature before effective boundary lubrication begins.

Jet A-1 produces severe wear, compared to regular DF-2 diesel fuel over an extended test duration. However, the effects of occasional operation or an initial break-in period with good lubricity fuel are unknown. Full-scale pump tests were performed using clay-treated Jet A-1 after an initial break-in period of 50 hours using DF-2. These tests were performed using Pump Nos. 3 and 4 in ambient humidity conditions of approximately 65 percent. The wear scar diameter obtained using the BOCLE test was 0.55 mm for the diesel fuel and 0.71 mm for the clay-treated Jet A-1 fuel.

Pump delivery remained constant during the initial 50 hours of testing with diesel fuel, as shown in Fig. B-4. However, conversion to Jet A-1 immediately affected pump delivery, due to its reduced viscosity compared to diesel (1.3 versus 3 cSt at 40°C), which promotes internal pump leakage. Reduced delivery with Jet A-1 has already been noted for new pumps (Appendix E) and is independent of fuel lubricity and wear. After several hours of operation, the total pump delivery recovered, due to wear of the roller shoes at the leaf spring contact, as shown in Fig. B-5. The comparatively mild wear on a similar component after 200 hours of operation in JP-8 is shown in Fig. B-5b for comparison. Wear at this point increases the stroke of the plungers with a concomitant increase in pump output. It should be noted that this component is not available with an improved metallurgy, producing similar, severe wear in both arctic and standard pumps.

A dramatic decrease in the transfer pump pressure on the standard unit was observed after only 4 hours of operation on neat Jet A-1, due to wear of the standard pump blades. The test was terminated after 8 hours of operation on neat Jet A-1 (a total of 58 hours). No change in transfer pump pressure was observed for the arctic pump unit that contains the improved metallurgy, and little or no wear was present on disassembly. Comparison of measurements taken prior to and after termination of the test indicates that approximately 0.133 mm (0.00525 in.) of wear occurred on the face of the standard transfer pump vane, compared with only 0.0051 mm (0.0002 in.) for the arctic metallurgy. Indeed, the dimensions of the standard pump blades were less than the manufacturer's recommended minimum after only 8 hours of operation with Jet A-1. A more detailed discussion of the measured wear rate is provided in Appendix D.

The initial 50 hours of operation with diesel had no quantifiable effect on subsequent operation with damp, neat Jet A-1 fuel. Wear of the standard pump during the subsequent 10-hour test was greater than that previously seen during 80 hours of operation with the same Jet A-1 fuel in dry ambient conditions. Disassembly of both pumps indicated that a golden film of iron oxide was present, causing both the cam ring and metering valve to bind.

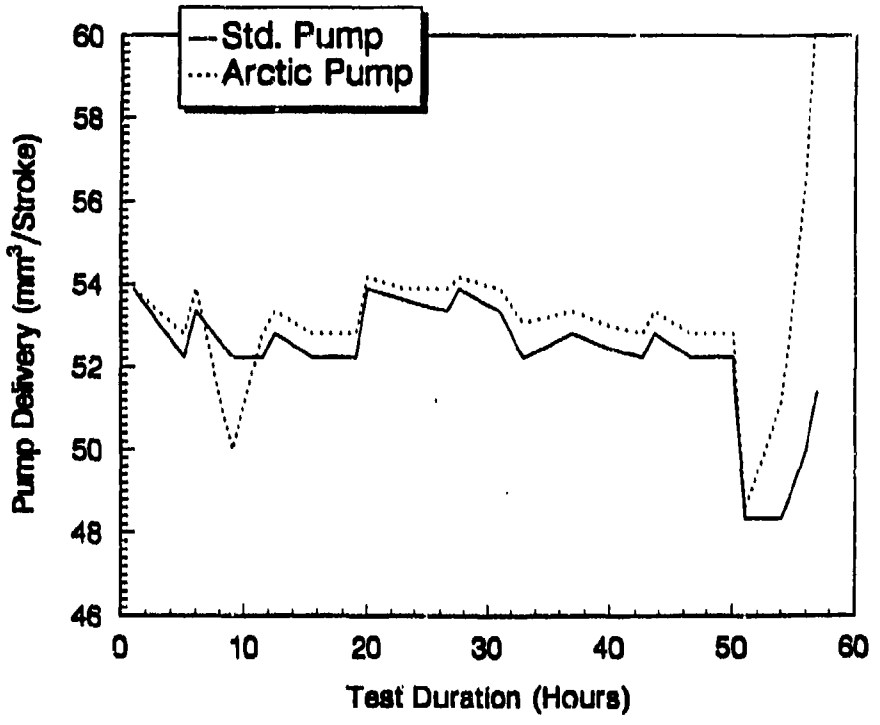

a. Fuel Delivery

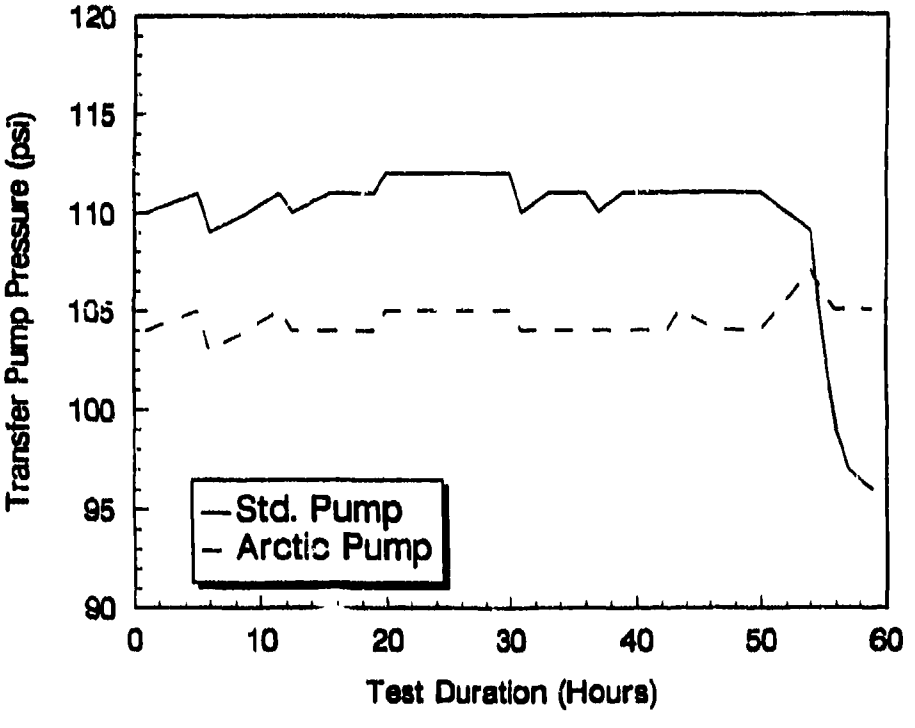

b. Transfer Pump Pressure

Figure B-4. Pump operating characteristics during initial break-in with diesel fuel (Fuel F) and subsequent operation with Jet A-1 (Fuel A)

a. Severe Wear on Neat Jet A-1

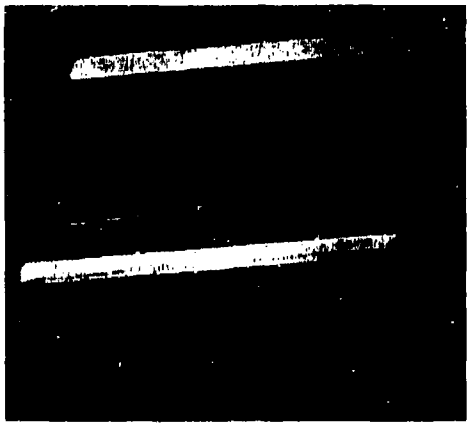

b. Mild Wear After Extended Operation on JP-8

Figure B-5. View of wear scar on pump roller shoe

F. List of References for Appendix B

1. Lacey P.I., "The Relationship Between Fuel Lubricity and Diesel Injection System Wear," Interim Report BFLRF No. 275 (AD A247927), prepared by Belvoir Fuels and Lubricants Research Facility (SwRI), Southwest Research Institute, San Antonio, TX, January 1992.

2. Lacey, P.I., "Effect of Low-Lubricity Fuels on Diesel Injection Pumps - Part II: Laboratory Evaluation," SAE Technical Paper No. 920823, February 1992.

3. *Handbook of Aviation Fuel Properties*, CRC Report No. 530, Coordinating Research Council, 219 Perimeter Center Parkway, Atlanta, GA, 1983.

4. Kubaschewski, O. and Hopkins, B.E., "Oxidation of Metals and Alloys," Butterworths, London, 1962.

APPENDIX C

Pump Calibration Stand Results

PUMP CALIBRATION STAND RESULTS

As in the previous study,* each of the pumps were precisely calibrated according to manufacturer specifications, which typically include some tolerance. As a result, the exact values were recorded for comparison with the post-test measurements with the results shown in TABLES C-1 through C-4.

It should be noted that Pump Nos. 1 and 2 (Model Nos. DB2829-4524 and DB2829-4523, standard and arctic units, respectively) conform to slightly different specifications than the remaining pumps, which have different model numbers (Model Nos. DB2-4979 and DB2-4980, standard and arctic units, respectively). A number of the pumps were judged to have failed during testing, i.e., Pump Nos. 1, 2, and 7, and were not recalibrated using the test stand. Neither of the two rebuilt pumps was calibrated using the test stand because of the relatively short nature of the tests performed.

The test stand conformed to ISO 4008 with SAE 0968/ISO 7440 calibrating injectors. The calibration fluid was Viscor conforming to SAE 0967/ISO 4113. The fluid supply temperature to the pump was maintained between 43° to 46°C (110° to 115°F) at a pressure of 5 ± 0.5 psi (34.5 ± 3 kPa).

Each pump was operated for 10 minutes prior to calibration to allow the system to stabilize. The computerized stand provided a digital readout of pump delivery per stroke at the required test speeds, eliminating errors. Injection advance is measured by a mechanical attachment that follows the movement of the cam ring (commonly known as a bat wing gauge).

* Lacey, P.I., "The Relationship Between Fuel Lubricity and Diesel Injection System Wear," Interim Report BFLRF No. 275 (AD A247927), prepared by Belvoir Fuels and Lubricants Research Facility (SwRI), Southwest Research Institute, San Antonio, TX, January 1992.

TABLE C-1. Pump Delivery

		Delivery, mm^3/stroke at designated rpm				
Speed, rpm		75	200	1000	1800	1875
Specification, mm^3/stroke		>28	>43	<56	>45	33.5 to 35.5
Pump No.	Test Time, Hours					
5	0	31.5	49.0	53.0	49.0	34.0
	200	30.1	47.2	52.5	48.7	46.4
6	0	36.5	49.0	52.0	47.7	35.0
	200	33.1	47.0	51.0	43.0	40.4
8	0	30.6	48.0	53.0	50.0	35.0
	26	37.5	50.9	55.1	52.1	50.6

Note: Readings at wide open throttle.

TABLE C-2. Transfer Pump Pressure

		Pressure, psi at designated rpm		
Speed, rpm		75	1000	2000
Specification, psi		>16	60 to 62	<125
Pump No.	Test Time, Hours			
5	0	19	62	105
	200	18	62	106
6	0	25	62	110
	200	18	60	97
8	0	20	62	107
	26	18	64	106

Note: Readings at wide open throttle.

TABLE C-3. Injection Advance Measurement, deg

Speed, rpm		325	1200	1600	1750
Throttle		LI*	WOT	LI	WOT
Specification, deg		>1	<3.25	<12	4.75
Pump No.	Test Time, Hours				
5	0	6.5	1.5	11.5	4.75
	200	6.0	2.5	12.0	5.00
6	0	5.5	1.5	11.5	4.75
	200	4.5	0.0	11.5	2.75
8	0	5.5	1.5	11.0	4.75
	26	6.5	2.0	12.0	5.25

TABLE C-4. Pump Measurements, Miscellaneous

Specification		RF*, cc/min	SO, mm^3/St	BA, mm^3/St
		225 to 375	<3	<15
Pump No.	Test Time, Hours			
5	0	300	0	1.0
	200	360	0	1.8
6	0	300	0	0.0
	200	300	0	0.0
8	0	350	0	0.0
	26	350	0	4.2

* RF = Return fuel from housing to tank (at 1,000 rpm).
SO = Shut off fuel flow.
BA = Fuel flow at breakaway speed (2,000 pump rpm).
St = Stroke.

APPENDIX D

Wear Measurement and Pump Disassembly

WEAR MEASUREMENT AND PUMP DISASSEMBLY

Severe test conditions combined with the very low lubricity Jet A-1 fuel caused premature termination of many full-scale pump tests noted in Appendix B. These pumps could not be evaluated using either the engine or the pump calibration stand, as had been the practice in earlier studies. However, each of the pumps was completely disassembled, and the sliding contacts throughout the pump were examined. A schematic diagram of the principal pump components is provided in Fig. D-1.

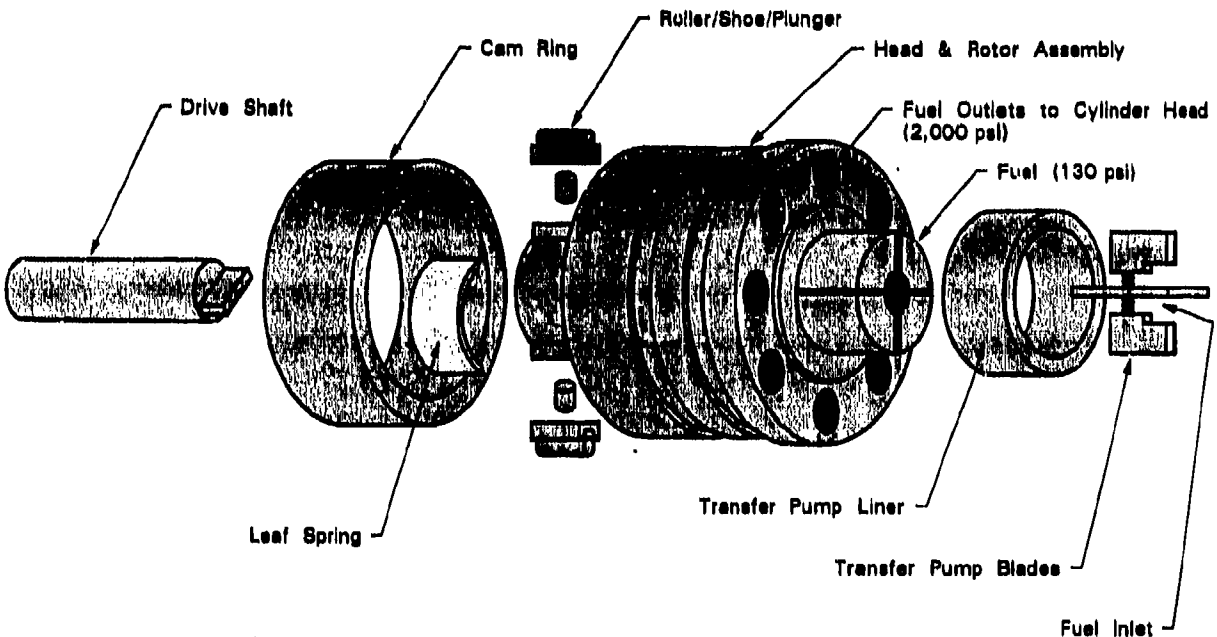

Figure D-1. Schematic diagram showing some components evaluated in the Stanadyne DB2 pump
(Courtesy of D. Lewicki, AMSRL-VPT.)

A. Quantitative Wear Measurements and Results

Previous reports in the present series gave particular attention to areas of the pump known to be susceptible to wear when used with low-lubricity fuels.(1)* Moreover, many of the components selected are available with the upgraded metallurgy of the arctic kit, as follows.

a. Transfer pump blades
b. Drive tang
c. Drive slot
d. Governor sleeve thrust washer
e. Governor weights†
f. Cam roller shoe†
g. Rotor retainers†

The dimensions of the wear scars formed on each component were determined using a Talysurf 10 surface profilometer. Wear measurement and subsequent analysis are analogous to that used in Reference 1 to facilitate direct comparison and is described in the Addendum 1 to this Appendix. The wear volume measured in each instance is summarized in TABLE D-1, along with the results obtained in Reference 1, which are denoted by the suffix a (for ease of reference, the test conditions for each pump are summarized in Addendum 2 to this appendix). The wear results were normalized using Archard's coefficient (2) to eliminate the effects of sliding distance and applied load, as some tests were terminated prematurely. Nonetheless, the normalized wear rate varied significantly, depending on fuel and test conditions, even for similar components.

In most instances, the improved arctic metallurgy was highly effective and decreased wear by several orders of magnitude. However, the arctic metallurgy was not effective on the thrust washer assembly, which appears largely insensitive to fuel lubricity and normally gives erratic wear results.

Previous work (1) indicated that the predominant wear mechanisms depend on contact severity; more highly loaded components produced unexpectedly high wear, possibly due to the onset of adhesion. The results of the present study for the lightly loaded pump blades, governor weights,

* Underscored numbers in parentheses refer to the list of references at the end of this appendix.
† Available in standard metallurgy only.

TABLE D-1. Archard's Wear Coefficient Calculated for Selected Pump Components

(NOTE: Bold text denotes arctic components with improved metallurgy.)

Pump No.	Pump Blades	Drive Tang	Drive Slot	Thrust Washer	Governor Weights	Roller Shoe	Rotor Retainers
1	92	400.0	515.0	190	--	176	7
2	1070	1224.0	1251.0	625	--	1476	652
3	1567	600.0	648.0	149	44	2071	699
4	**991**	**8.2**	**67.0**	**5223**	40	2028	201
5	2	0.9	0.8	167	13	13	23
6	**3**	**0.1**	**2.0**	**57**	5	15	68
7	15182	708.0	965.0	35	18	548	34
8	**389**	**2.4**	**12.0**	**1324**	28	629	4
The following pump results were obtained from Reference 1:							
1a	67	503.0	705.0	107	15	236	69
2a	**7**	**2.0**	**2.0**	**79**	10	582	107
3a	12	7.0	6.0	41	5	9	38
4a	**12**	**1.5**	**3.0**	**55**	4	15	38
5a	14	156.0	25.0	14	1	5	17
6a	**8**	**2.0**	**3.0**	**26**	3	38	30
7a	17	5.0	2.0	0	1	19	3
8a	**10**	**8.0**	**2.0**	**39**	1	10	4

and rotor retainer are plotted in Fig. D-2a, while the highly loaded drive tang, drive slot, and roller shoe are plotted in Fig. D-2b. A logarithmic scale is used due to the very large variation in wear rates observed. In each instance, the results are plotted by fuel category from both this and preceding reports where applicable. This procedure decreases random variation by allowing

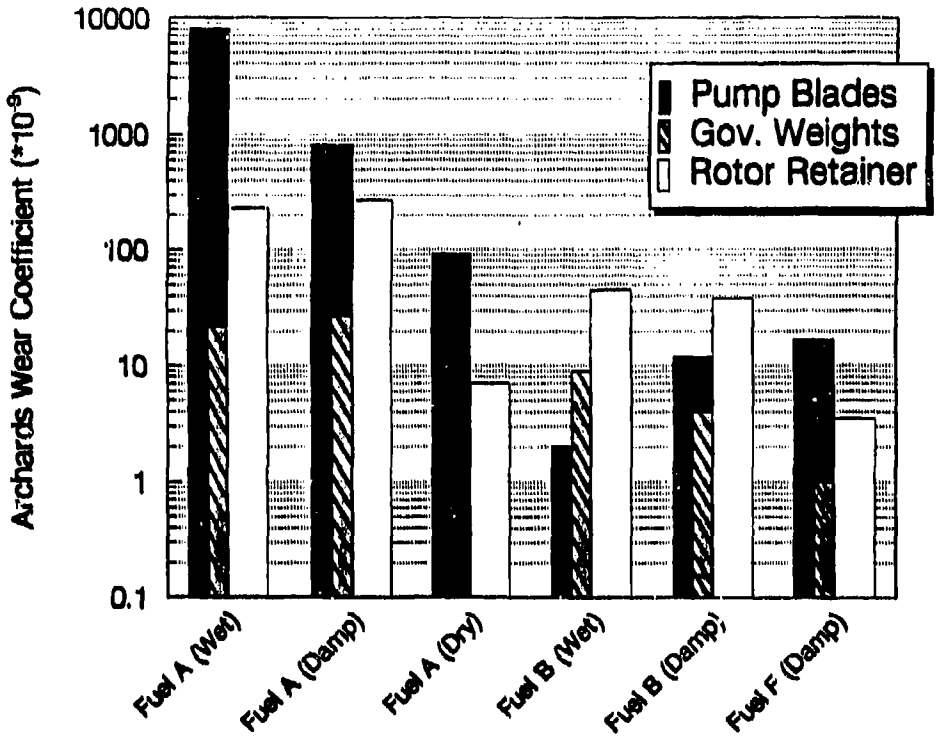

a. Lightly Loaded Pump Components

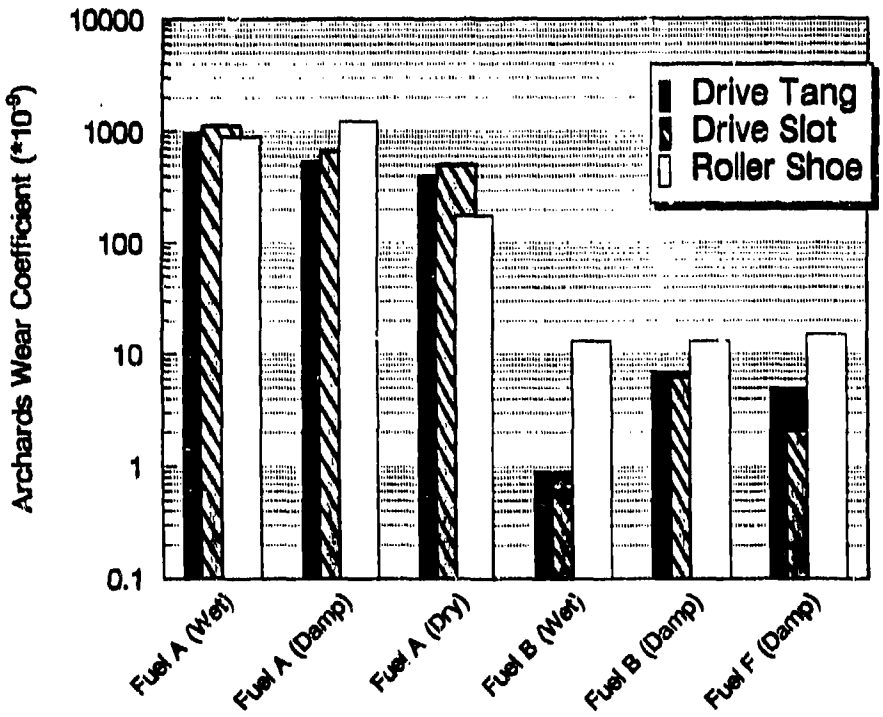

b. Highly Loaded Pump Components

Figure D-2. Wear measurements from individual pump components with fuel categories detailed in TABLE D-2

averaging within similar categories, as detailed in TABLE D-2. The erratic wear measurements obtained for the thrust washer are not included.

TABLE D-2. Description of Fuel Categories Used in Figs. 2 (Main Report) and D-2

Fuel Type	Description of Test Fuels Considered
Wet Jet A-1	Average measurements obtained from Pumps Nos. 2 and 7, with Fuel A. Nonarctic components from Pump No. 8 are also considered. The fuel was saturated with dissolved moisture.
Damp Jet A	Average measurements obtained from nonarctic components in Pump Nos. 3, 4, 1a, and 2a. Refers to pump stand tests in which the moisture content was not controlled and depended solely on atmospheric humidity.
Dry Jet A	Pump No. 3. The fuel was blanketed in dry air.
Wet JP-8	Average measurements obtained from Pump No. 5, with Fuel B. Nonarctic components from Pump No. 6 are also considered. The fuel was saturated with dissolved moisture.
Damp JP-8	Average measurements obtained for nonarctic components in Pump Nos. 3a, 4a, 5a, and 6a, with Fuel B. Refers to pump stand tests in which the moisture content was not controlled and depended solely on atmospheric humidity.
Diesel	Average measurements obtained for nonarctic components in Pump Nos. 7a and 8a, with Fuel D.

B. Qualitative Wear Measurements

The preceding section described quantitative wear measurements on seven pump components. Previous reports in this series developed a quantitative rating that could be applied to the numerous sliding contacts within each pump.(1, 3, 4) In this procedure, each component is assigned a numerical rating between 0 and 5, with 0 corresponding to no wear and 5 corresponding to severe wear and failure. The results obtained from this process are provided in TABLE D-3.

TABLE D-3. Subjective Wear Level* on Critical Pump Components

Component		Pump 1	2	3	4	5	6	7	8
Hydraulic Head & Rotor	Hydraulic Head	-	-	0	0	0	0	1	0
	Discharge Fittings	-	-	0	0	0	0	0	0
	Distributor Rotor	-	-	1	0	1	1	1	1
	Delivery Valve	-	-	2	2	2	2	2	1
	Plungers	-	-	2	1	1	1	2	1
	Cam Rollers & Shoes	3	4	3	4	2	2	3	3
	Leaf Spring & Screw	2	3	2	3	2	1	2	3
	Cam	-	-	2	1	1	1	1	1
	Governor Weight Retainer	-	-	2	2	1	1	2	3
	Governor Weights	-	-	1.5	1.5	2	2	2	1
	Governor Thrust Washer	1	1.5	1	2	2	1	1	2
	Governor Thrust Sleeve	-	-	1	1	1	1	1	1
	Drive Shaft Tang	-	-	3	1	2	2	4	2
Transfer Pump	Inlet Screen (0 = Clean; 5 = Clogged)	-	-	0	0	0	0	0	0
	Regulating Adj. Plug	-	-	0	0	0	0	0	0
	Regulating Piston	-	-	1	1	2	2	2	3
	Regulator	1	4	3.5	2	2	2	2	2
	Blades	1.5	4.5	4.5	1	1	1	4.5	1
	Liner	1	4.5	4	2	2	2	1	2
	Rotor Retainers	1.5	2	3.5	2	3	3	2	2
Governor	Metering Valve	-	1.5	2	1	1	1	1	2
	Metering Valve Arm	-	1	1	1	0	0	1	1
Advance	Piston	-	-	3	3	3	2.5	3	2
	Cam Advance Screw	-	-	1.5	1	1	1	2	1

* 0 = No Wear; 5 = Failure.

Pump 1: Rebuilt, 80 hours with Jet A-1 in dry air.
Pump 2: Rebuilt, 10 hours with wet Jet A-1.
Pump 3: New pump, 50 hours with diesel and 8 hours with Jet A-1.
Pump 4: New pump, 50 hours with diesel and 8 hours with Jet A-1.
Pump 5: New pump, 200 hours with wet JP-8.
Pump 6: New pump, 200 hours with wet JP-8.
Pump 7: New Pump, 26 hours with damp Jet A-1 at 90°F.
Pump 8: New Pump, 26 hours with damp Jet A-1 at 90°F.

However, unlike the previous reports, many of the pump tests discussed in the present study were terminated prematurely, as summarized in Appendix B. The different operating times

experienced by the pumps could not be accounted for, severely limiting the information available from simple qualitative analysis. Nonetheless, it is clear that the quantitative wear measurements on isolated components described in the preceding section are in good qualitative correlation with the remainder of the pump, i.e., severe wear was produced in a short period of time with unadditized moist fuel. By comparison, relatively mild wear was observed for Pump Nos. 5 and 6, which operated for a longer time period on moist fuel containing a lubricity additive (i.e., JP-8).

The transfer pump blades were among the components most affected by fuel lubricity. A very deep wear track was present on the standard pump blade after only 26 hours of operation on neat Jet A-1, as shown in Fig. D-3a, while only mild polishing was present on the arctic component in Fig. D-3b under the same conditions. By comparison, little or no wear is present on either the standard or the arctic blades after 200 hours of operation on JP-8, as shown in Figs. D-3c and D-3d, respectively.

The pump blades are lightly loaded but have a high sliding speed, with a correspondingly large sliding distance. Such conditions appear to maximize the effects of oxidative/corrosive wear. It is likely that high sliding speeds rapidly remove the surface oxide layer and provide nascent material that maximizes the oxidation reaction. Lower sliding speeds would allow formation of a thicker oxide layer. However, the reaction rate for the oxidation process decreases rapidly with increasing thickness due to the need for oxygen to diffuse through the oxide layer to the metallic substrate.(5, 6) The decrease in reaction rate may follow a logarithmic, asymptotic, or parabolic law, depending on metallurgy and temperature.

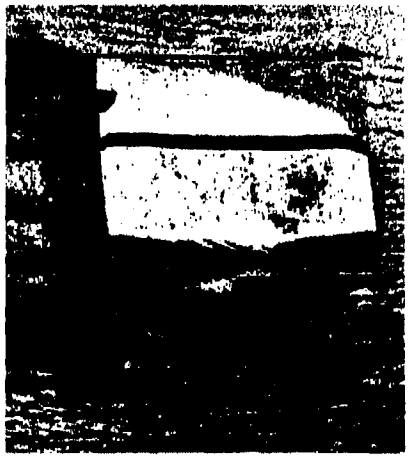

a. Pump 7 (Wet Jet A-1/Standard)

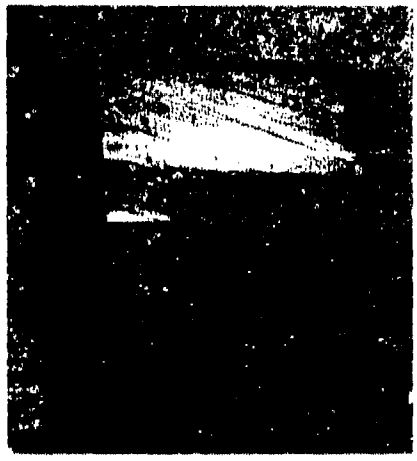

b. Pump 8 (Wet Jet A-1/Arctic)

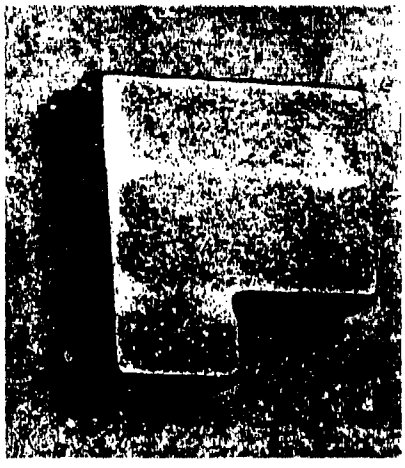

c. Pump 5 (Wet JP-8/Standard)

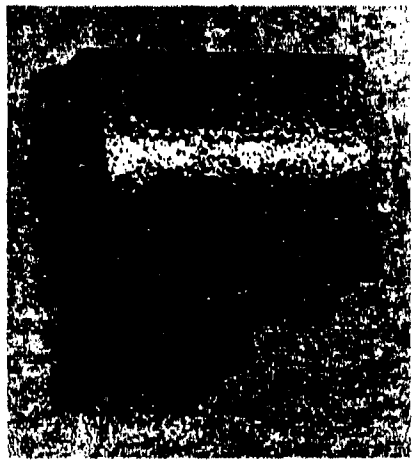

d. Pump 6 (Wet JP-8/Arctic)

Figure D-3. Comparison of wear scars on pump blades

C. List of References for Appendix D

1. Lacey P.I., "The Relationship Between Fuel Lubricity and Diesel Injection System Wear, Interim Report BFLRF No. 275 (AD A247927), prepared by Belvoir Fuels and Lubricants Research Facility (SwRI), Southwest Research Institute, San Antonio, TX. January 1992.

2. Archard, J.F., "Contact and Rubbing of Flat Surfaces," *Journal of Applied Physics*, **24**, pp. 981–988, 1953.

3. Lacey, P.I. and Lestz, S.J., "Failure Analysis of Fuel Injection Pumps From Generator Sets Fueled With Jet A-1,' Interim Report BFLRF No. 268 (AD A234930) prepared by Belvoir Fuels and Lubricants Research Facility (SwRI), Southwest Research Institute, San Antonio, TX, January 1991.

4. Lacey, P.I., "Wear Analysis of Diesel Engine Fuel Injection Pumps From Military Ground Equipment Fueled With Jet A-1," Interim Report BFLRF No. 272 (AD A239022), prepared by Belvoir Fuels and Lubricants Research Facility (SwRI), Southwest Research Institute, San Antonio, TX, May 1991.

5. Kubaschewski, O. and Hopkins, B.E., "Oxidation of Metals and Alloys," Butterworths, London, 1962.

6. Evans, U.R., "The Corrosion and Oxidation of Metals: Scientific Principals and Practical Applications," St. Martins Press Inc., New York, 1960.

ADDENDUM 1

CALCULATION OF ARCHARD'S WEAR COEFFICIENT ON PUMP COMPONENTS

A. Wear Measurements on Transfer Pump Blades

A reciprocating action is formed between the rotor and the transfer pump blade. This action forms a wear scar with a sharp step at the limit of the cycle. The depth of the wear scar was measured at this step using a Talysurf 10 profilometer. Scar depth was assumed to decrease linearly across the contact area, and the wear volume was calculated accordingly. An improved metallurgy is available in the arctic pump vanes, and the appropriate indentation hardness was used in calculating Archard wear coefficient as detailed in TABLE D-4. The cumulative sliding distance was calculated for an eccentricity of 4 mm.

Note: Hardness of Arctic Pump Vanes, Hv = 750
Hardness of Standard Pump Vanes, Hv = 460
Sliding Distance in 200 Hours, km = 173
Approximate Contact Load, kg = 0.36

TABLE D-4. Wear Measurements on Transfer Pump Blades

Pump No.	Wear Scar Dimensions: Max Depth, $mm \times 10^{-3}$	Wear Scar Dimensions: Final Area, mm^2	Wear Scar Dimensions: Volume, $mm^3 \times 10^{-3}$	Wear Coefficient, $K \times 10^{-9}$
1	4.5	11.1	24.9	1567
2	2.5	7.7	9.6	991
3	5.5	5.3	14.7	92
4	4.0	10.7	21.5	1070
5	1.0	2.3	1.1	2
6	1.0	1.5	0.7	3
7	100.0	15.4	771.0	15182
8	2.0	12.3	12.3	389

B. Wear Measurements on Governor Thrust Washer

The present wear scar is in the shape of a ring, formed by the action of the six governor weights on the governor thrust washer. The average depth of the wear scar was measured using a Talysurf profilometer and was found to be approximately constant around the complete circumference. The applied load was derived from the thrust required to counteract centripetal force on each governor weight at 1800 rpm. The indentation hardness of both the arctic and standard components were similar, and calculation of Archard's wear coefficient for this component is summarized in TABLE D-5. New thrust washers were placed in both reconditioned pumps, i.e., Pump Nos. 3 and 4.

Note: Hardness of Both Arctic and Standard Parts, Hv = 670
Sliding Speed, km/hr = 1.94
Approximate Contact Load, kg = 2
Circumference of Contact, mm = 83.2

TABLE D-5. Wear Measurements on Governor Thrust Washer

Pump No.	Scar Depth, mm $\times 10^{-3}$	Scar Width, mm	Volume, $mm^3 \times 10^{-3}$	Wear Coefficient, $K \times 10^{-9}$
1	0.2	1.2	20	149
2	3.5	2.5	728	5223
3	1.6	2.0	266	190
4	0.7	1.9	109	625
5	3.5	2.0	582	167
6	1.2	2.0	200	57
7	0.2	1.0	16	35
8	3.2	2.2	600	1324

C. Wear Measurements on Governor Weights

The six governor weights mate with the thrust washer described in the previous section. A narrow wear scar is formed across the 12-mm width of each weight. The wear scar is triangular in cross section and was measured using a Talysurf surface profilometer. Calculation of Archard's wear coefficient for this component is summarized in TABLE D-6. The tabulated results are the average derived from three individual traces along each wear scar. Used thrust washers were placed in Pump Nos. 3 and 4, so no wear measurements were taken.

Note: Approximate Contact Load, kg = 2
Vickers Hardness, kg/mm^2 = 410

TABLE D-6. Wear Measurements on Governor Weights

	Wear Scar Dimensions			
Pump No.	Max Depth, $mm \times 10^{-3}$	Width, mm	Volume, $mm^3 \times 10^{-3}$	Wear Coefficient, $K \times 10^{-9}$
1	23	0.35	48	44
2	23	0.31	43	40
3	-	-	-	-
4	-	-	-	-
5	90	0.65	351	13
6	55	0.45	148	5
7	40	0.27	64	18
8	52	0.32	100	28

D. Wear Measurements on Cam Roller Shoe

This wear scar is formed by a counterformal contact between the cam roller shoe and the pumping plunger. Little relative motion should occur other than that caused by vibration. The approximate sliding distance was calculated by assuming that the shoe vibrated once each time

the roller strikes the cam ring. The amplitude of the movement is equal to the tolerance between the shoe and the slot in the hydraulic head after testing. The wear volume was approximated by assuming that pumping plunger is cone-shaped close to the area of contact. Calculation of Archard's wear coefficient for this component is summarized in TABLE D-7. The tabulated result is an average value derived from both shoes on each pump. It should be noted that considerable variation existed between the two shoes on many of the pumps. New roller shoes were placed in the reconditioned pumps.

Note: Vickers Hardness, kg/mm^2 = 730
Approximate Sliding Distance per hour, km/hr = 0.0425
Total Contact Load During Injection, kg = 57

TABLE D-7. Wear Measurements on Cam Roller Shoe

Pump No.	Scar Depth, mm × 10^{-3}	Scar Diameter, mm	Volume, mm^3 × 10^{-3}	Wear Coefficient, K × 10^{-9}
1	45	3.75	165	2071
2	44	3.75	161	2028
3	30	4.25	141	176
4	40	3.75	147	1476
5	9	3.25	26	13
6	16	2.75	31	15
7	42	3.60	142	548
8	39	4.00	163	629

E. Wear Measurements on Rotor Retainers

The wear scar is a circular ring and was formed by the motion of the pump rotor. The depth of the wear scar was measured using the Talysurf profilometer, and the tabulated result is the average of four individual measurements. The depth of the wear scar was relatively constant in each measurement. The radial width of the wear scar was normally 2 mm, corresponding to the

overlap between the pump rotor and the washers. However, only a portion of the apparent contact area was worn in the two pumps that operated with diesel fuel. The applied load was approximated from the end loading on the shaft due to the transfer pump pressure and opposing reaction force from the governor weights. End loading from the driveshaft will also be a contributing factor. Calculation of Archard's wear coefficient for this component is summarized in TABLE D-8. New rotor retainers were placed in the reconditioned pumps, i.e., Pump Nos. 3 and 4.

Note: Sliding Distance per hour, km/hr = 7.125
Approximate Applied Load, kg = 4
Vickers Hardness, kg/mm^2 = 560
Average Circumference, mm = 66

TABLE D-8. Wear Measurements on Rotor Retainers

Pump No.	Max Depth, mm $\times 10^{-3}$	Width, mm	Volume, $mm^3 \times 10^{-3}$	Wear Coefficient, $K \times 10^{-9}$
1	6.5	2.00	858	699
2	2.5	1.50	247	201
3	1.2	1.12	92	7
4	2.2	1.50	222	652
5	5.7	1.87	709	23
6	17.0	1.87	2098	68
7	0.6	3.50	138	34
8	0.5	0.50	16	4

F. Wear Measurements on Drive Tang

A wedge-shaped wear scar is formed where the drive tang mates with the pump rotor. The maximum wear scar depth (at the deepest portion of the wedge) was measured using a micrometer and compared with unworn portions of the drive tang. The depth of the wear scar

was then assumed to decrease linearly to zero at the opposite edge of the scar. The tabulated value is an average calculated from measurements taken from each side of the drive tang.

Pump Nos. 1 and 2 ran for 50 hours on diesel, followed by 8 hours on Jet A-1. The total wear volume on diesel fuel is negligible. Only the 8 hours of testing on Jet A-1 is considered in the calculation of Archard's wear coefficient. It should be noted that the drive tang on reconditioned Pumps Nos. 3 and 4 had suffered a very slight amount of wear prior to testing. This initial wear volume was considered negligible compared to the material removed during the present test process.

A single deviation of 0.1 mm is assumed to occur at the drive tang for each injection cycle, i.e., eight times per revolution. The contact load is calculated for an average radius of 6.35 mm (0.25 in.) at a torque of 250 in.-lb.* Calculation of Archard's wear coefficient for this component is summarized in TABLE D-9.

Note: Approximate Applied Load, kg = 250
Sliding Distance per hour, km/hr = 0.086
Vickers Hardness, kg/mm^2 = 650

TABLE D-9. Wear Measurements on Drive Tang

Pump No.	Max Depth, $mm \times 10^{-3}$	Contact Area, mm^2	Volume, $mm^3 \times 10^{-3}$	Wear Coefficient, $K \times 10^{-9}$
1	44	24.0	527.0	600.0
2	5	2.9	7.2	8.2
3	203	32 0	3248.0	400.0
4	84	32.0	1340.0	1224.0
5	14	3.1	21.0	0.9
6	2	3.1	3.9	0.1
7	104	38.5	2002.0	708.0
8	11	1.9	6.9	2.4

* Hess, T. and Salzgeber, D., "The Stanadyne DB2 Distributor Pump for Medium Duty Diesels," Off-Highway Vehicle Meeting and Exposition MECCA, Milwaukee, WI, 10-13 September 1979.

G. Wear Measurements on Drive Slot

The drive slot mates with the drive tang. The wear measurements for the drive slots are described in TABLE D-10. The maximum depth of each wear scar was measured using a Talysurf surface profilometer. The tabulated result is an average value derived from readings obtained on both sides of the slot. The contact area in each instance was taken from TABLE D-9. The depth of the wear scar was then assumed to decrease linearly to zero at the opposite edge of the scar and the wear volume calculated accordingly.

Pump Nos. 1 and 2 ran for 50 hours on diesel, followed by 8 hours on Jet A-1. The total wear volume on diesel fuel is negligible. Only the 8 hours of testing on Jet A-1 is considered in the calculation of Archard's wear coefficient. The original pump rotor was used in the reconditioned pump (the pump rotor and body are a matched pair). As a result, the drive slot on reconditioned Pumps Nos. 3 and 4 had suffered a very slight amount of wear prior to testing. This initial wear volume was considered negligible compared to the material removed during the present test process.

TABLE D-10. Wear Measurements on Drive Slot

Pump No.	Max Depth, $mm \times 10^{-3}$	Contact Area, mm^2	Volume, $mm^3 \times 10^{-3}$	Wear Coefficient, $K \times 10^{-9}$
1	21	24.00	516	648.0
2	18	2.90	53	67.0
3	125	32.00	4000	515.0
4	39	32.00	1248	1251.0
5	7	3.12	21	0.8
6	17	3.12	53	2.0
7	65	38.50	2502	965.0
8	16	1.90	31	12.9

ADDENDUM 2

SUMMARY OF PUMP TEST CONDITIONS USED IN PRESENT STUDY AND REFERENCE 1

Code No.	Pump Type	Serial No.	Test Fuel	Test Duration	Wet/Dry	Comments
1	Standard	5608689	Jet A-1	80	Dry	--
2	Standard	5608690	Jet A-1	10	Wet	Terminated
3	Standard	6627499	DF-2/Jet A	50/8	Uncontrolled	Break-In Test
4	Arctic	6624980	DF-2/Jet A	50/8	Uncontrolled	Break-In Test
5	Standard	7136688	JP-8	200	Wet	--
6	Arctic	6913740	JP-8	200	Wet	--
7	Standard	7136689	Jet A-1	26	Wet	32°C (90°F)
8	Arctic	6913741	Jet A-1	26	Wet	32°C (90°F)

The following pumps were previously tested, and the results provided in Reference 1:

1a	Standard	6627504	Jet A-1	200	Uncontrolled	Severe Wear
2a	Arctic	6624985	Jet A-1	200	Uncontrolled	--
3a	Standard	6627505	MIL-I-25017*	200	Uncontrolled	--
4a	Arctic	6624984	MIL-I-25017	200	Uncontrolled	--
5a	Standard	6627506	MIL-S-53021†	200	Uncontrolled	--
6a	Arctic	6624983	MIL-S-53021	200	Uncontrolled	--
7a	Standard	6627499	DF-2	200	Uncontrolled	--
8a	Arctic	6627980	DF-2	200	Uncontrolled	--

* The MIL-I-25017 fuel consists of neat Jet A-1 and 15 mg/L DCI-4A dilinoleic acid-based corrosion inhibitor.

† The combination of BIOBOR-JF/FOA-15 are the only fuel additives qualified under MIL-I-53021 that are known to enhance fuel lubricity.

APPENDIX E

Engine Test Procedure and Results

ENGINE TEST PROCEDURE AND RESULTS

The engine test procedure used is the same as that reported by Lacey, 1992.* A brief description of the procedure is repeated for completeness. The engine tests were performed using a General Motors (GM) 6.2L engine with the specifications given in TABLE E-1. The engine was completely overhauled prior to testing, with new injectors (Bosch NA52X with DNOSD 248 Nozzle) and piston rings fitted. The normal opening pressure on each injector was established to be 1900 psi. The break-in procedure defined in the GM 210-hour wheeled vehicle cycle endurance test† was used.

The power curve was defined from 1400 to 3600 rpm in 200-rpm increments with the results shown in Figs. E-1 through E-5. The engine was warmed up prior to testing for 30 minutes at 1200 rpm and allowed to stabilize for 10 minutes between each test speed. The fuel return from the governor housing was collected in a day tank at the inlet side of the pump. The fuel flow meter was connected prior to the day tank to measure the net volume of fuel burned with the results shown in Figs. E-6 through E-8. Measured exhaust temperature is plotted in Figs. E-9 through E-11.

TABLE E-1. Specifications of the 6.2L Diesel Engine

Engine Type	Naturally Aspirated, Ricardo Swirl Precombustion Chamber, Four-Stroke, Compression Ignition
No. of Cylinders, Arrangement	8, V
Displacement, Liters (in.^{3})	6.2 (380)
Bore × Stroke, mm (in.)	101 × 97 (3.98 × 3.82)
Rated Power, kW (Bhp)	107.7 (145) (With HMMWV Pump)
Rated Torque, Nm (ft-lb)	325 (240)
Engine Structure	Cast Iron Head and Block (No Cylinder Liners), Aluminum Pistons
Injection System	Stanadyne DB-2 F/I Pump With Bosch Pintle Injectors

* Lacey, P.I., "The Relationship Between Fuel Lubricity and Diesel Injection System Wear," Interim Report BFLRF No. 275 (AD A247927), prepared by Belvoir Fuels and Lubricants Research Facility (SwRI), Southwest Research Institute, San Antonio, TX, January 1992.

† "Accelerated Fuel-Engines Qualification Procedures Methodology Engine Test 210-Hour Wheeled Vehicle Cycle Using the GM 6.2L Diesel Engine Operating on JP-8 Fuel," prepared by U.S. Army Fuels and Lubricants Research Laboratory, Southwest Research Institute, San Antonio, TX, October 19[illegible]

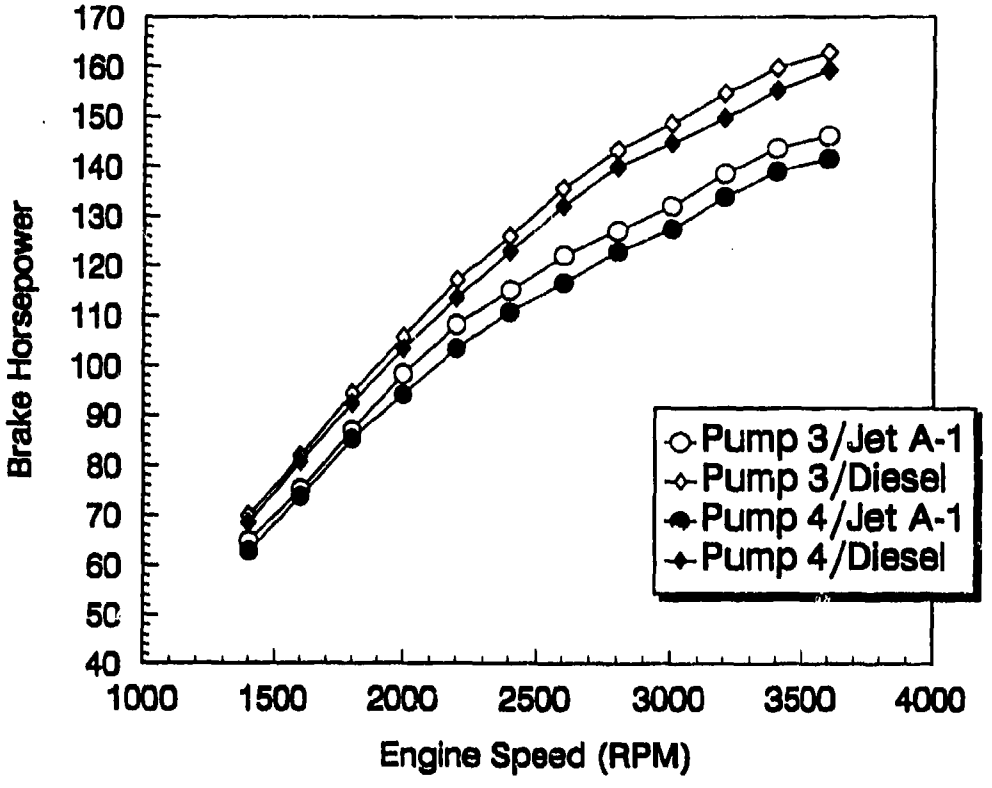

Figure E-1. Pretest engine power curves for Pump Nos. 3 and 4

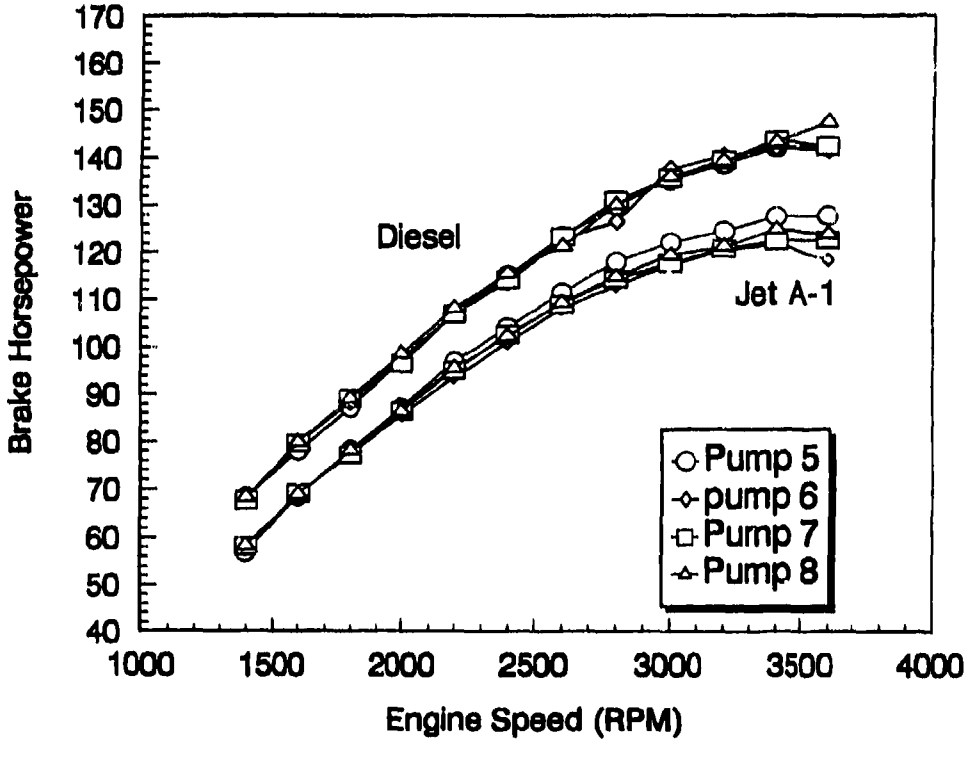

Figure E-2. Pretest engine power curves for Pump Nos. 5 through 8

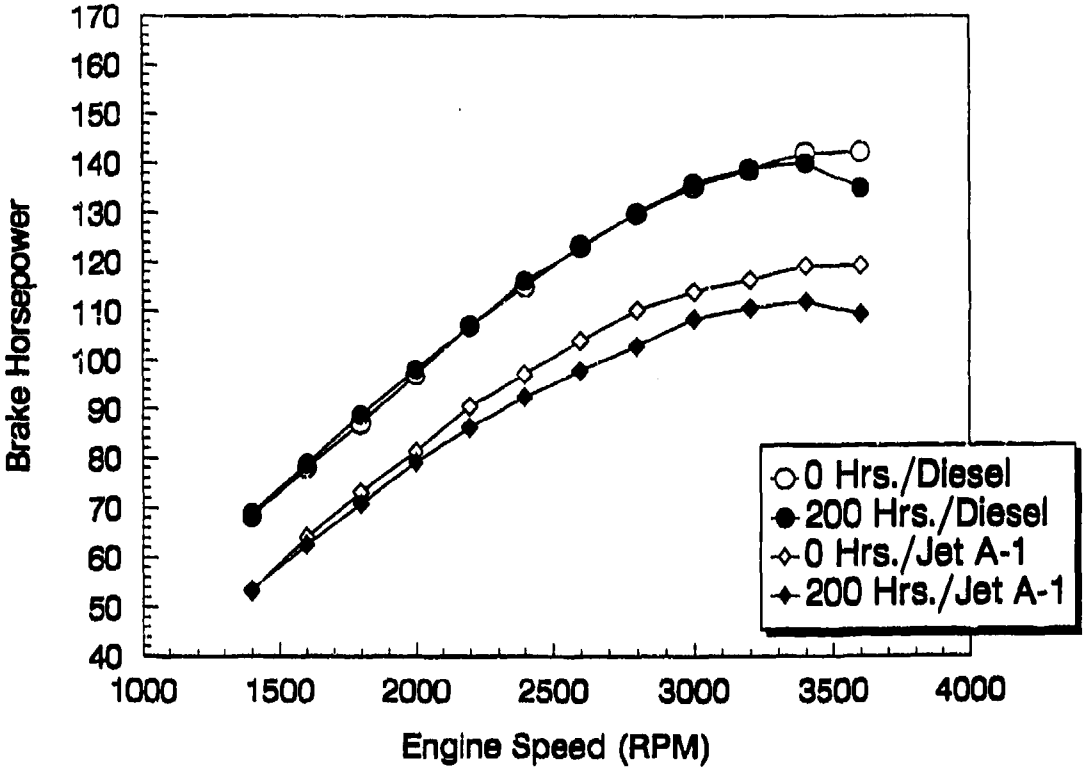

Figure E-3. Engine power curves for Pump No. 5 — standard pump tested for 200 hours on wet JP-8

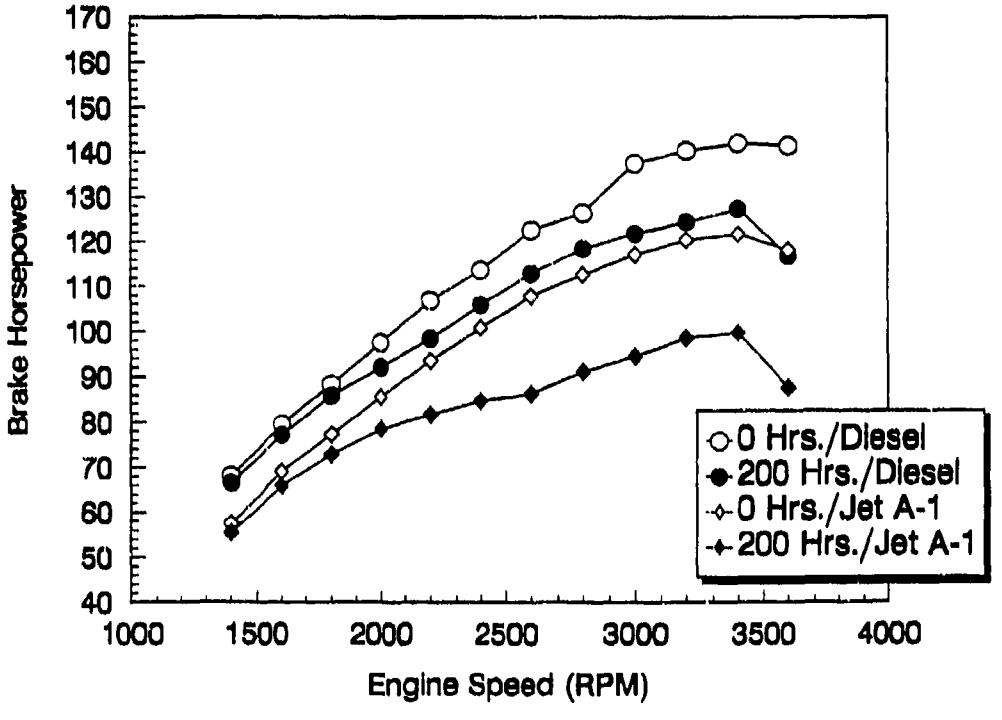

Figure E-4. Engine power curves for Pump No. 6 — arctic pump tested for 200 hours on wet JP-8

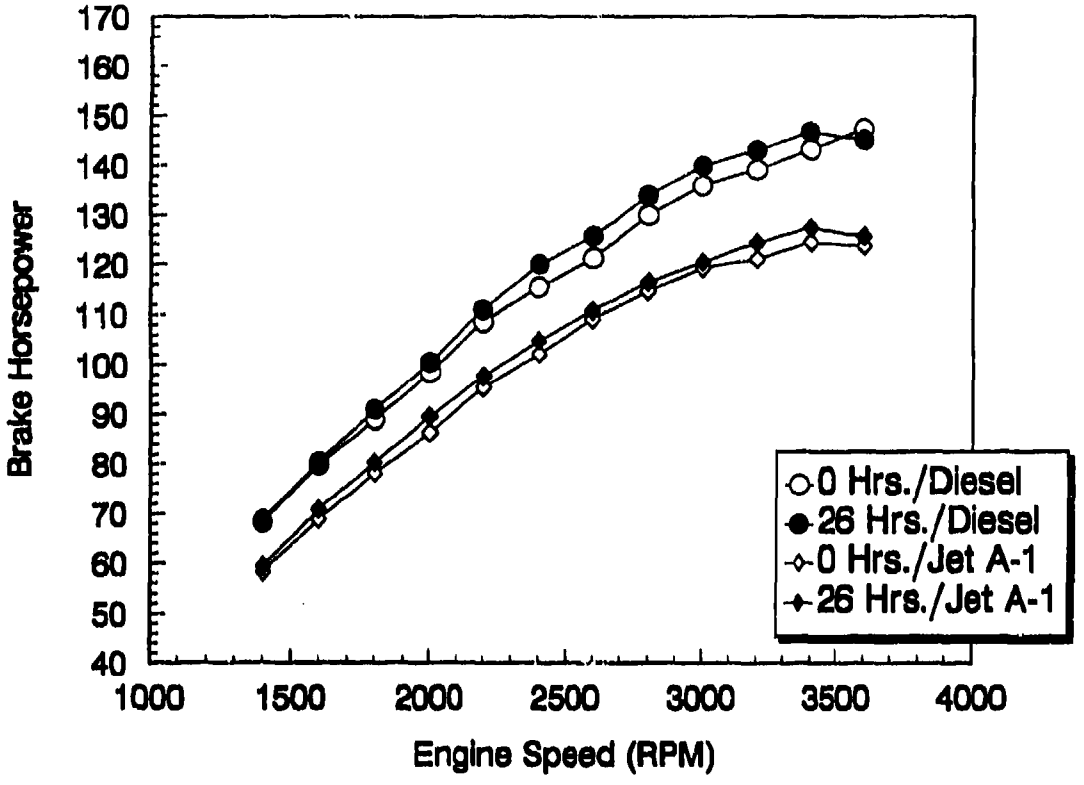

Figure E-5. Engine power curves for Pump No. 8 — arctic pump tested for 26 hours on wet Jet A-1 at 32°C (90°F)

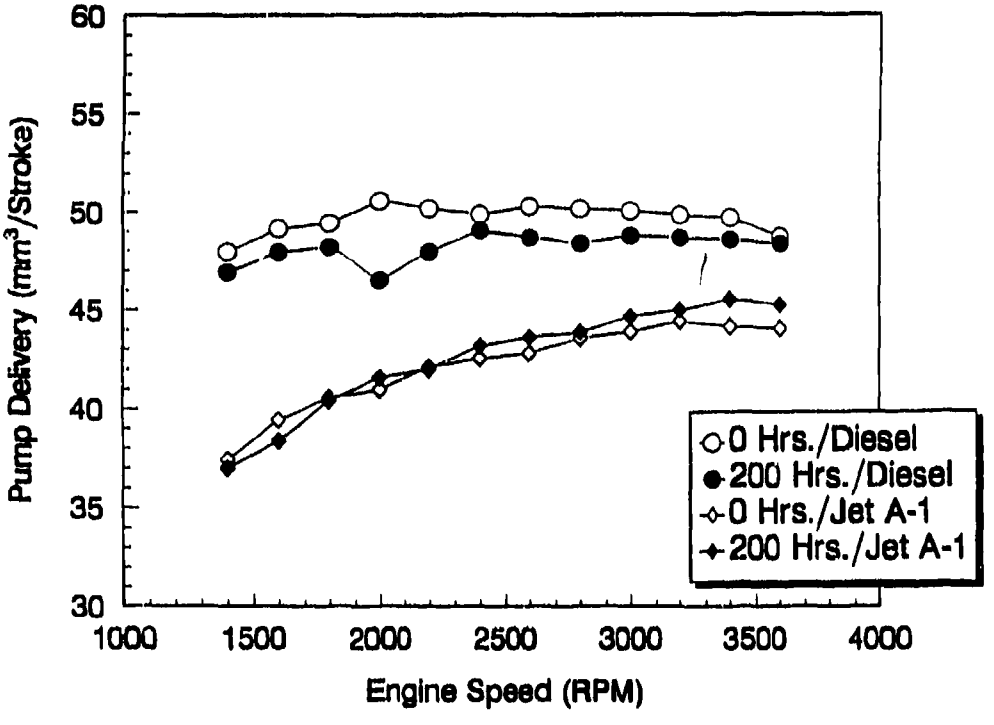

Figure E-6. Fuel delivery during engine tests with Pump No. 5 — standard pump tested for 200 hours on wet JP-8

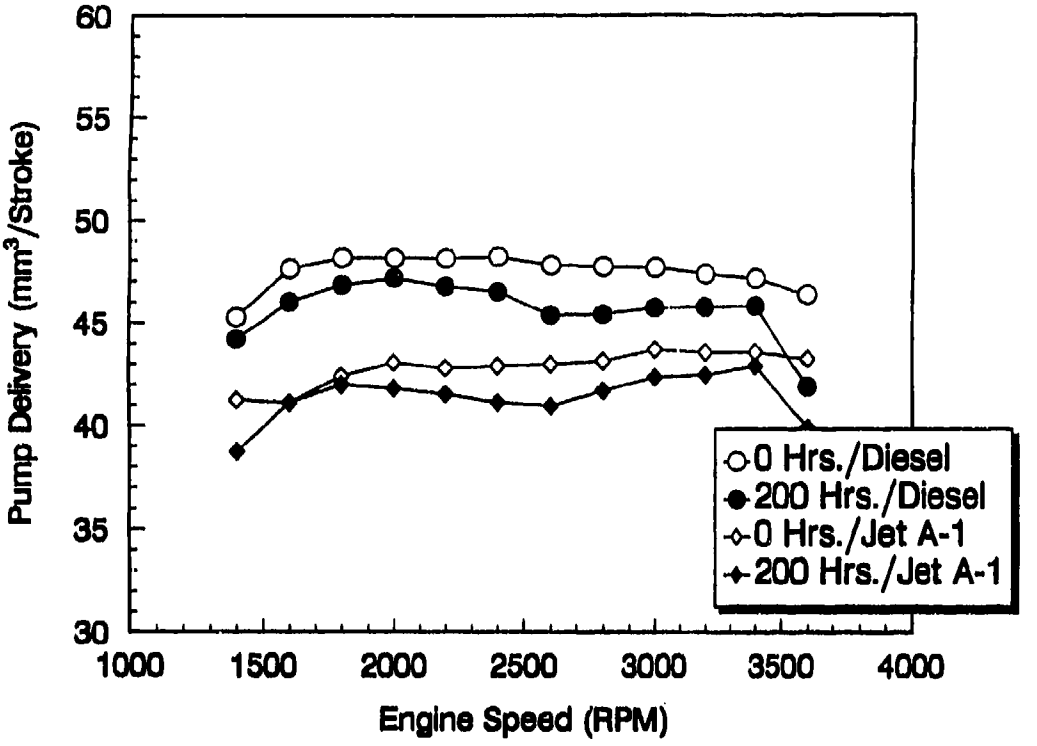

Figure E-7. Fuel delivery during engine tests with Pump No. 6 — arctic pump tested for 200 hours on wet JP-8

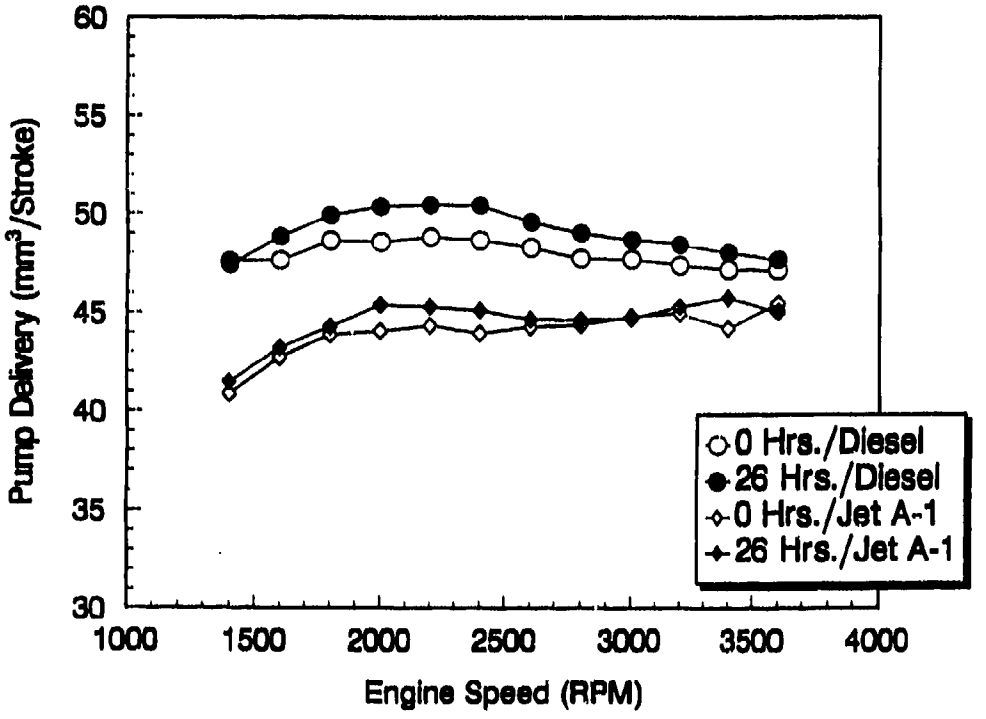

Figure E-8. Fuel delivery during engine tests with Pump No. 8 — arctic pump tested for 26 hours on wet Jet A-1 at 32°C (90°F)

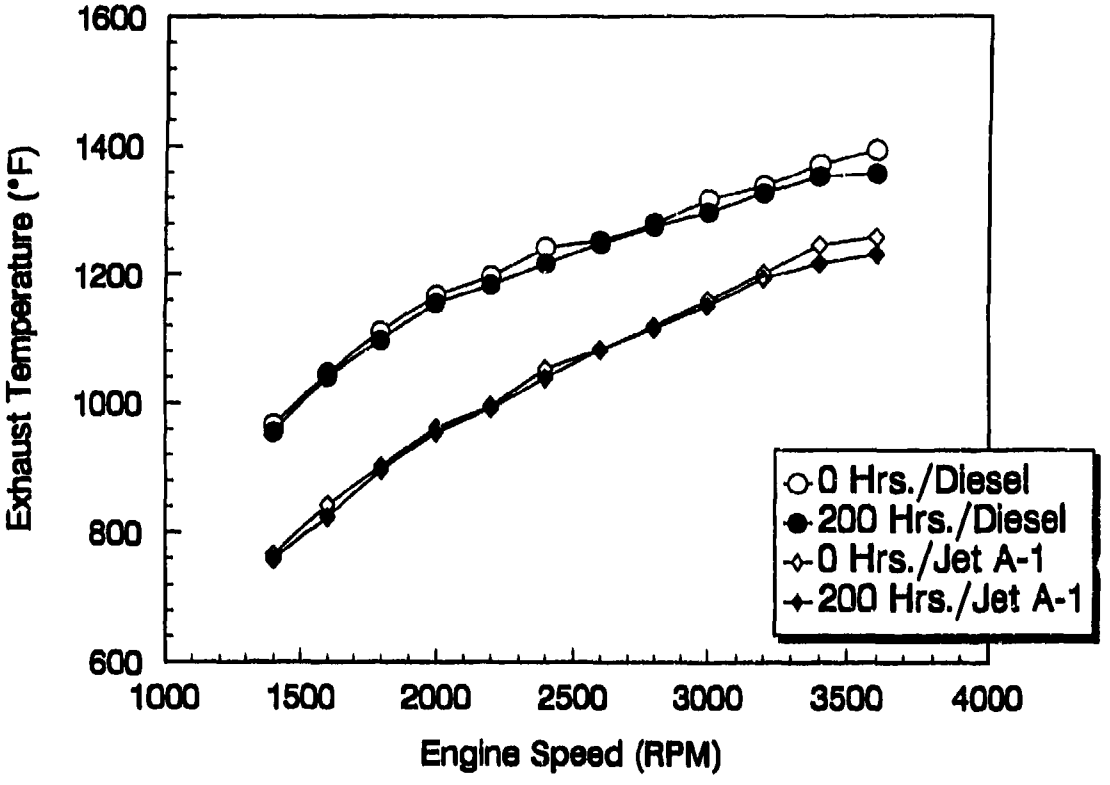

Figure E-9. Average exhaust temperature during engine tests with Pump No. 5 — standard pump tested for 200 hours on wet JP-8

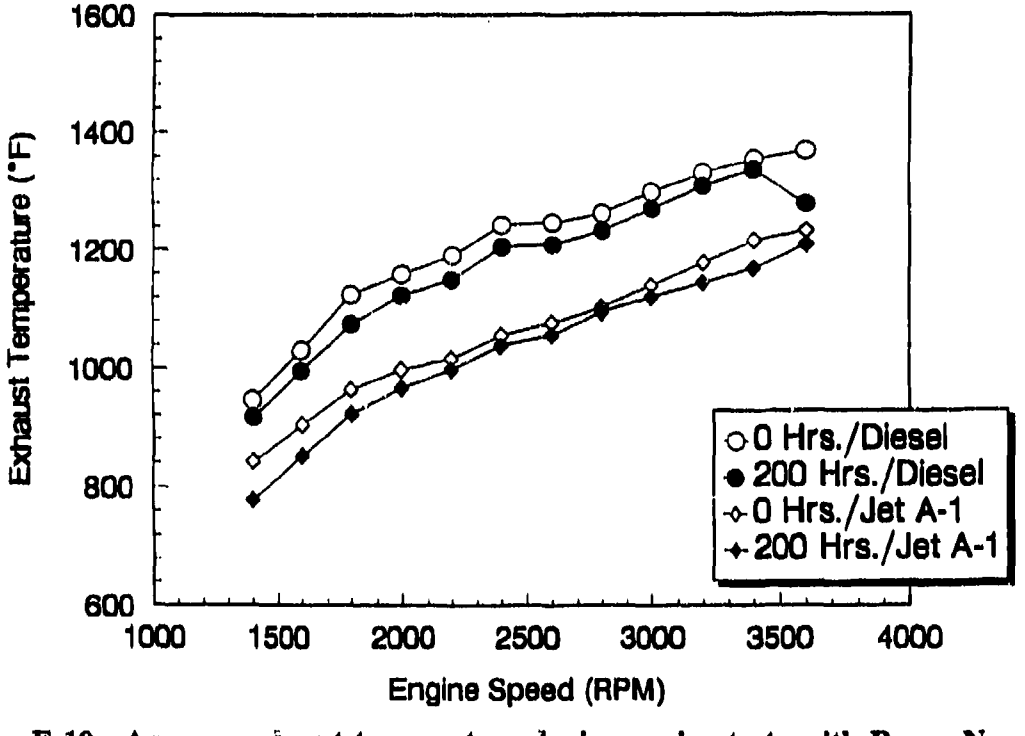

Figure E-10. Average exhaust temperature during engine tests with Pump No. 6 — arctic pump tested for 200 hours on wet JP-8

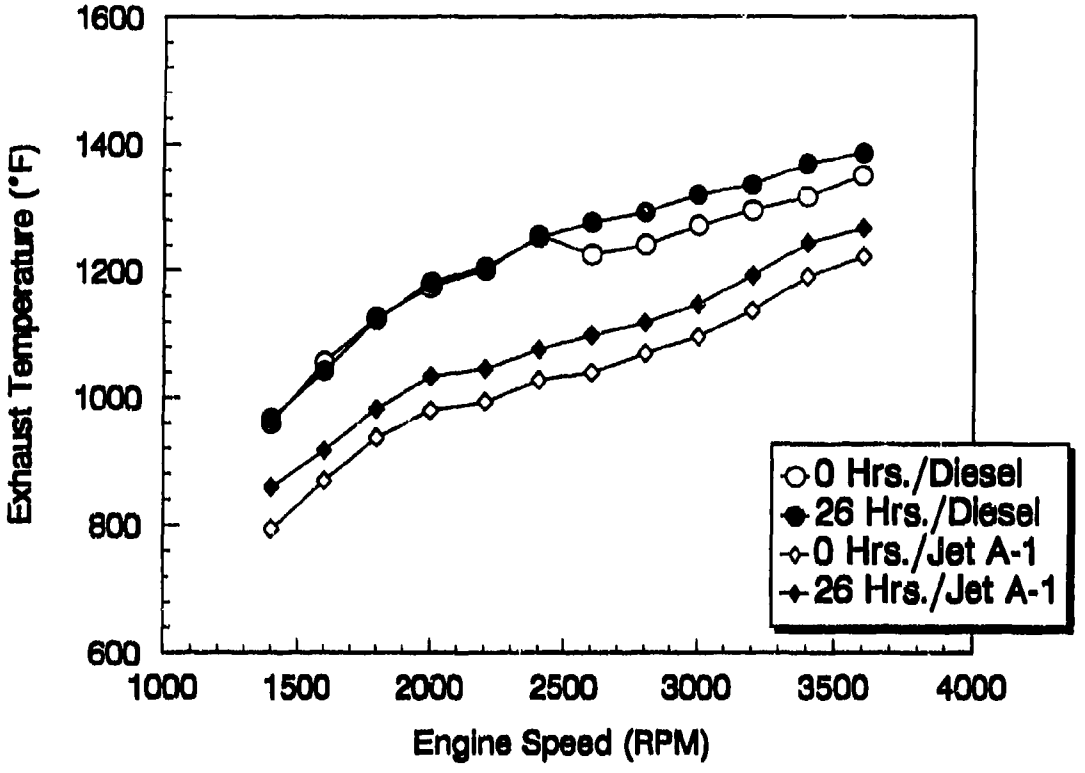

Figure E-11. Average exhaust temperature during engine tests with Pump No. 8 — arctic pump tested for 26 hours on wet Jet A-1 at 32°C (90°F)

APPENDIX F

Selected Fuel Characteristic Illustrations

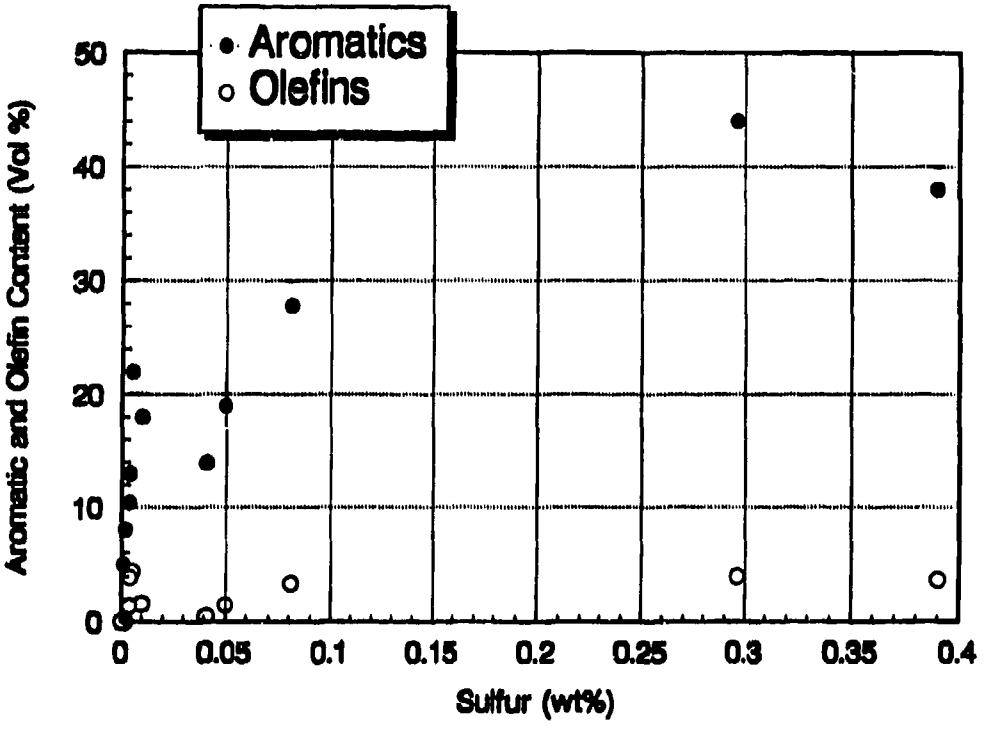

a. Relationship Between Sulfur, Aromatic, and Olefin Content

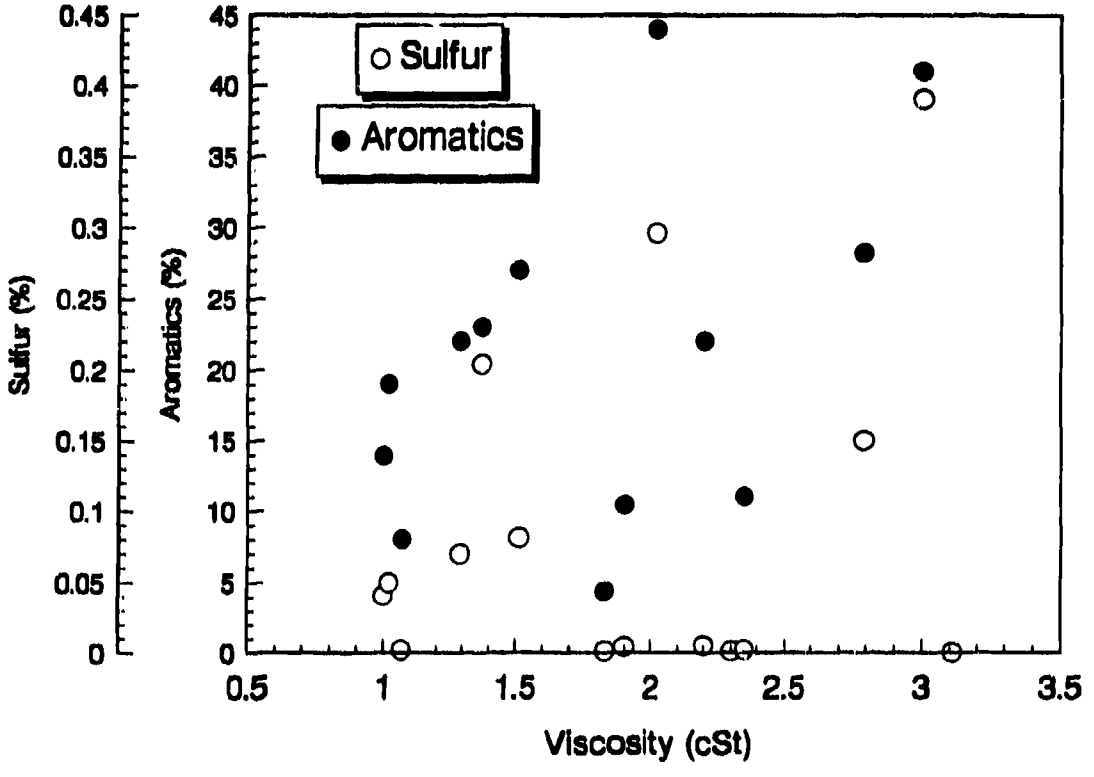

b. Relationship Between Sulfur/Aromatic Content and Viscosity

Figure F-1. Effects of refinery severity

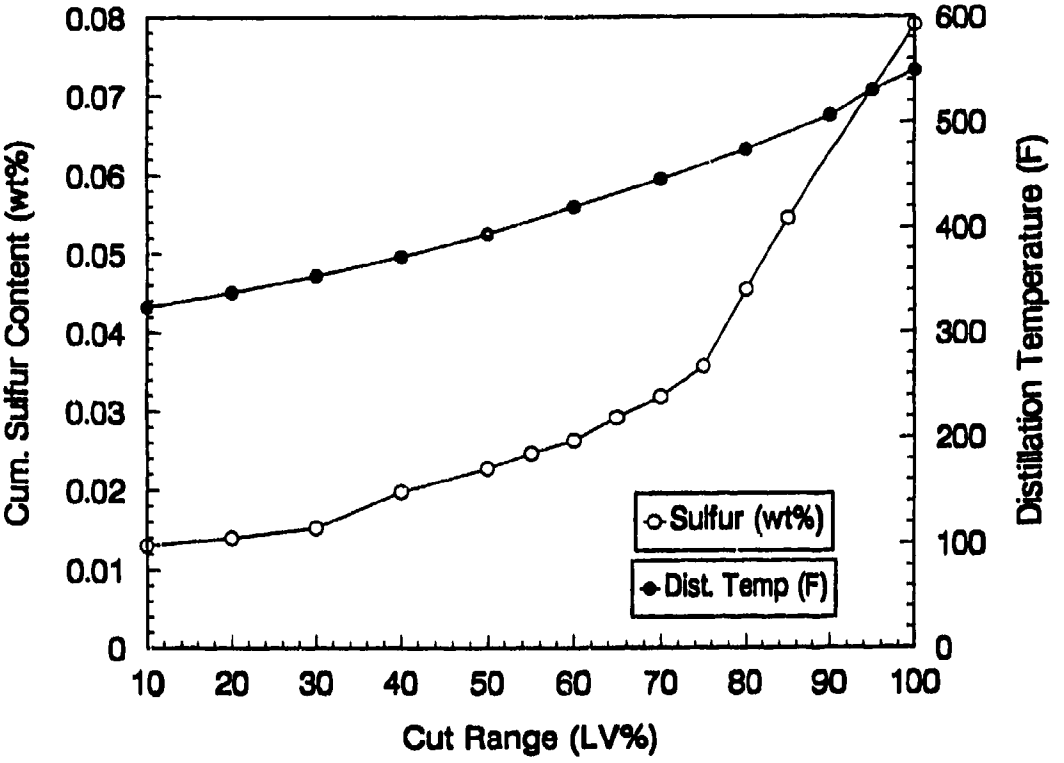

a. Fuel O

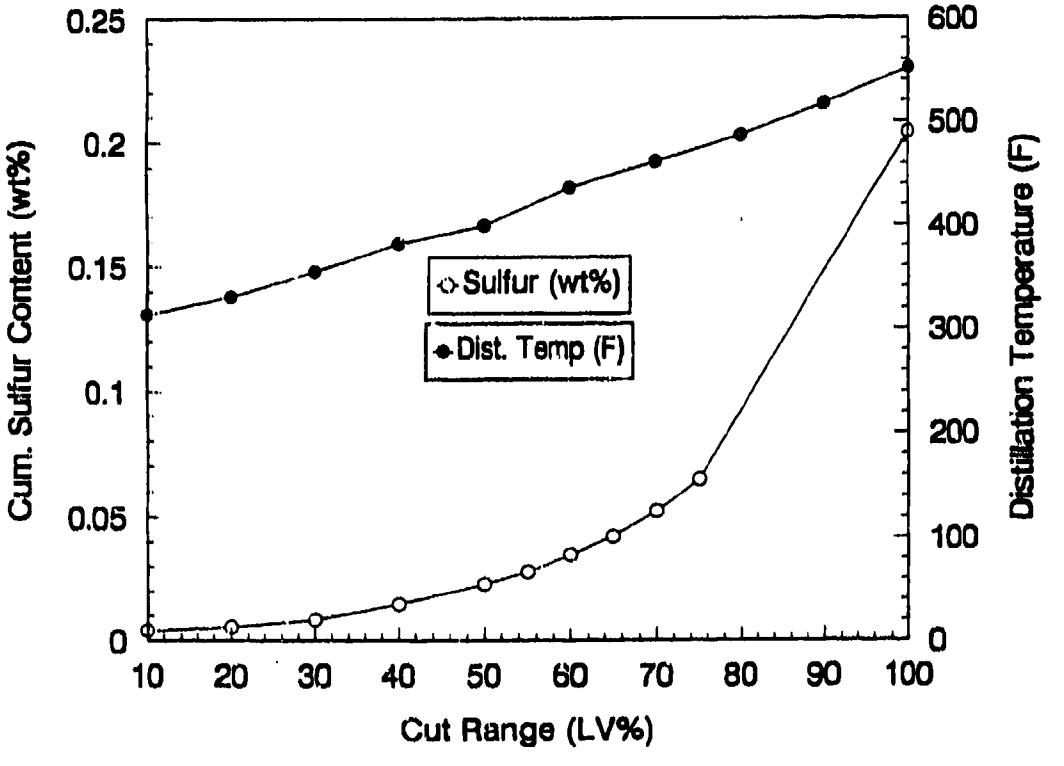

b. Fuel P

Figure F-2. Distillation properties of selected fuels from TABLE 2

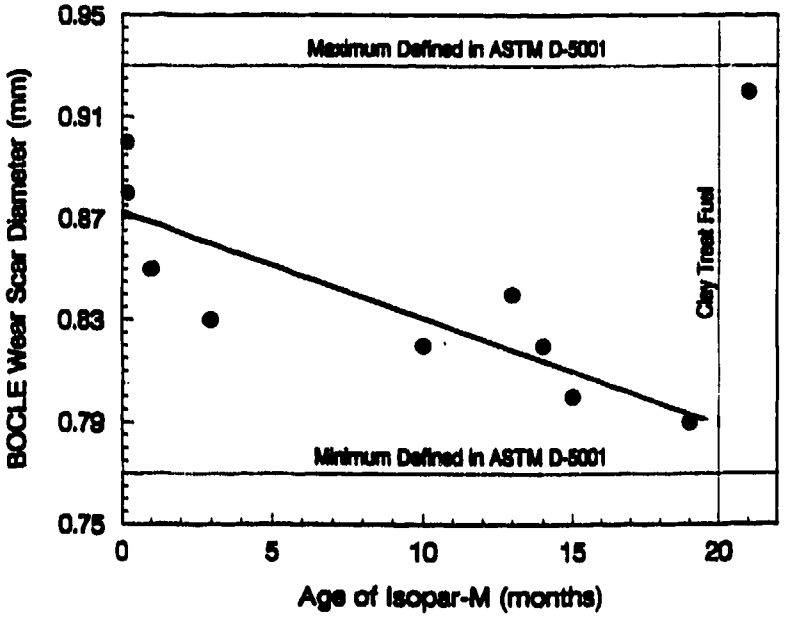

(Fuel was stored in an unlined steel container.)

Figure F-3. Effect of reference fluid (ISOPAR M) age on tests performed according to ASTM D 5001

APPENDIX G

Effects of Temperature on the BOCLE

EFFECTS OF TEMPERATURE ON THE BOCLE

Low-lubricity fuels have been successfully used in arctic conditions with no apparent effect on durability. However, full-scale pump tests over a range of temperatures higher than those found in the arctic failed to show any correlation with temperature, as detailed in Appendix B. To better define the effects of low temperatures, a nonstandard chilled BOCLE test procedure was developed. During these tests, the base of the fuel reservoir was cooled using recirculated ethylene glycol provided by a small refrigeration unit. However, no facilities were available to chill the incoming air or the humidifier in the BOCLE unit. Instead, 1 milliliter of distilled water was added to the standard 50 milliliters of fuel to ensure complete moisture saturation, reflecting the full-scale pump test conditions reported in Appendix B.

Initially, the fuel reservoir including the test ball and ring was insulated from the surrounding atmosphere and allowed to reach thermal equilibrium over a period of 45 minutes. However, severe wear at all temperatures and very poor repeatability was achieved, due to moisture condensation on the cool test ring. Subsequently, 3.8 liters of dry air were passed over the test fluid per minute to eliminate the humid surrounding environment. (Note: moisture remained available to the fuel from the 1 cubic centimeter of water present in the reservoir.)

The BOCLE result is a strong function of temperature, and wear volume increases by approximately an order of magnitude between –7° and 50°C, with the results shown in Fig. G-1. Previous workers have noted directionally similar effects, but over a narrow temperature range.* This temperature dependence is unlikely to be due solely to increasing hydrodynamic lift, as a very low viscosity Jet A-1 was used (1.07 cSt at 40°C). Surprisingly, wear rate at 25°C under the present nonstandard saturated moisture conditions is less than the 0.72 mm obtained for this fuel during the standard aerated test at the same temperature. This effect may be due to evaporation of moisture from the otherwise saturated fuel carried by the test ring to the perfectly dry surrounding atmosphere.

* "Aviation Fuel Lubricity Evaluation," CRC Report No. 560, Coordinating Research Council, 219 Perimeter Center Parkway, Atlanta, GA, July 1988.

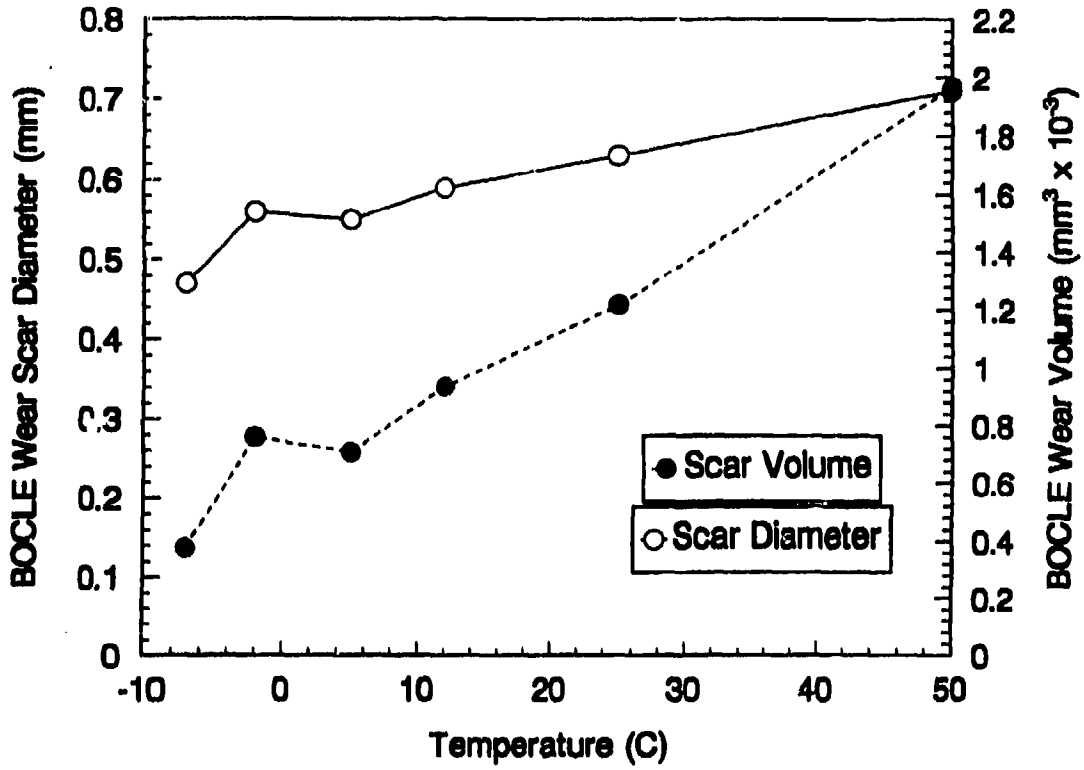

Figure G-1. Effect of fuel temperature on nonstandard BOCLE wear test results

The quantity of water dissolved in aircraft fuels is determined by the partial pressure of water in the vapor space above the fuel as illustrated in Fig. G-2.* When this vapor space is saturated with water at a given temperature, i.e., 100 percent relative humidity, the water dissolved in the fuel will reflect the values shown in Appendix F. Under cool conditions, such as those typically encountered in Alaska, the moisture content of the fuel will remain low. This effect was not observed during the full-scale pump test at the lower temperature described in Appendix B, as the temperature of the fuel reservoir remained unchanged at 90°C. As a result, the fuel moisture content was unchanged, even though the fuel inlet temperature to the pump was reduced, i.e., the fuel heater is between the reservoir and the pump.

* "Handbook of Aviation Fuel Properties," CRC Report No. 530, Coordinating Research Council, 219 Perimeter Center Parkway, Atlanta, GA, 1983.

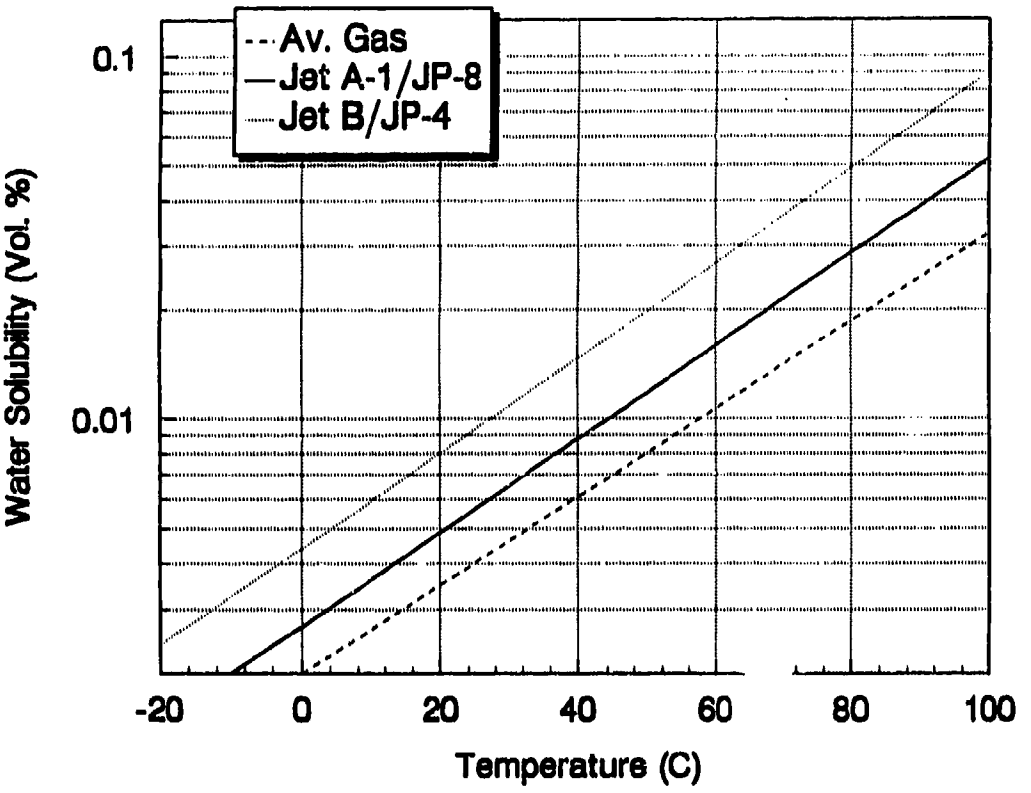

Figure G-2. Water solubility versus temperature for aircraft fuels*

Previously, nonstandard BOCLE wear tests were performed at higher temperatures than those of the present report.** However, erratic test results were obtained for clay-treated Jet A-1. Other workers have also observed this effect and suggest that it may be due to competition between increased rates of fuel oxidation and surface corrosion at temperatures above the standard 25°C specified in ASTM D 5001.† Fuel evaporation may also be a contributing factor. Indeed, low-volatility fuels are known to give more precise results, even under the standard ASTM test conditions.‡

---

* "Handbook of Aviation Fuel Properties," CRC Report No. 530, Coordinating Research Council, 219 Perimeter Center Parkway, Atlanta, GA 30346, 1983.

** Lacey, P.I. and Lestz, S.J., "Fuel Lubricity Requirements for Diesel Injection Systems," Interim Report BFLRF No. 270, AD A235972, February 1991.

† Biddle, T.B. and Edwards, W.H., "Evaluation of Corrosion Inhibitors as Lubricity Improvers," AD A198743, AF Wright Aeronautical Laboratories, July 1988.

‡ "Aviation Fuel Lubricity Evaluation," CRC Report No. 560, Coordinating Research Council, 219 Perimeter Center Parkway, Atlanta, GA 30346, July 1988.

APPENDIX H

Results Obtained in Scuffing Load Tests

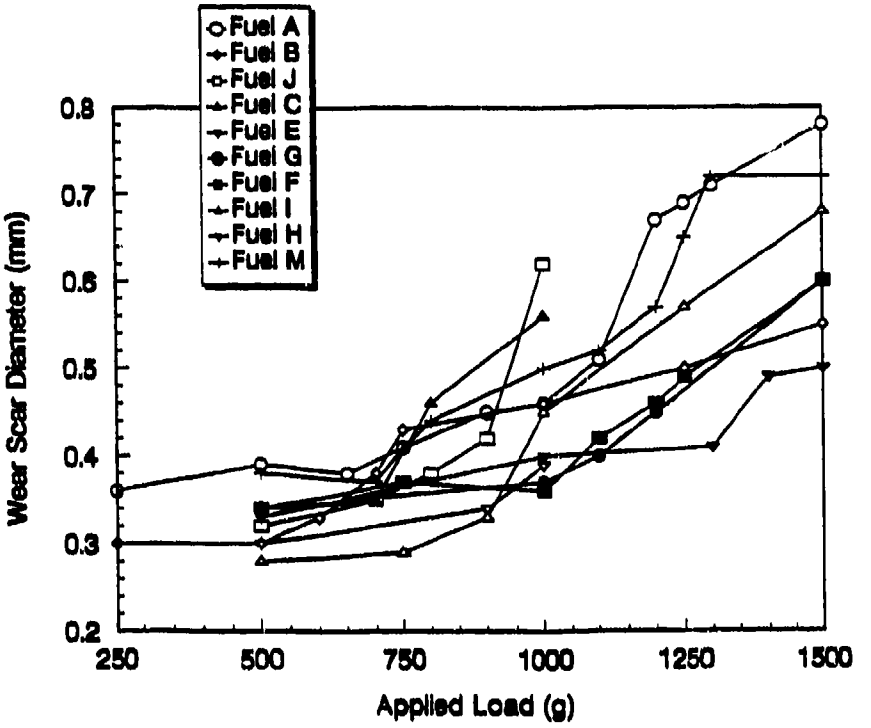

a. Wear Scar Diameter

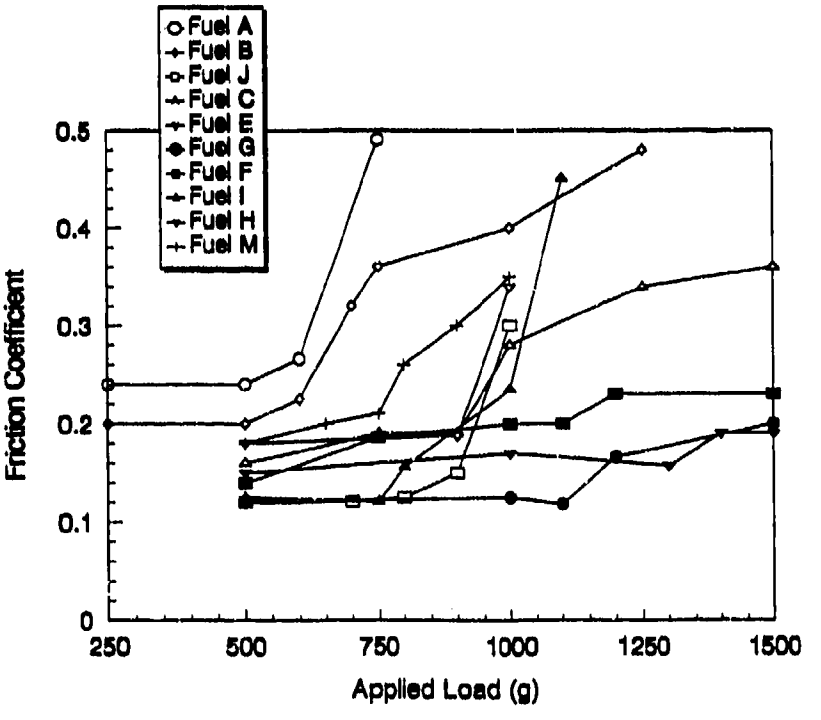

b. Friction Coefficient

Figure H-1. Data obtained during BOCLE scuffing load wear test performed according to *Procedure C* with fuels detailed in TABLE 2 of main report

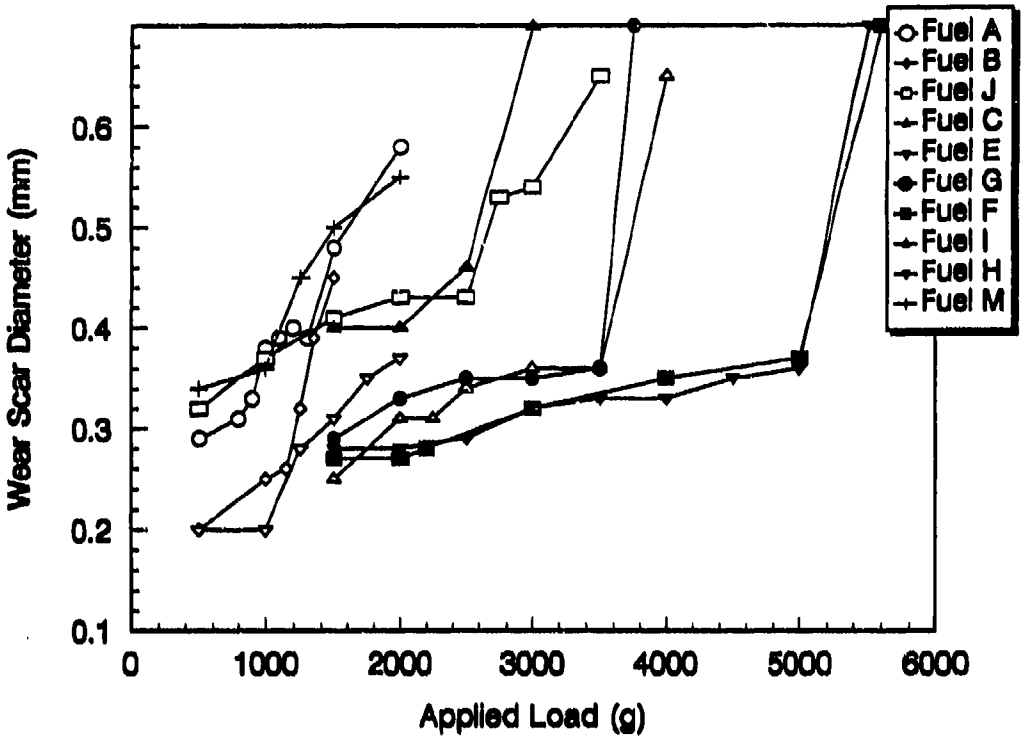

a. Wear Scar Diameter

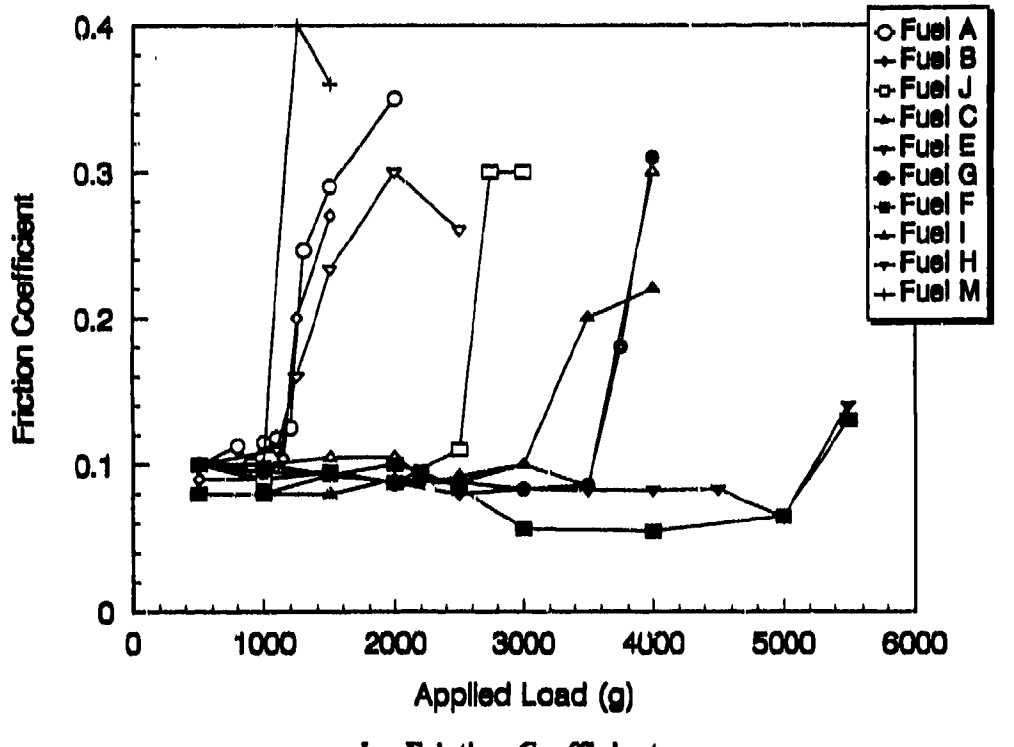

b. Friction Coefficient

Figure H-2. Data obtained during BOCLE scuffing load wear test performed according to *Procedure D* with fuels detailed in TABLE 2 of main report

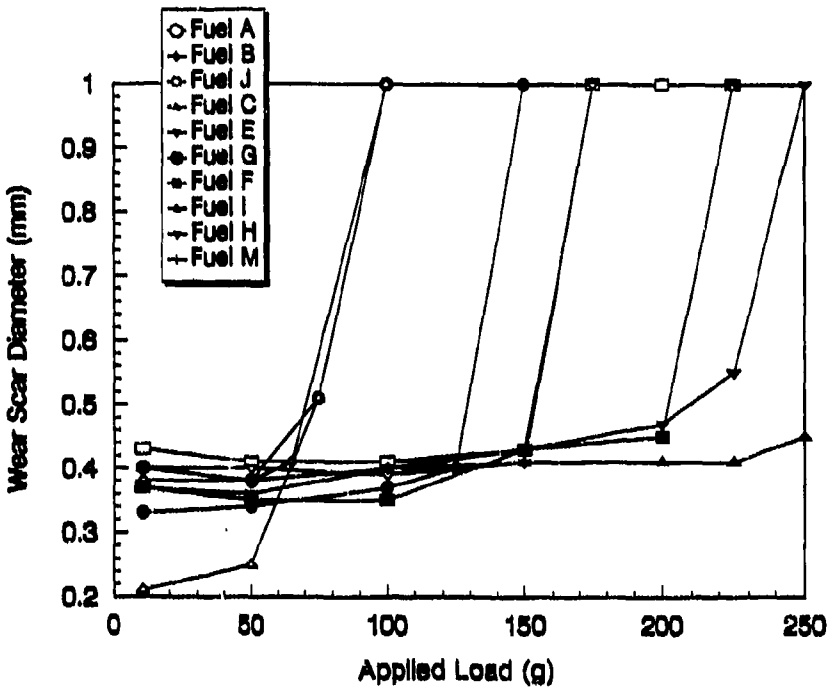

Figure H-3. Data obtained during Cameron-Plint scuffing load wear tests performed according to *Procedure F* with fuels detailed in TABLE 2 of main report

APPENDIX I

Calculation of Hertzian Contact Diameter

CALCULATION OF HERTZIAN CONTACT DIAMETER

The geometrical contact area formed by two normally loaded counterformal contacts may be calculated using the Hertzian equations as described in Wear Control Handbook, 1980. The analysis assumes that the surfaces are perfectly smooth, the effects of tangential loading and friction are negligible, and that the deformation is elastic (rather than plastic).

The ball-on-cylinder geometry formed in the BOCLE produces an elliptical contact. A simplified technique to derive the major (a) and minor (b) axis dimensions produced by two contacting solids with different radii of curvature in a pair of principal planes (x and y), is as follows:

$$a = \left[\frac{\left(6 * K^2 * E * w * R_s\right)}{\left(\pi * E\right)} \right]^{0.333}$$

$$b = \left[\frac{\left(6 * F * w * R_s\right)}{\left(\pi * E * K\right)} \right]^{0.333}$$

Where: $K = 1.0399(R^x/R^y)^{0.636}$

$R_x = (1/R_{x1} + 1/R_{x2})^{-1}$

$R_y = (1/R_{y1} + 1/R_{y2})^{-1}$

$R_s = (1/R_x + 1/R_y)^{-1}$

$F = 1.0003 + 0.5968/(R_y/R_x)$

w = Applied Load (N)

$E = 2\,[(1-\upsilon_1^2)/E_1 + (1-\upsilon_2^2)/E_2]$

For the contact geometry formed by the BOCLE:

$E = 0.227 * 10^6$ N/mm^2

$R_{x1} = R_{y1} = 6.35$ mm

$R_{x2} = 24.5$ mm

$R_{y2} = \alpha$

$w = 9.81$ N.

For an initial applied load of 1 kg, the length of the semimajor and semiminor axis formed during the BOCLE test are 0.16 and 0.135 mm, respectively. The mean contact pressure is predicted to be 578 N/mm^2.

The radial contact deformation at the center of the contact may be calculated from the following equation:

$$\delta = G\left[\left(\frac{1}{2} * R_S * F\right)\left(3 * \frac{w}{\pi KE}\right)^2\right]^{0.0333}$$

where $F = 1.5277 + 0.6023\ln(R_y/R_x)$.

For the standard contact conditions in the BOCLE test, the calculated radial contact deflection is 0.19 μm.

APPENDIX J

Characteristics of Test Surfaces

CHARACTERISTICS OF TEST SURFACES

Ring specimens of varying roughness were obtained by successively polishing the surface of ASTM standard test ring to obtain the required finish. (Note: The original surface finish on many test rings was marginally greater than that specified in ASTM D 5001.) The test rings were initially treated using 600-grit abrasive paper, followed by crocus cloth and finished using successively finer grades of diamond lapping paste. The duration of each step was varied, depending on the finish required. Particular attention was given to the polished specimen to ensure a repeatable mirror finish, free of waviness and blemishes. The ring must be maintained perpendicular to the cloth during treatment to prevent formation of bevelled edges.

Surface roughness was measured using a Talysurf 10 profilometer with a stylus tip width of 0.0025 mm. The trace was taken over 7 mm of surface and filtered with a cut off of 0.25 mm to remove long wavelength undulations. This value approximates the wear scar diameter of many scuffing load tests. A segment of the surface trace and corresponding height density/distribution (bearing area) is shown in Figs. J-1 through J-5 for each of the ring types used in the present study. (Note: Traces for the most highly polished specimen are not included as little surface roughness was apparent.)

The probability distribution (bearing area curve) represents the fraction of solid material [$P(z)$] lying above a certain datum (z) and may be defined as:

$$P(z) = \int_{-\infty}^{\infty} p(z)d(z)$$

with $P(-\infty) = 0$ and $P(\infty) = 1$.

The probability density function [$p(z)$] is the first derivative of the probability distribution and can be defined as $p(z) = dP(z)/d(z)$ and a gaussian or normal distribution is given by:

$$P(z) = \left(\frac{1}{\sigma_H\sqrt{2\pi}}\right)\exp\left(\frac{-z^2}{2\sigma_H{}^2}\right)$$

with $\sigma_H = Rq$.

The Root Mean Square (*Rq*), skewness (*Rsk*), and kurtosis (*Rk*) of the profile height distribution are also provided, and may be defined as follows:

$$Rq = \sigma_H = \sqrt{-\infty\int^{\infty} z^2\ p(z)d(z)}$$

$$Rsk = 1/\sigma_H{}^3 \ _{-\infty}\int^{\infty} z^3\ p(z)d(z)$$

$$Rk = 1/\sigma_H{}^4 \ _{-\infty}\int^{\infty} z^4\ p(z)d(z)$$

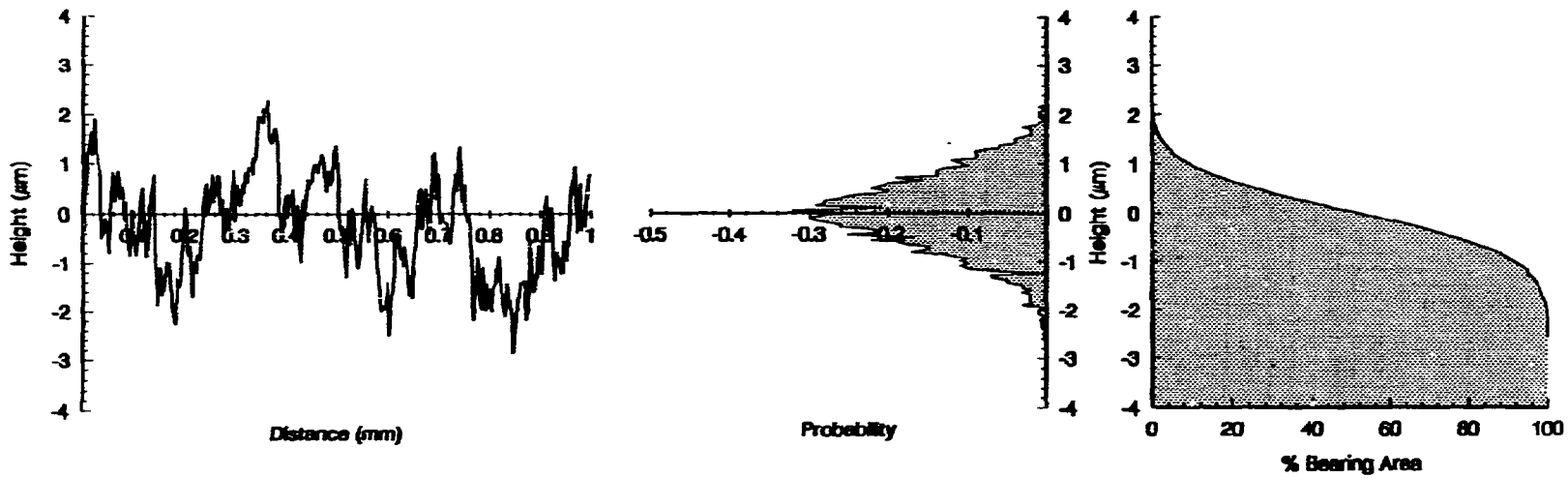

Figure J-1. Standard specimen, Rq = 0.7 µm, Rku = 2.91, Rsk = -0.7 (*Procedures A, B,* and *C*)

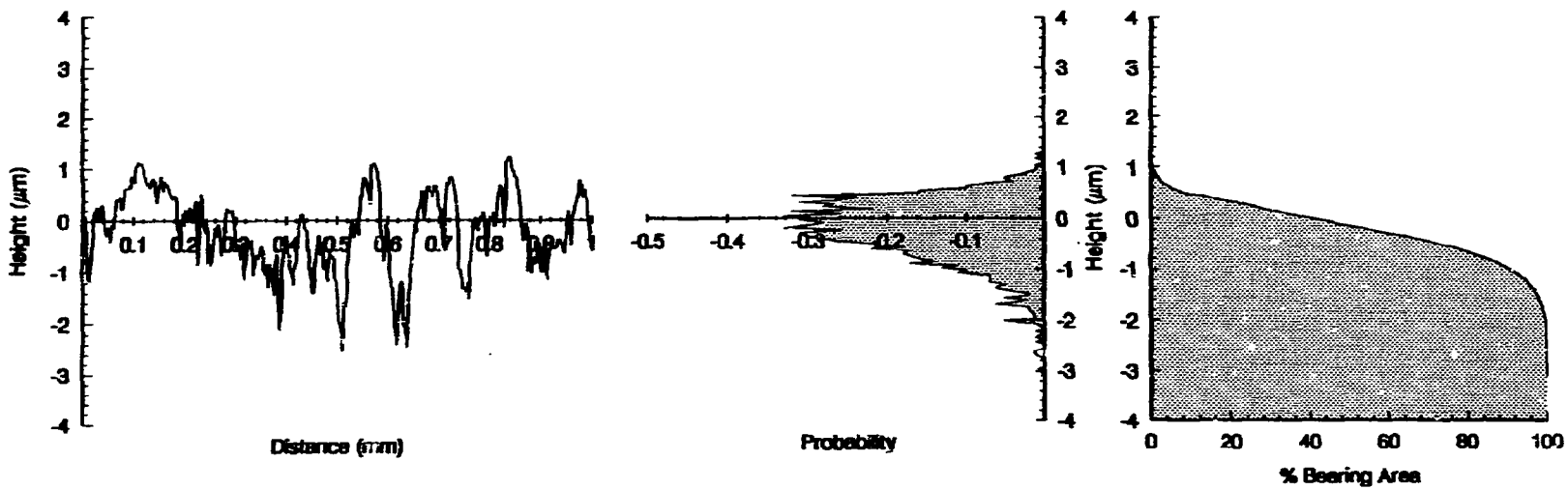

Figure J-2. Two-process finish, Rq = 0.59 µm, Rku = 3.6, Rsk = -0.67

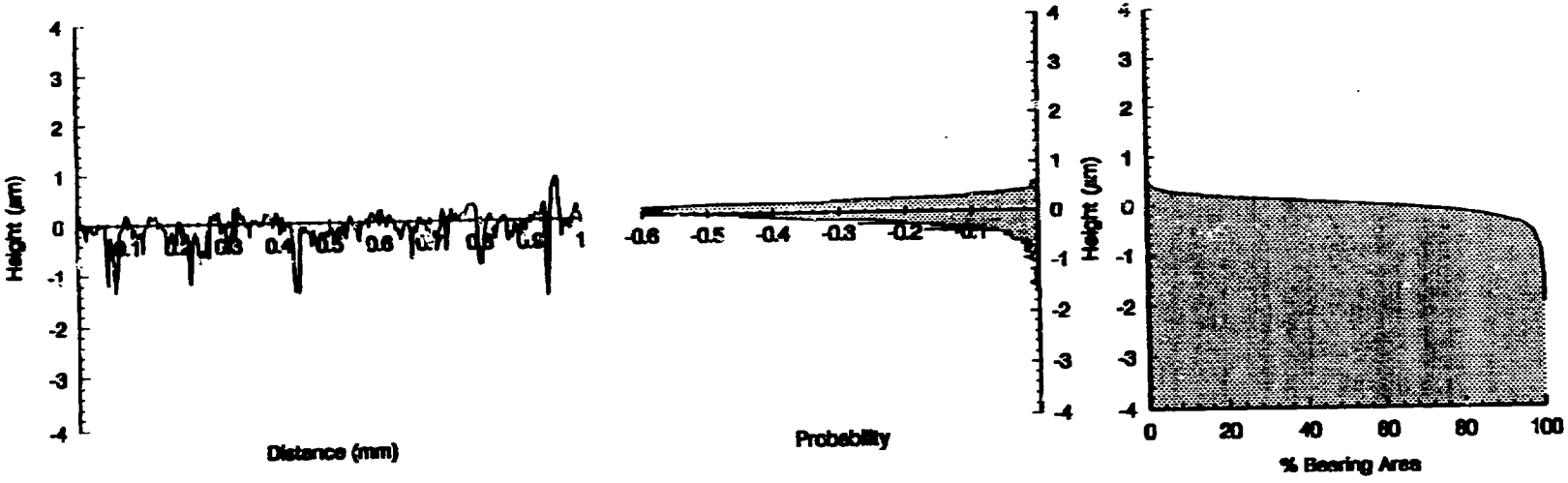

Figure J-3. Two-process finish, Rq = 0.25 µm, Rku = 9.81, Rsk = -1.85

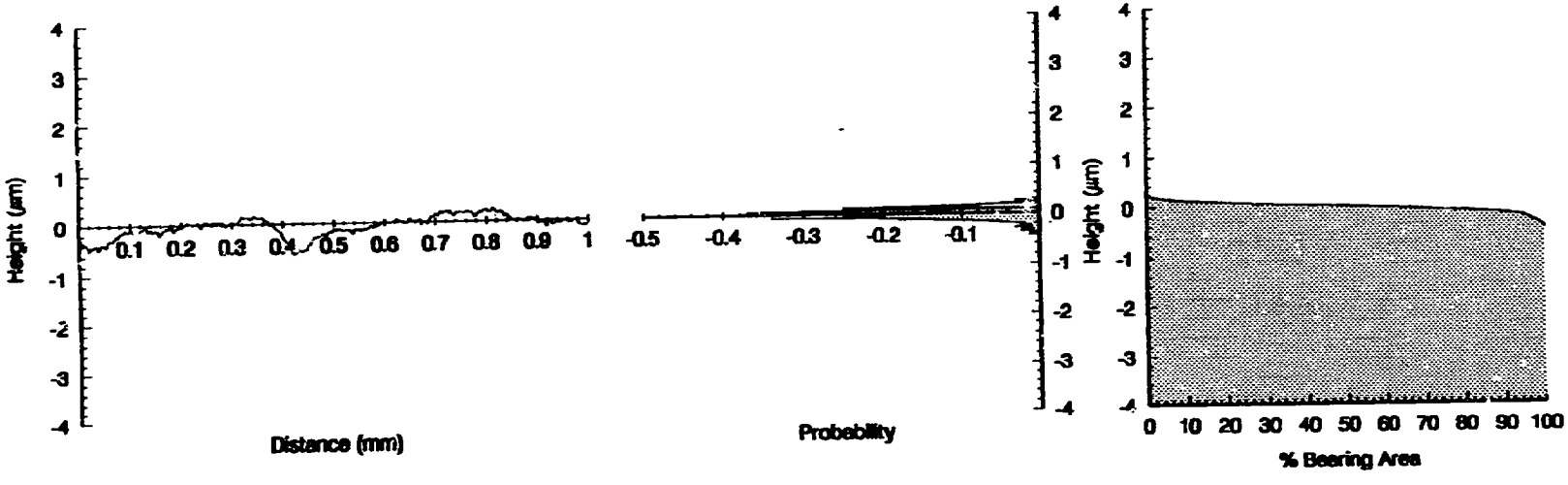

Figure J-4. Two-process finish, Rq = 0.11 µm, Rku = 3.88, Rsk = -0.63

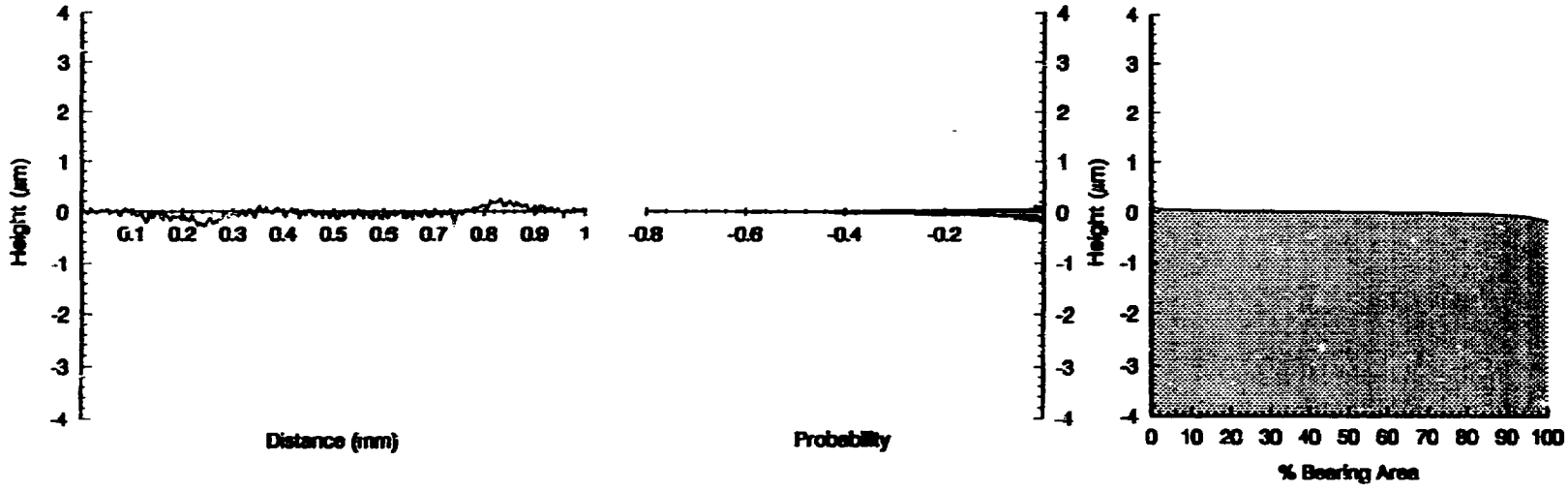

Figure J-5. Polished specimen, Rq = 0.04 µm, Rku = 5.06, Rsk = -0.94 (*Procedures D* and *E*)

APPENDIX K

Suggested Test Procedure for Measurement of Scuffing Load Capacity Using the Ball-on-Cylinder Lubricity Evaluator (BOCLE)

THE U.S. ARMY SCUFFING LOAD WEAR TEST

Suggested Test Procedure for Measurement of Scuffing Load Capacity Using the Ball-on-Cylinder Lubricity Evaluator (BOCLE)*

01 January 1994

* Note: The following is a draft test procedure. This test procedure is based on ASTM D 5001 and contains changes made solely by the Belvoir Fuels and Lubricants Research Facility (BFLRF). Comments, additions, and changes should be addressed to Dr. P.I. Lacey, Belvoir Fuels and Lubricants Research Facility (SwRI), Southwest Research Institute, P.O. Drawer 28510, San Antonio, Texas 78228-0510.

1. Scope

1.1. This test method assesses the severe wear aspects of the boundary lubrication properties of fuels intended for use in compression ignition equipment on rubbing steel surfaces.

1.2. The values stated in SI units are to be regarded as the standard.

2. Referenced Documents

2.1. *ASTM Standards:*

D 329 Specification for Acetone[1]

D 770 Specification for Isopropyl Alcohol[1]

D 1016 Test Method for Purity of Hydrocarbons From Freezing Points[2]

D 4306 Practice for Sampling Aviation Fuel for Tests Affected by Trace Contamination[3]

2.2. *Military Specification:*

MIL-I-25017, Inhibitor, Corrosion/Lubricity Improver, Fuel Soluble[4]

2.3. *American Iron and Steel Institute Standard:*

AISI E-52100 Chromium Alloy Steel[5]

2.4. *American National Standards Institute Standard:*

ANSI B3.12, Metal Balls[6]

2.5. *Society of Automotive Engineers Standard:*

SAE 8720 Steel[7]

3. Terminology

3.1. *Descriptions of Terms Specific to This Procedure:*

3.1.1. *Cylinder*—the polished test ring and mandrel assembly.

3.1.2. *Lubricity*—a property of the fluid, measured by the minimum applied load, in grams, that will produce a transition from mild boundary lubricated wear to adhesive scuffing between a stationary ball and a fluid-wetted rotating ring operating under closely controlled conditions.

4. Summary of Test Method

4.1. The fluid under test is placed in a test reservoir in which atmospheric air is maintained at 50% relative humidity. A nonrotating steel ball is held in a vertically mounted chuck and forced against an axially mounted *polished* steel ring. The applied load is increased until a disproportionate change in friction and wear is observed. Any sequence of increasing loads may be selected to most efficiently define

---

1 *Annual Book of ASTM Standards*, Vol 06.03.
2 *Annual Book of ASTM Standards*, Vols 05.01 and 06.03.
3 *Annual Book of ASTM Standards*, Vol 05.03.
4 Available from Naval Publications and Form Center, 5801 Tabor Ave., Philadelphia, PA 19120.
5 Available from American Iron and Steel Institute, 1000 16th Street, NW, Washington, DC 20036.
6 Available from American National Standards Institute, 1430 Broadway, New York, NY 10018.
7 Available from Society of Automotive Engineers, Inc., 400 Commonwealth Ave., Warren, PA 15096.

the point at which either friction or wear exceeds defined limits. The fuel is not renewed between load increments during a normal test sequence. The test cylinder is rotated at a fixed speed while being partially immersed in the fluid reservoir. This partial immersion maintains the cylinder in a wet condition and continuously transports the test fluid to the ball/cylinder interface. The minimum applied load required to produce a transition to severe friction and wear is a measure of the fluid-lubricating properties.

5. Significance and Use

5.1. Severe wear resulting in shortened life of components on compression-ignition engines such as fuel pumps has sometimes been ascribed to lack of lubricity in highly refined fuel.

5.2. The relationship of test results to rotary fuel injection pump distress due to wear has been demonstrated for some fuel/hardware combinations in which boundary lubrication is a factor in the operation of the component.

5.3. The scuffing load capacity in the Ball-on-Cylinder Lubricity Evaluator (BOCLE) test is sensitive to contamination of the fluids and test materials, the presence of oxygen and water in the atmosphere, and the temperature of the test. Lubricity measurements are also sensitive to trace materials acquired during sampling and storage. Containers specified in Practice D 4306 shall be used.

5.4. Initial tests with many different procedures indicate that correlation achieved with full-scale equipment may be affected by viscosity, particularly if viscosity is below approximately 1.8 cSt at 40°C.

5.5 *Simplification of Procedure*

5.5.1. If desired, the incremental-load procedure described in Section 10 may be modified to a single-load test at a test load to be defined.

5.5.2. The single-load test has been found to approximate full-scale equipment needs and to provide a simple pass/fail result.

5.5.3. The single-load test does not provide a quantitative ranking of fuels in either the pass or fail categories.

6. Apparatus

6.1. *Ball-on-Cylinder Lubricity Evaluator (BOCLE).*

6.1.1. The test requirements are listed in TABLE K-1.[8]

6.1.2. If possible, the apparatus should facilitate accurate measurement of tangential friction. However, accurate determination of scuffing load capacity is possible without friction measurement.

6.1.3. The inclusion of a small splash guard within the fluid reservoir is necessary to prevent loss of fluid from the joint between the reservoir cover and reservoir.

6.2. *Constant Temperature Bath-Circulator,* capable of maintaining the fluid sample at 25° ± 1°C when circulating coolant through the base of the sample reservoir.

---

[8] BOCLE units, BOC 100, made by InterAv, Inc., P.O. Box 792228, San Antonio, TX 78279 have been found to be satisfactory.

TABLE K-1. Operating Conditions

Fluid Volume	50 ± 1.0 mL
Fluid Temperature	25° ± 1°C
Conditioned Air*	50 ± 1% relative humidity at 25° ± 1°C

Fluid pretreatment 0.50 L/min air flowing through and 3.3 L/min over the fluid for 15 min.
8.1 ft^3/hr = 3.8 L/min.
Fluid test conditions 3.8 L/min flowing over the fluid.

Applied Load	
Break-In Period	500 g
Incremental-Load Test	500 to 8,000 g
Single-Load Test	To be defined
Cylinder Rotational Speed	525 ± 1 r/min
Test Duration	
Break-In Period	30 sec
Scuff Tests	60 sec

*Note: 50% humidity should be achieved using equal volumes of dry and saturated air.

6.3. *Microscope,* capable of 100× magnification in graduations of 0.1 mm and incremented in divisions of 0.01 mm.

6.3.1. *Glass Slide Micrometer,* with a scale ruled in 0.01 mm divisions.[9]

6.4. *Cleaning Bath*—Ultrasonic seamless stainless steel tank with a capacity of 1.9 L (0.5 gal) and a cleaning power of 40 W.

7. Reagents and Materials

7.1. *Test Ring,* of SAE 8720 steel, having a Rockwell hardness "C" scale (HRC) number of 58 to 62 and a surface finish of 0.015 μm root mean square. The remaining dimensions are similar to that described in ASTM D 5001.[10]

7.2. *Mandrel,* a 10° tapered short cylindrical section used for holding test ring.[11]

[9] Catalog No. 31-16-99 from Bausch and Lomb, Inc. has been found satisfactory. A certificate of traceability from the National Institute of Standards and Technology is available.

[10] Test Rings, Part No. F25061 from Falex Corp., 2055 Comprehensive Drive, Aurora, IL 60505, have been found satisfactory if polished to the required surface finish using only the procedure defined by the U.S. Army Belvoir Fuels and Lubricants Research Facility, P.O. Drawer 28510, San Antonio, TX 78228. Correct surface finish is central to test accuracy.

[11] Mandrel, Part No. M-O from Falex Corp., or P/N BOC-2101 from InterAv. Inc., P.O. Box 792228, San Antonio, TX 78279, has been found satisfactory.

7.3. *Test Ball,* chrome alloy steel, made from AISI standard steel No. E-52100, with a diameter of 12.7 mm (0.5 in.) grade 5 to 10 EP finish. The balls are described in ANSI Specification B3.12. The extra-polish finish is not described in that specification. The HRC shall be 64 to 66, a closer limit than found in the ANSI requirement.[12]

7.4. *Compressed Air,* containing less than 0.1 ppm hydrocarbons and 50 ppm water.

7.5. *Desiccator,* containing a nonindicating drying agent, capable of storing test rings, balls, and hardware.

7.6. *Gloves,* clean, lint-free, cotton, disposable.

7.7. *Wiper,* wiping tissue, light-duty, lint-free, hydrocarbon-free, disposable.

7.8. *Isooctane,* conforming to Test Method D 1016, 95% purity minimum, 2,2,4-trimethylpentane.

7.9. *Isopropyl Alcohol,* conforming to Specification D 770.

7.10. *Acetone,* conforming to Specification D 329.

7.11. *Reference Fluids.*

7.11.1. *Fluid A*—Shall be Reference No. 2 (Cat 1-H) diesel fuel.[13] Store in borosilicate glass with an aluminum foil lined insert cap. Store in dark area.

7.11.2. *Fluid B*—Shall be a narrow-cut isoparaffinic solvent.[14]

8. Preparation of Apparatus

8.1. *Cleaning of Apparatus and Test Components:*

8.1.1. *Test Rings:*

8.1.1.1. The test rings shall be partially stripped of any wax-like protective coatings by manually rubbing them with rags or paper towels saturated with isooctane.

8.1.1.2. Place partially cleaned rings in a clean 500-mL beaker. Transfer a sufficient volume of a 1 to 1 mixture of isooctane and isopropyl alcohol to the beaker such that the test rings are completely covered.

8.1.1.3. Place beaker in ultrasonic cleaner and turn on for 15 min.

8.1.1.4. Remove test rings and repeat ultrasonic cleaning cycle of 8.1.1.2 and 8.1.1.3 with a clean beaker and fresh solvents.

8.1.1.5. Handle all clean test rings with clean forceps or disposable gloves. Remove test rings from beaker and rinse with isooctane. Dry. Rinse with acetone.

NOTE 1: Drying operations can be accomplished using a compressed air (7.4) jet at 140 to 210 kPa (20 to 30 psi) pressure.

8.1.1.6. Dry and store in a desiccator.

---

[12] Test Balls, SKF Swedish, Part No. 310995A, RB 12.7, grade 5 to 10 EP Finish, AISI 52100 Alloy from SKF Industries, Component Systems, 1690 East Race Street, Allentown, PA 90653, have been found satisfactory.

[13] Available from Howell Hydrocarbons, P.O. Box 429, Channelview, TX 77530.

[14] Solvent is ISOPAR M, manufactured by the Exxon Company, USA, P.O. Box 2180, Houston, TX 77001.

8.1.2. *Test Balls as Received.*

8.1.2.1. Place balls in 300-mL beaker. Transfer a sufficient volume of a 1 to 1 mixture of isooctane and isopropyl alcohol to the beaker such that the test balls are completely covered by the cleaning solvent.

NOTE 2: Approximately a 5-day supply can be processed at one time.

8.1.2.2. Place beaker in ultrasonic cleaner and turn on for 15 min.

8.1.2.3. Repeat the cleaning cycle of 8.1.2.1 and 8.1.2.2 with a clean beaker and fresh solvent.

8.1.2.4. Remove and rinse with isooctane, dry, rinse with acetone.

8.1.2.5. Dry and store in a desiccator.

8.1.3. *Reservoir, Reservoir Cover, Ball Chuck, Ball Lock Ring, and Ring Mandrel Assembly Components:*

8.1.3.1. Rinse with isooctane.

8.1.3.2. Clean for 5 min. in an ultrasonic cleaner with a 1 to 1 mixture of isooctane and isopropyl alcohol.

8.1.3.3. Remove and rinse with isooctane, dry, rinse with acetone.

8.1.3.4. Dry and store in a desiccator.

8.1.4. *Hardware:*

8.1.4.1. The hardware and utensils, that is, shaft, wrenches, and tweezers, that come in contact with the test fluid shall be cleaned by washing thoroughly with isooctane and wiping with a lint-free cloth.

8.1.4.2. Store parts in desiccator when not in use.

8.1.5. *After Test:*

8.1.5.1. Remove reservoir and cylinder.

8.1.5.2. Disassemble components and clean for 5 min. in an ultrasonic cleaner using a 1 to 1 mixture of isooctane and isopropyl alcohol. Rinse with isooctane, dry, rinse with acetone. Reassemble components.

8.1.5.3. Dry and store in a desiccator.

8.1.5.4. Care shall be taken to ensure that the fuel aeration tube is rinsed and dried during the cleaning procedure. Store parts in desiccator when not in use.

9. Calibration and Standardization

9.1. Visually inspect test balls and rings before each test. Discard specimens that exhibit pits, corrosion, or surface abnormalities.

9.2. *Reference Fluids:*

9.2.1. Test each new batch of the reference fluids and verify machine accuracy in accordance with Section 10.

9.2.2. The machine calibration should be verified once every twelve tests.

9.2.3. If desired, the test need only be performed at the two loads defined in Section 9.2.6 to verify test performance and accuracy.

9.2.4. Additional tests are necessary if the scuffing load capacities on Reference Fluids A and B lie outside the acceptable range.

9.2.5. Calculate the scuffing load capacity (SLC) in accordance with Section 13.0.

9.2.6. The following reference fluid values are preliminary: No scuffing should be produced at 4,500 and 900 g with Reference Fluids A and B, respectively. Scuffing should be produced at 5,100 and 1,400 g with Reference Fluids A and B, respectively.

9.3. *Leveling of Load Arm:*

9.3.1. The level of the load arm shall be inspected prior to each test. Level the motor platform by use of the circular bubble level and adjustable stainless steel legs.

9.3.2. Install a test ball in the retaining nut as described in Section 10.4.

9.3.3. Lower load arm. Attach required weight to end of load beam. Lower ball onto ring manually or by use of arm actuator switch.

9.3.4. Check level on top of load arm. The indicator bubble shall be centered in the middle of the two lines. If required, adjust the retaining nut screw to achieve a level load arm.

9.4. *Assembly of Cylinder:*

9.4.1. Place a clean test ring on the mandrel and bolt the back plate to the mandrel.

10. Procedure

10.1. The summary of test conditions is included in TABLE K-1.

10.1.2. The test procedure described in Sections 10.2 through 10.29 is repeated with a finite load change until scuffing is observed, as described in Section 13.

10.1.3. Any desired sequence of load increments may be selected to most rapidly converge on the scuffing transition. The loading sequence provided in the Addendum to this appendix is strongly recommended.

10.1.4. The test fluid should be replaced/aerated and the apparatus thoroughly cleaned after every eighth load increment.

10.2. *Installation of Cleaned Test Cylinder:*

NOTE 3: The BOCLE is very sensitive to contamination problems.

10.2.1. The greatest care shall be taken to adhere strictly to cleanliness requirements and to the specified cleaning procedures. During handling and installation procedures, protect cleaned test parts (cylinder, balls, reservoir, and reservoir cover) from contamination by wearing clean cotton gloves.

10.2.2. Rinse shaft with isooctane and wipe with disposable wiper.

10.2.3. Push the shaft through the left bearing and support bracket.

10.2.4. Hold the cylinder with the set screw hub facing left. Push the shaft through the cylinder bore, through the right bearing support bracket, and into the coupling as far as the shaft will go.

10.2.5. Align the coupling set screw with the flat keyway side of the cylinder shaft. Tighten set screw.

10.2.6. Set micrometer at 2.50 mm and slide cylinder to the left until it is firmly against micrometer probe. Ensure that cylinder set screw is directed toward the keyway (flat surface of shaft) and tighten set screw.

10.2.7. Back micrometer probe away from the cylinder before drive motor is engaged.

10.3. Record on the data sheet the ring number, if assigned, and the position of the test cylinder as indicated by the micrometer. The first and last wear tracks on a ring shall be approximately 1 mm in from either side.

10.3.1. For subsequent tests, reset cylinder to a new test position with the micrometer.

10.3.2. If the fuel is not to be changed, the cylinder should be adjusted by loosening the coupling set screw rather than at the mandrel, to minimize atmospheric contamination between tests. Unnecessary removal of the reservoir cover should be avoided after the initial aeration is completed.

10.3.3. If the fuel sample is to be changed/aerated, then the adjustment may be made at the mandrel. (Fuel is changed only after eight consecutive tests.)

10.3.4. The new position is to be 0.75 mm from the last wear track on the ring and noted on the data sheet.

10.3.5. After tightening the coupling set screw to lock the cylinder/shaft in a new test position, the micrometer probe should be backed off, then advanced to the cylinder again. Check micrometer reading to ensure correct track spacing. Readjust position, if required. When the correct ring position is ensured, back the micrometer probe away from the cylinder.

10.4. Install a clean test ball prior to each test by first placing the ball in the retaining nut, followed by the blue retaining ring. Screw retaining nut onto the threaded chuck located on the load arm and hand tighten.

10.5. Secure the load beam in the Up position by insertion of the blue pin.

10.6. If necessary, install the clean reservoir. Install the blue spacing platform by raising the reservoir. Slide blue spacer platform into position under the reservoir. Place thermocouple in the hole provided at the rear left side of the reservoir. Insert splash guards.

10.7. Check load beam level. Adjust, if necessary.

10.8. If necessary, supply test fluid in accordance with Practice D 4306. Transfer 50 ± 1 mL of the test fluid to the reservoir. Place cleaned reservoir cover in position and attach the 1/4 to 1/8 in. air lines to reservoir cover.

10.9. Move power switch to On position.

10.10. Turn on compressed air cylinder. Adjust the delivery pressure to 210 to 350 kPa (30 to 50 psi) and the console air pressure to approximately 100 kPa (14.5 psi).

10.11. Lower load beam by pulling blue pull pin. Do not allow the ball specimen to contact the ring.

10.12. Start rotation of cylinder by switching motor drive to On. Set rotation to 525 ± 1 r/min.

10.13. Using the flowmeters that control the wet and dry airflows, adjust conditioned airflow to read 3.8 L/min. Maintain 50 ± 0.2% relative humidity.

NOTE 4: 50% relative humidity should require approximately equal volumes of wet and dry air.

10.14. Adjust reservoir temperature as required until temperature stabilizes at 25° ± 1°C. Adjust thermostat of the heat exchanger circulating bath to obtain the required temperature.

10.15. If necessary, set fuel aeration timer for 15 min and adjust fuel aeration flowmeter to 0.5 L/min. (First test in load sequence only.)

10.16. At completion of aeration (if performed), the whistle will sound and aeration will cease. Continue 3.8 L/min flow through the reservoir.

10.17. *Break-In*

10.17.1. Place 500-g load on load arm.

10.17.2. Gently lower load arm. The pneumatic lift arm actuator must not be used.

10.17.3. Switch timer on for 30 seconds.

10.17.4. At the end of 30 seconds, the whistle will sound, and the test load must be immediately removed.

10.18. Switch on chart recorder to measure friction trace (if available).

10.19. Check all test condition readouts and adjust as necessary. Record all necessary information on data sheet.

10.20. Place required load on load arm. Do not replace test ball or adjust test cylinder. (See the Addendum at the end of this appendix for suggested loading sequence.)

10.21. Gently lower load arm. The pneumatic lift arm actuator must not be used.

10.22. Switch timer on for 60 seconds.

10.23. At the end of 60 seconds, the whistle will sound, and the test load must be immediately removed.

10.24. Manually remove test weight. Lift test load arm up and secure with blue pull pin.

10.25. Do not remove reservoir cover unless fuel is to be replaced. If fuel is not to be replaced, wipe revolving ring with an unused disposable lint free cloth to remove residue from the test ring. Turn motor drive and power switch to Off.

10.26. Remove test ball from locking nut. Do not remove ball from blue retaining ring. Wipe ball clean with disposable wipe prior to microscopic examination. Replace with new ball.

10.27. Measure the MAXIMUM friction coefficient (if available) and wear scar diameter as described in Section 11.

10.28. Determine if scuffing has occurred at the last applied load, as defined in Section 13.

10.29. If scuffing has not occurred, repeat from Section 10.2 with appropriate load increment as defined in the Addendum to this appendix.

11. Measurement of Wear Scar and Friction

11.1. *Wear Scar Measurement*

11.1.1. Turn on microscope light and position test ball under microscope at 100× magnification.

11.1.2. Focus microscope and adjust stage such that wear scar is centered within the field of view.

11.1.3. Align the wear scar to a divisional point of reference on the numerical scale with the mechanical stage controls. Measure the major axis to the nearest 0.01 mm. Record the readings on the data sheet.

11.1.4. Align the wear scar to a divisional point of reference on the numerical scale with the mechanical stage controls. Measure the minor axis to the nearest 0.01 mm. Record the readings on the data sheet.

11.1.5. Record condition of wear area if different from the reference standard test, that is, debris color, unusual particles or wear pattern, visible galling, etc., and presence of particles in the reservoir.

11.2. *Friction Measurement*

11.2.1. Measure maximum tangential friction force in grams from output on stripchart recorder.

11.2.2. Calculate friction coefficient as described in Section 12.

11.2.3. Record applied load and friction coefficient.

12. Calculation

12.1. Calculate the wear scar diameter as follows:

$$WSD = \frac{(M + N)}{2} \qquad \text{(Eq. 1)}$$

where: WSD = Wear scar diameter, mm
M = Major axis, mm
N = Minor axis, mm.

12.2 Calculate the maximum friction coefficient as follows:

$$\mu = \frac{Ft}{Fn} \qquad \text{(Eq. 2)}$$

where: μ = Coefficient of Friction
Ft = Maximum tangential friction force, g
Fn = Contact load, g (= 2× applied Load).

13. Adhesive Scuffing

13.1. Scuffing may be defined as the transition from mild boundary lubricated wear or oxidative corrosion wear to more severe adhesive wear.

13.2. The onset of scuffing is accompanied by a marked increase in both friction and wear. Typical friction traces are provided in Fig. K-1.

13.2.1. Scuffing is considered to occur if the friction coefficient exceeds 0.175 at any time during the test.

13.2.2. Scuffing is considered to occur if the plotted friction coefficient or wear scar diameter increases disproportionately with increasing load. (Requires additional tests.)

13.3. A subjective measure of the wear mechanisms present is often possible from a visual examination of the wear scar, with a distinct change in the surface topography after scuffing has been initiated. Scuffing is typically accompanied by a change in the sound of the test apparatus.

13.4. The scuffing load capacity is considered to be the minimum applied load at which scuffing *is* observed.

13.5. Scuffing onset is most easily defined through observation of the friction traces.

14. Report

14.1. Report the following information:

14.1.1. The applied load (not contact load) required to produce scuffing to the nearest 100 g.

14.1.2. Deviations from the standard conditions of the test load, relative humidity, and fuel temperature, etc.

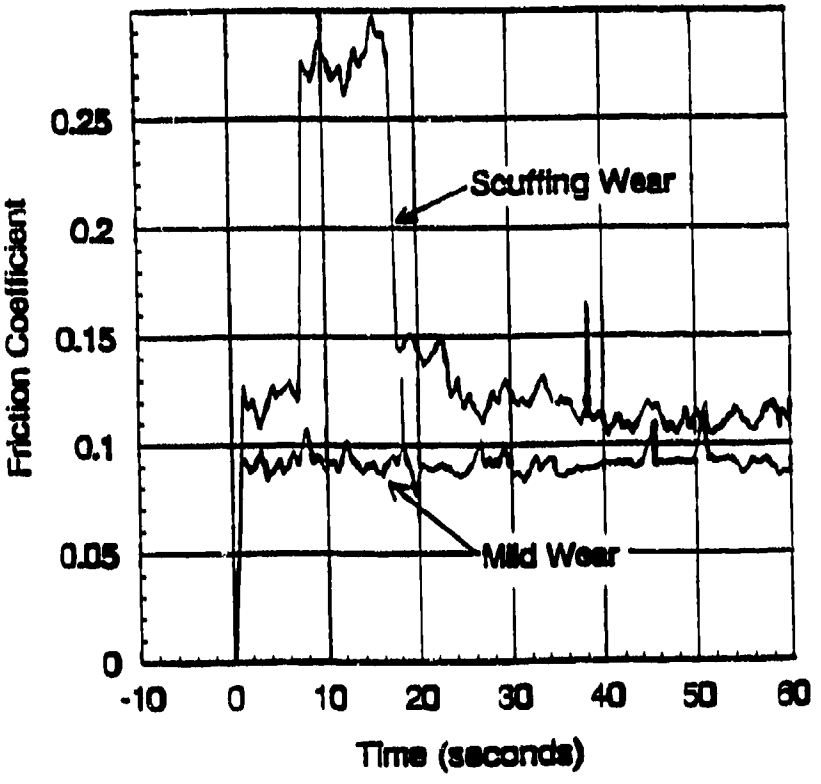

Figure K-1. Typical friction traces obtained during scuffing load wear tests

ADDENDUM

Suggested Test Load Sequence

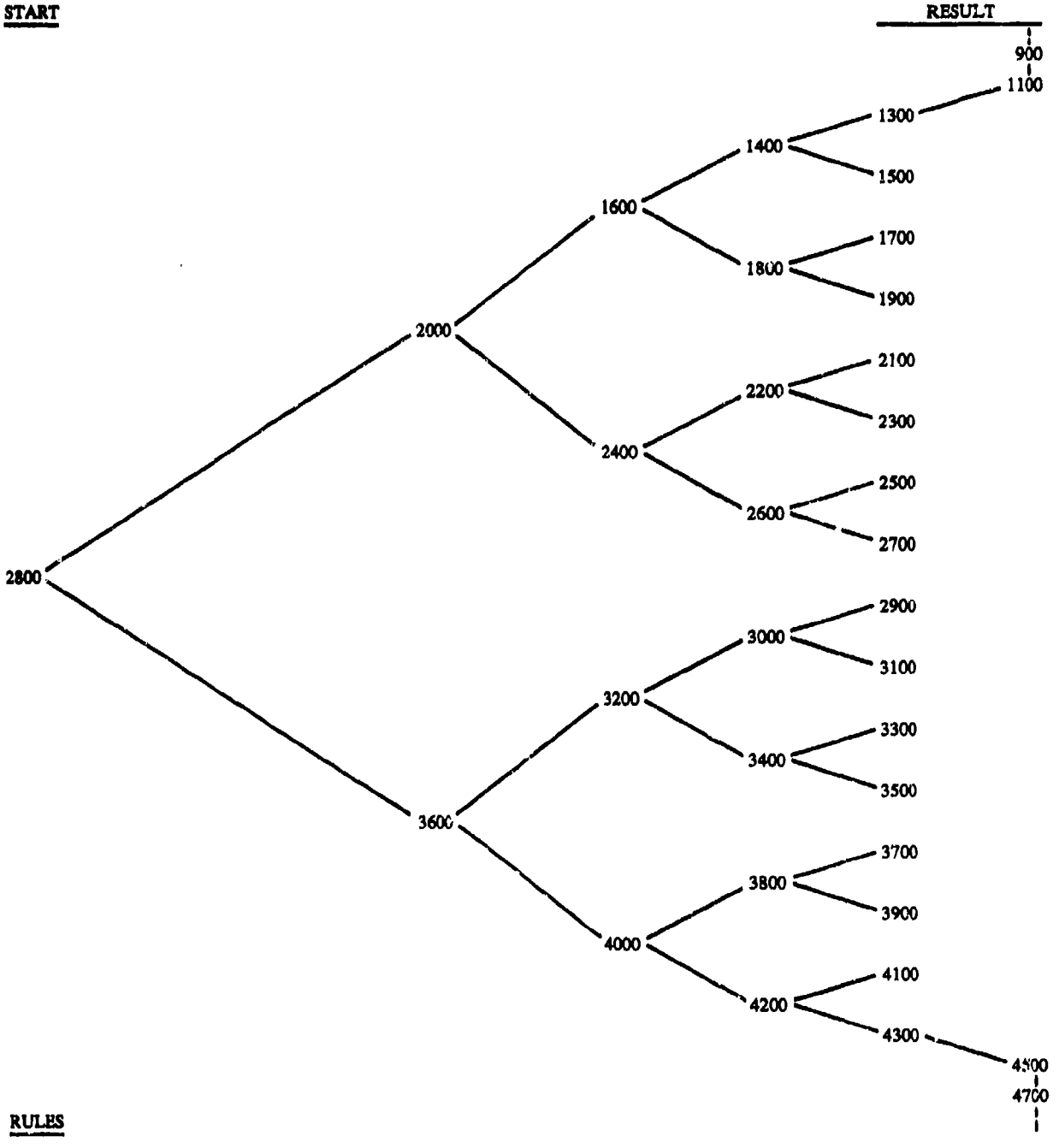

RULES

1. Move left to right when selecting load, start at 2,800 g.
2. If scuffing is observed, select the next lower load to the right (i.e., follow the upward arrow).
3. If no scuffing is observed, select the next higher load to the right (i.e., follow the downward arrow).
4. The result is the value obtained in the rightmost column to the nearest 200 g.
5. If necessary, additional tests may be performed to assess results outside the range 1,300 to 4,300 g. However, few fuels exceed the given range.

DISTRIBUTION LIST

Department of Defense

DEFENSE TECH INFO CTR 12
CAMERON STATION
ALEXANDRIA VA 22314

ODUSD
ATTN: (L) MRM 1
PETROLEUM STAFF ANALYST
PENTAGON
WASHINGTON DC 20301-8000

ODUSD
ATTN: (ES) CI 1
400 ARMY NAVY DR
STE 206
ARLINGTON VA 22202

HQ USEUCOM
ATTN: ECJU L1J 1
UNIT 30400 BOX 1000
APO AE 09128-4209

US CINCPAC
ATTN: J422 BOX 64020 1
CAMP H M SMITH
HI 96861-4020

DIR DLA
ATTN: DLA MMDI 1
DLA MMSB 1
CAMERON STA
ALEXANDRIA VA 22304-6100

CDR
DEFENSE FUEL SUPPLY CTR
ATTN: DFSC Q BLDG 8 1
DFSC S BLDG 8 1
CAMERON STA
ALEXANDRIA VA 22304-6160

DIR ADV RSCH PROJ AGENCY
ATTN: ARPA/ASTO 1
3701 N FAIRFAX DR
ARLINGTON VA 22203-1714

Department of the Army

HQDA
ATTN: DALO TSE 1
DALO SM 1
PENTAGON
WASHINGTON DC 20310-0103

SARDA
ATTN: SARD TL 1
PENTAGON
WASHINGTON DC 20310-0103

CDR AMC
ATTN: AMCRD S 1
AMCRD IM 1
AMCRD IT 1
AMCEN A 1
AMCLG MS 1
AMCLG MT 1
AMCICP ISI 1
5001 EISENHOWER AVE
ALEXANDRIA VA 22333-0001

TARDEC
ATTN: AMSTA CMA 1
AMSTA CMB 1
AMSTA CME 1
AMSTA HBM 1
AMSTA N 1
AMSTA R 1
AMSTA RG 1
AMCPM ATP 1
AMSTA Q 1
AMSTA UE 1
AMSTA UG 1
CDR TACOM
WARREN MI 48397-5000

CDR ARMY TACOM
ATTN: AMSTA FP 1
AMSTA KL 1
AMSTA MM 1
AMSTA MT 1
AMSTA MC 1
AMSTA GT 1
AMSTA FNG 1
AMSTA FR 1
USMC LNO 1
AMCPM LAV 1
AMCPM M 113/M60 1
AMCPM CCE/SMHE 1
WARREN MI 48397-5000

DEPARTMENT OF THE ARMY
MOBILITY TECH CTR BELVOIR
ATTN: AMSTA RBF 10
AMSTA RBXA 1
10115 GRIDLEY RD STE 128
FT BELVOIR VA 22060-5843

PROG EXEC OFFICER
ARMORED SYS MODERNIZATION
ATTN: SFAE ASM S 1
SFAE ASM BV 1
SFAE ASM CV 1
SFAE ASM AG 1
CDR TACOM
WARREN MI 48397-5000

PROG EXEC OFFICER
ARMORED SYS MODERNIZATION
ATTN: SFAE ASM FR 1
SFAE ASM AF 1
PICATINNY ARSENAL
NJ 07806-5000

PROG EXEC OFFICER
COMBAT SUPPORT
ATTN: SFAE CS TVL 1
SFAE CS TVM 1
SFAE CS TVH 1
CDR TACOM
WARREN MI 48397-5000

PROG EXEC OFFICER
ARMAMENTS
ATTN: SFAE AR HIP 1
SFAE AR TMA 1
PICATINNY ARSENAL
NJ 07806-5000

PROJ MGR
UNMANNED GROUND VEH
ATTN: AMCPM UG 1
REDSTONE ARSENAL
AL 35898-8060

DIR
ARMY RSCH LAB
ATTN: AMSRL CP PW 1
2800 POWDER MILL RD
ADELPHIA MD 20783-1145

VEHICLE PROPULSION DIR
ATTN: AMSRL VP (MS 77 12) 1
NASA LEWIS RSCH CTR
21000 BROOKPARK RD
CLEVELAND OH 44135

CDR AMSAA
ATTN: AMXSY CM 1
AMXSY L 1
APG MD 21005-5071

CDR ARO
ATTN: AMXRO EN (D MANN) 1
RSCH TRIANGLE PK
NC 27709-2211

CDR AEC
ATTN: SFIM AEC ECC (T ECCLES) 1
APG MD 21010-5401

CDR ARMY ATCOM
ATTN: AMSAT I ME (L HEPLER) 1
AMSAT I LA (V SALISBURY) 1
AMSAT R EP (V EDWARD) 1
4300 GOODFELLOW BLVD
ST LOUIS MO 63120-1798

CDR ARMY NRDEC
ATTN: SATNC US (J SIEGEL) 1
SATNC UE 1
NATICK MA 01760-5018

CDR ARMY CRDEC
ATTN: SMCCR RS 1
APG MD 21010-5423

CDR ARMY DESCOM
ATTN: AMSDS MN 1
AMSDS EN 1
CHAMBERSBURG PA 17201-4170

CDR ARMY WATERVLIET ARSN
ATTN: SARWY RDD 1
WATERVLIET NY 12189

CDR APC
ATTN: SATPC Q 1
SATPC QE (BLDG 85 3) 1
NEW CUMBERLAND PA 17070-5005

PETROL TEST FAC WEST 1
BLDG 247 TRACEY LOC
DDRW
P O BOX 96001
STOCKTON CA 95296-0960

CDR ARMY LEA
ATTN: LOEA PL 1
NEW CUMBERLAND PA 17070-5007

CDR ARMY TECOM
ATTN: AMSTE TA R 1
AMSTE TC D 1
AMSTE EQ 1
APG MD 21005-5006

PROJ MGR PETROL WATER LOG
ATTN: AMCPM PWL 1
4300 GOODFELLOW BLVD
ST LOUIS MO 63120-1798

PROJ MGM MOBILE ELEC PWR
ATTN: AMCPM MEP 1
7798 CISSNA RD STE 200
SPRINGFIELD VA 22150-3199

CDR
ARMY COLD REGION TEST CTR
ATTN: STECR TM 1
STECR LG 1
APO AP 96508-7850

CDR
ARMY BIOMED RSCH DEV LAB
ATTN: SGRD UBZ A 1
FT DETRICK MD 21702-5010

CDR FORSCOM
ATTN: AFLG TRS 1
FT MCPHERSON GA 30330-6000

CDR TRADOC
ATTN: ATCD SL 5 1
INGALLS RD BLDG 163
FT MONROE VA 23651-5194

CDR ARMY ARMOR CTR
ATTN: ATSB CD ML 1
ATSB TSM T 1
FT KNOX KY 40121-5000

CDR ARMY QM SCHOOL
ATTN: ATSM CD 1
ATSM PWD 1
FT LEE VA 23001-5000

CDR
ARMY COMBINED ARMS SPT CMD
ATTN: ATCL CD 1
ATCL MS 1
FT LEE VA 23801-6000

CDR ARMY FIELD ARTY SCH
ATTN: ATSF CD 1
FT SILL OK 73503

CDR ARMY TRANS SCHOOL
ATTN: ATSP CD MS 1
FT EUSTIS VA 23604-5000

CDR ARMY INF SCHOOL
ATTN: ATSH CD 1
ATSH AT 1
FT BENNING GA 31905-5000

CDR ARMY AVIA CTR
ATTN: ATZQ DOL M 1
ATZQ DI 1
FT RUCKER AL 36362-5115

CDR ARMY CACDA
ATTN: ATZL CD 1
FT LEAVENWORTH KA 66027-5300

CDR ARMY ENGR SCHOOL
ATTN: ATSE CD 1
FT LEONARD WOOD MO 65473-5000

CDR ARMY ORDN CTR
ATTN: ATSL CD CS 1
APG MD 21005

CDR ARMY SAFETY CTR
ATTN: CSSC PMG 1
CSSC SPS 1
FT RUCKER AL 36362-5363

CDR ARMY CSTA
ATTN: STECS EN 1
STECS LI 1
STECS AE 1
STECS AA 1
APG MD 21005-5059

CDR ARMY YPG
ATTN: STEYP MT TL M 1
YUMA AZ 85365-9130

CDR ARMY CERL
ATTN: CECER EN 1
P O BOX 9005
CHAMPAIGN IL 61826-9005

DIR 1
AMC FAST PROGRAM
10101 GRIDLEY RD STE 104
FT BELVOIR VA 22060-5818

CDR I CORPS AND FT LEWIS
ATTN: AFZH CSS 1
FT LEWIS WA 98433-5000

CDR
RED RIVER ARMY DEPOT
ATTN: SDSRR M 1
SDSRR Q 1
TEXARKANA TX 75501-5000

PS MAGAZINE DIV
ATTN: AMXLS PS 1
DIR LOGSA
REDSTONE ARSENAL AL 35898-7466

CDR 6TH ID (L)
ATTN: APUR LG M 1
1060 GAFFNEY RD
FT WAINWRIGHT AK 99703

Department of the Navy

OFC OF NAVAL RSCH
ATTN: ONR 464 1
800 N QUINCY ST
ARLINGTON VA 22217-5660

CDR
NAVAL SEA SYSTEMS CMD
ATTN: SEA 03M3 1
2531 JEFFERSON DAVIS HWY
ARLINGTON VA 22242-5160

CDR
NAVAL SURFACE WARFARE CTR
ATTN: CODE 630 1
CODE 632 1
CODE 859 1
3A LEGGETT CIRCLE
ANNAPOLIS MD 21401-5067

CDR
NAVAL RSCH LABORATORY
ATTN: CODE 6181 1
WASHINGTON DC 20375-5342

CDR
NAVAL AIR WARFARE CTR
ATTN: CODE PE33 AJD 1
P O BOX 7176
TRENTON NJ 08628-0176

CDR 1
NAVAL PETROLEUM OFFICE
CAMERON STA T 40
5010 DUKE STREET
ALEXANDRIA VA 22304-6180

OFC ASST SEC NAVY (I & E) 1
CRYSTAL PLAZA 5
2211 JEFFERSON DAVIS HWY
ARLINGTON VA 22244-5110

CDR
NAVAL AIR SYSTEMS CMD
ATTN: AIR 53623C 1
1421 JEFFERSON DAVIS HWY
ARLINGTON VA 22243-5360

Department of the Navy/U.S. Marine Corps

HQ USMC
ATTN: LPP 1
WASHINGTON DC 20380-0001

PROG MGR COMBAT SER SPT 1
MARINE CORPS SYS CMD
2033 BARNETT AVE STE 315
QUANTICO VA 22134-5080

PROG MGR GROUND WEAPONS 1
MARINE CORPS SYS CMD
2033 BARNETT AVE
QUANTICO VA 22134-5080

PROG MGR ENGR SYS 1
MARINE CORPS SYS CMD
2033 BARNETT AVE
QUANTICO VA 22134-5080

CDR
MARINE CORPS SYS CMD
ATTN: SSE 1
2033 BARNETT AVE STE 315
QUANTICO VA 22134-5010

CDR
BLOUNT ISLAND CMD
ATTN: CODE 922/1 1
5880 CHANNEL VIEW BLVD
JACKSONVILLE FL 32226-3404

CDR
MARINE CORPS LOGISTICS BA
ATTN: CODE 837 1
814 RADFORD BLVD
ALBANY GA 31704-1128

CDR 1
2ND MARINE DIV
PSC BOX 20090
CAMP LEJEUNNE NC 28542-0090

CDR 1
1ST MARINE DIV
CAMP PENDLETON CA 92055-5702

CDR 1
FMFPAC G4
BOX 64118
CAMP H M SMITH HI 96861-4118

Department of the Air Force

HQ USAF/LGSSF
ATTN: FUELS POLICY 1
1030 AIR FORCE PENTAGON
WASHINGTON DC 20330-1030

HQ USAF/LGTV
ATTN: VEH EQUIP/FACILITY 1
1030 AIR FORCE PENTAGON
WASHINGTON DC 20330-1030

AIR FORCE WRIGHT LAB
ATTN: WL/POS 1
WL/POSF 1
1790 LOOP RD N
WRIGHT PATTERSON AFB
OH 45433-7103

AIR FORCE MEEP MGMT OFC 1
615 SMSQ/LGTV MEEP
201 BISCAYNE DR STE 2
ENGLIN AFB FL 32542-5303

SA ALC/SFT
1014 ANDREWS RD STE 1
KELLY AFB TX 78241-5603 1

WR ALC/LVRS
225 OCMULGEE CT
ROBINS AFB GA 31098-1647 1

Other Federal Agencies

NASA
LEWIS RESEARCH CENTER
CLEVELAND OH 44135 1

NIPER
PO BOX 2128
BARTLESVILLE OK 74005 1

DOT
FAA
AWS 110
800 INDEPENDENCE AVE SW
WASHINGTON DC 20590 1

DOE
CE 151 (MR RUSSEL)
1000 INDEPENDENCE AVE SW
WASHINGTON DC 20585 1

EPA
AIR POLLUTION CONTROL
2565 PLYMOUTH RD
ANN ARBOR MI 48105 1